US Army Corps of Engineers

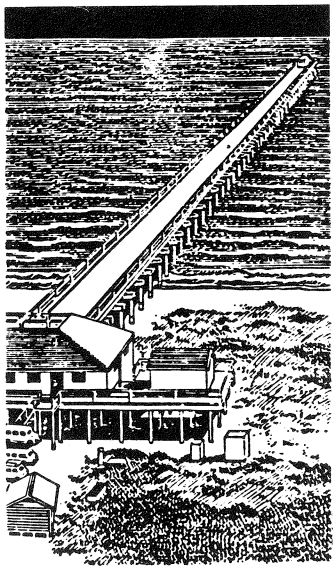

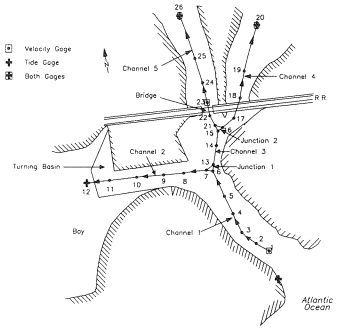

TECHNICAL REPORT CERC-91-10

DYNLET1: DYNAMIC IMPLICIT NUMERICAL MODEL OF ONE-DIMENSIONAL TIDAL FLOW THROUGH INLETS

by

Michael Amein

Amein & Associates
9424 Chapel Hill Road
Raleigh, North Carolina 27607

and

Nicholas C. Kraus

Coastal Engineering Research Center

DEPARTMENT OF THE ARMY
Waterways Experiment Station, Corps of Engineers
3909 Halls Ferry Road, Vicksburg, Mississippi 39180-6199

September 1991

Final Report

Approved For Public Release; Distribution Is Unlimited

REPORT DOCUMENTATION PAGE

Form Approved
OMB No. 0704-0188

Public reporting burden for this collection of information is estimated to average 1 hour per response, including the time for reviewing instructions, searching existing data sources, gathering and maintaining the data needed, and completing and reviewing the collection of information. Send comments regarding this burden estimate or any other aspect of this collection of information, including suggestions for reducing this burden, to Washington Headquarters Services, Directorate for Information Operations and Reports, 1215 Jefferson Davis Highway, Suite 1204, Arlington, VA 22202-4302, and to the Office of Management and Budget, Paperwork Reduction Project (0704-0188), Washington, DC 20503.

1. AGENCY USE ONLY *(Leave blank)*

2. REPORT DATE
September 1991

3. REPORT TYPE AND DATES COVERED
Final report

4. TITLE AND SUBTITLE
DYNLET1: Dynamic Implicit Numerical Model of One-Dimensional Tidal Flow Through Inlets

5. FUNDING NUMBERS
Work Unit 32526

6. AUTHOR(S)
Michael Amein
Nicholas C. Kraus

7. PERFORMING ORGANIZATION NAME(S) AND ADDRESS(ES)
See reverse

8. PERFORMING ORGANIZATION REPORT NUMBER
Technical Report
CERC-91-10

9. SPONSORING/MONITORING AGENCY NAME(S) AND ADDRESS(ES)
US Army Corps of Engineers
Washington, DC 20314-1000

10. SPONSORING/MONITORING AGENCY REPORT NUMBER

11. SUPPLEMENTARY NOTES
Available from National Technical Information Service, 5285 Port Royal Road, Springfield, VA 22161

12a. DISTRIBUTION/AVAILABILITY STATEMENT
Approved for public release; distribution is unlimited

12b. DISTRIBUTION CODE

13. ABSTRACT *(Maximum 200 words)*

The development and verification of a simple model of inlet hydrodynamics for use in reconnaissance-level quantitative studies of inlets are presented. The model, named DYNLET1 for its one-dimensional modeling of the dynamic (time-dependent) behavior of tidal flow at inlets, is based on the full one-dimensional shallow-water equations employing an implicit finite difference technique. The model is intended for personal computer (PC) users having little or no experience in numerical modeling and facilitates minimal data entry and numerical grid generation.

DYNLET1 can predict flow conditions in channels with varied geometry, and it accepts varying friction factors across an inlet channel, geometric boundary conditions. Values of water surface elevation and average velocity are computed at locations across and along inlet channels and displayed on the PC monitor and written to output files for possible further analysis.

(Continued)

14. SUBJECT TERMS
Indian River Inlet, Delaware
Inlet
Masonboro Inlet, North Carolina
Numerical Model
Tidal flow
Tidal inlet hydrodynamics

15. NUMBER OF PAGES
130

16. PRICE CODE

17. SECURITY CLASSIFICATION OF REPORT
UNCLASSIFIED

18. SECURITY CLASSIFICATION OF THIS PAGE
UNCLASSIFIED

19. SECURITY CLASSIFICATION OF ABSTRACT

20. LIMITATION OF ABSTRACT

7. (Continued)

Amein & Associates
9424 Chapel Hill Road
Raleigh, NC 27607;

USAE Waterways Experiment Station
Coastal Engineering Research Center
3909 Halls Ferry Road
Vicksburg, MS 39180-6199

13. (Continued)

The inlet to be modeled may consist of a single channel connecting the sea to the bay, or it can be a system of interconnected channels, with or without bays. The principal limitation of DYNLET1 is potential inaccuracy in situations where strong two-dimensional flow fields, such as gyres, exist perpendicular to the major axis of channels comprising the modeled inlet.

This report also includes a short review of existing, similar simple models of tidal inlet hydrodynamics. Application and verification of the model are illustrated with two case studies for which extensive data are available: Masonboro Inlet, North Carolina, and Indian River Inlet, Delaware.

PREFACE

The study described herein was authorized as part of the Civil Works Research and Development Program by Headquarters, US Army Corps of Engineers (HQUSACE). Work was performed under the Inlet Stability Work Unit 32526, which is part of the Harbor Entrances and Coastal Channels Program conducted at the Coastal Engineering Research Center (CERC), US Army Engineer Waterways Experiment Station (WES), Vicksburg, MS. Messrs. John H. Lockhart, Jr.; John G. Housley; Robert H. Campbell; and James E. Crews were HQUSACE Technical Monitors. Dr. Charles L. Vincent, CERC, was Program Manager.

This study was performed and the report prepared over the period 1 March through 30 December 1990 by Dr. Michael Amein, Amein and Associates, Raleigh, NC, and Dr. Nicholas C. Kraus, Senior Scientist, CERC. Ms. Kathryn J. Gingerich, formerly of the Coastal Processes Branch (CPB), Research Division (RD), was Principal Investigator of Work Unit 32526 during the inception and research stages of the study, and Ms. Julie Dean Rosati, CPB, was the Principal Investigator during report preparation and publication. Dr. Kraus was under the administrative supervision of Dr. James R. Houston, Chief, CERC, and Mr. Charles C. Calhoun, Jr., Assistant Chief, CERC. Mses. Gingerich and Rosati were under the direct supervision of Mr. Bruce A. Ebersole, Chief, CPB, RD, and Mr. H. Lee Butler, Chief, RD, CERC. Technical reviews were provided by Messrs. Ebersole and Butler, Ms. Rosati, and Mr. W. Jeffrey Lillycrop, Coastal Structures and Evaluation Branch, Engineering Development Division, CERC. Mses. Marsha W. Darnell and Carolyn J. Dickson, CPB, RD, assisted in text formatting and figure preparation under the supervision of Ms. Rosati. Ms. Lee T. Byrne, Information Technology Laboratory, WES, edited the report.

COL Larry B. Fulton, EN, was Commander and Director of WES. Dr. Robert W. Whalin was Technical Director.

CONTENTS

	Page
PREFACE	1
LIST OF FIGURES	3
CONVERSION FACTORS, NON-SI TO SI (METRIC) UNITS OF MEASUREMENT	4
PART I: INTRODUCTION	5
Background and Motivation	5
Organization of This Report	8
PART II: THEORETICAL BACKGROUND	10
Review of Basic Equations	10
Numerical Solution Method	15
PART III: DYNLET1 NUMERICAL SOLUTION PROCEDURE	18
Model Setup	18
Solution of the Finite-Difference Equations	25
PART IV: DYNLET1	34
Preparation to Run DYNLET1	34
Input Files	41
Output Files	46
Auxiliary Programs	48
PART V: EXAMPLE APPLICATION 1: MASONBORO INLET, NORTH CAROLINA	50
Masonboro Inlet	50
DYNLET1	52
GITI Models for Masonboro Inlet	57
Evaluation of Flow Parameters from DYNLET1	59
PART VI: EXAMPLE APPLICATION 2: INDIAN RIVER INLET, DELAWARE	65
Indian River Inlet	65
DYNLET1	68
PART VII: SUMMARY AND CONCLUSION	74
REFERENCES	76

CONTENTS (Concluded)

		Page
APPENDIX A:	DATA FILES FOR MASONBORO INLET	A1
APPENDIX B:	DATA FILES FOR INDIAN RIVER INLET	B1
APPENDIX C:	NOTATION	C1

LIST OF FIGURES

No.		Page
1	Definition sketch for flow in inlet channel	11
2	Definition sketch for inlet channel cross section	11
3	Definition sketch for inlet channel network (modeled after Moorhead Harbor, North Carolina	19
4	Computation grid on the y - t plane	21
5	DYNLET1 input and output file structure	41
6	Auxiliary program input and output file structure	47
7	Schematic for Masonboro Inlet model	51
8	Computed and measured velocities (Gage 2C), Masonboro Inlet	55
9	Computed and measured velocities (Gage 2S), Masonboro Inlet	55
10	Computed and measured discharges, Masonboro Inlet	56
11	Cross section through Node 1, Masonboro Inlet	57
12	Schematic plan for Indian River Inlet	66
13	Computed and measured velocities (Gage INLET3), Indian River, using DYNLET1	71
14	Computed and measured velocities (Gage MIDIS3), Indian River, using DYNLET1	71
15	Computed and measured stage (Gage USCG), Indian River, using DYNLET1	72
16	Computed and measured stage (Gage Dewey), Indian River, using DYNLET1	72

CONVERSION FACTORS, NON-SI TO SI (METRIC) UNITS OF MEASUREMENT

Non-SI units of measurement used in this report can be converted to SI (metric) units as follows:

Multiply	By	To Obtain
cubic feet per second	0.02831685	cubic meters per second
degree	0.01745329	radians
feet	0.3048	meters
miles (US statute)	1.609344	kilometers
square feet	0.09290304	square meters

DYNLET1: DYNAMIC IMPLICIT NUMERICAL MODEL OF ONE-DIMENSIONAL TIDAL FLOW THROUGH INLETS

PART I: INTRODUCTION

Background and Motivation

1. The US Army Corps of Engineers (USACE) has responsibility for creating and maintaining navigable US waterways. Tidal inlets that connect the ocean with bays, estuaries, and sounds constitute a major component of this navigation system. The design and construction of navigation improvements to existing inlets is an important part of the USACE responsibility, and each year the USACE dredges millions of cubic yards of sediments from tidal inlets to maintain navigability.

2. To a great extent, the sand-trapping capacity of inlets determines the long-term evolution of the shoreline position on adjacent beaches. The sand-trapping capacity depends on such factors as the strength of the tidal flow, morphology of the shoals at the inlet, wave action, and condition and configuration of the navigation channel and inlet structures, such as jetties.

3. The channel shoaling rate, inlet shoal morphology, and inlet bank position are to a great extent controlled by the tidal flow through an inlet. Accurate and efficient calculation of the hydraulic characteristics of inlets is, therefore, important for project planning and engineering involving navigation, inlet stability, beach and side bank evolution, and the flushing of bays and lagoons. Quantitative understanding of tidal flow at inlets is, of course, also required to achieve understanding of fundamental hydrodynamic and morphodynamic processes at inlets.

4. In the past two decades, sophisticated two- and three-dimensional numerical simulation models have been developed for computing detailed processes of inlet hydrodynamics (Butler 1980, 1982; Johnson et al. 1989; Cialone, in preparation) and water-quality aspects (Kim, Johnson, and Sheng 1989) of inlets. Special expertise and a powerful mainframe computer are required to set up and run these types of models, however, and they are not, as yet, available to the non-modeling coastal or dredging planner, engineer, and geophysical researcher.

5. There is, therefore, a gap between the requirements to perform sophisticated inlet hydrodynamics modeling and the needs, knowledge base, and computer resources of the project-level planner and engineer. The development and verification of a simple, yet accurate model of inlet hydrodynamics for use in reconnaissance-level quantitative studies of inlets at the project level are identified as a research need to be addressed.

6. The research conducted in this study was directed toward answering the question of whether it would be possible to develop an accurate and easy-to-use numerical model suited for operating with computer resources available in any engineering office, namely a modern desk-top or personal computer. The model should be suitable for reconnaissance-level studies for most inlets by providing reliable and accurate answers to users who do not have experience in numerical modeling, facilitating minimal data entry and numerical grid-generation.

7. The objective of this study was, therefore, development of a state-of-the-art reconnaissance-level model for predicting tide-dominated velocities and water level fluctuations at an inlet and verification of the model by comparison to field measurements. The model would have a rigorous theoretical foundation, be numerically implemented in a sound manner, and be capable of describing realistic situations. It should provide detailed velocity information across the inlet channels, be able to describe multichannel inlets, be flexible to allow inclusion of new features, and importantly, be easy to operate on a personal computer.

8. This report describes a numerical model developed to satisfy the above requirements. The model is based on the full one-dimensional shallow-water equations employing an implicit finite-difference technique. The model was named DYNLET1, reflecting the fact that it is a one-dimensional model of the dynamic (time-dependent) behavior of the tidal flow at inlets. It is asserted that use of the full one-dimensional hydrodynamic equations and a rigorous treatment of the cross-sectional inlet and flow properties meet the objective of this study.

9. The principal limitation of DYNLET1 is potential inaccuracy in situations where strong two-dimensional flow fields, such as gyres, exist perpendicular to the major axis of channels comprising the modeled inlet. However, the model is well suited for applications to narrow inlets connected

to large bay systems as compared with two-dimensional models because the primary flow directions are known and cross-sectional data at high resolution can be represented in the main inlet. Inlets with multiple channels are also appropriately modeled with DYNLET1. Transition head losses arising from sudden changes in channel width are well modeled by the one-dimensional approach taken here; rigorous description of this phenomenon in two-dimensional models is unknown to the authors.

10. The model DYNLET1 also provides an alternative to the "linked-node" models developed in the 1960's (Roesner, Aldrich, and Dickinson 1989). Standard linked-node models use explicit numerical solution schemes and, therefore, have restrictions severely limiting the size of the allowable time step. Also, channel cross sections must be greatly idealized, use of local bottom friction coefficients is not possible, and only an average velocity for a cross section can be obtained (as opposed to computing local velocities at different stations corresponding to different locations along a cross section). These and other limitations inherent in the linked-node models, which were originally developed for pipe flow analysis, do not exist in DYNLET1.

11. As will be described in subsequent chapters, DYNLET1 can analyze the flow in channels of varied geometry, ranging from prismatic channels to natural channels with flood banks, and it accepts varying friction factors across an inlet channel, geometric data at variable distances across and along an inlet channel, and a variety of boundary conditions. Flooding and drying on the channel banks are automatically part of the calculation process if the cross sections include these areas. Values of water surface elevation and average velocity are computed at locations across and along inlet channels, and displayed on the computer monitor and written to output files for possible further analysis and enhanced visual display. The inlet to be modeled may consist of a single channel connecting the sea to the bay, or it can be a system of interconnected channels, with or without bays.

12. The numerical model also includes a number of useful enhancements beyond simply implementing an efficient and accurate numerical solution scheme, including incorporation of a transition-loss term, user-friendly interface for data entry, preparation of data files for viewing on the monitor, and printer output of cross-section geometry, velocity, and stage.

For future research and applications, the model can be easily coupled to transport models to compute thermal effects, and salinity, sediment, and water-quality constituent transport.

13. This report also includes a short review of existing, similar simple models of tidal inlet hydrodynamics for comparison of capabilities and for parallel structure for placement of study results in the context of models presently available to the project planner and engineer who may be involved in navigation and beach protection projects.

14. Application and verification of the model are illustrated with two case studies for which extensive data are available. The first example is Masonboro Inlet, North Carolina, which has a system of interconnected channels but does not have a well-defined bay. Velocity and tidal measurements are available at five locations in the Masonboro Inlet system for 12 September 1969. Flow conditions for that date were represented in DYNLET1, and model predictions were compared with field measurements.

15. The second example is Indian River Inlet, Delaware, an inlet protected by two jetties at its entrance and having two well-defined bays. A significant flow-related problem at this inlet is scour occurring at pilings of a major highway bridge crossing its entrance. Velocity measurements at two locations and tidal height measurements at five locations are available for the period of 29 June to 1 July 1989. The results of model calculations are compared with these measurements.

Organization of This Report

16. Part I describes the motivation for the study and presents the problem statement and study objective. Parts II and III respectively give the theoretical background and numerical solution scheme defining the model developed in the study, DYNLET1. The main portion of the original numerical modeling work is given in Part III.

17. Part IV mainly deals with the general procedures for model operation, the user interface, and preparations for running DYNLET1. Parts V and VI give detailed examples of model application and testing for Masonboro Inlet, North Carolina, and Indian River Inlet, Delaware, respectively. Part VII contains conclusions and summarizes results.

18. Appendices A and B respectively give the data files and additional graphical output for the Masonboro Inlet and Indian River Inlet test cases, and Appendix C contains a list of notation used in this report.

PART II: THEORETICAL BACKGROUND

Review of Basic Equations

19. The shallow-water hydrodynamic equations forming the basis of the numerical model for one-dimensional depth-averaged flow consist of the equations for the conservation of mass, momentum, and energy. Their derivations are given in standard reference works (for example, Chow 1959, Stoker 1957, Ippen 1966, French 1984). For most applications, the equations for the conservation of momentum and energy provide identical information. A short derivation of the equations for the conservation of mass and momentum is given here to review concepts and introduce notation.

20. Consider a short reach of a channel of length Δy with the flow taking place from Section 1 to Section 2 as shown in Figure 1. A typical channel cross section is shown in Figure 2. These figures introduce the following notation*:

A = cross-sectional area

B = top width of the channel cross section

g = acceleration due to gravity

h = water depth from the channel bottom to the free surface

P = wetted perimeter of channel cross section

q = the lateral inflow or outflow per unit channel length per unit time

Q = the volume flow rate

t = time

Δt = small time increment

v = average flow velocity

x = distance across channel

y = distance along channel

z = water surface elevation

z_b = channel bottom elevation

z_t = water elevation at time t

---

* For convenience, symbols and abbreviations are listed in the Notation, Appendix C.

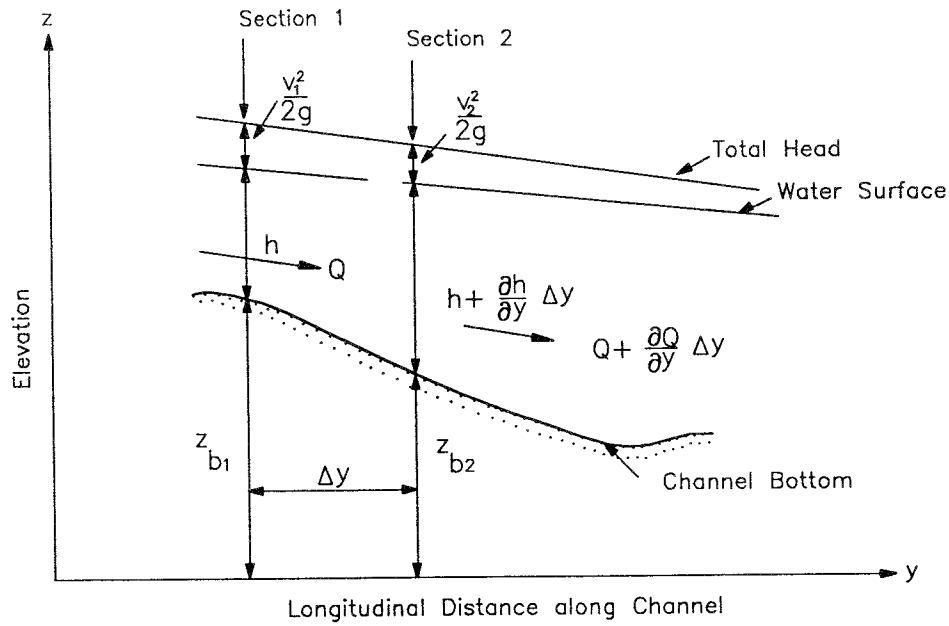

Figure 1. Definition sketch for flow in inlet channel

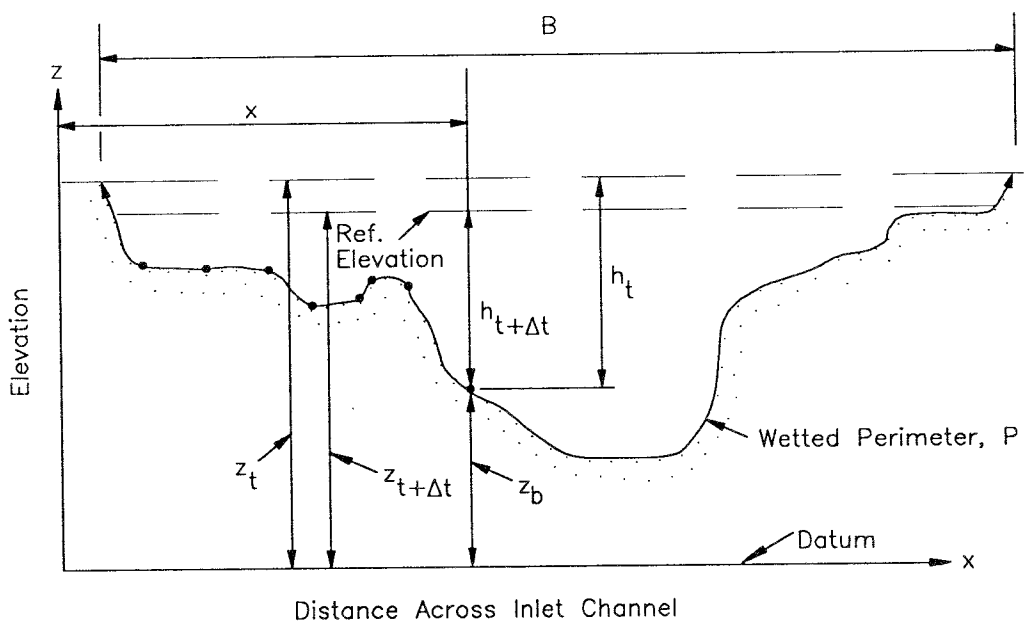

Figure 2. Definition sketch for inlet channel cross section

$z_{t+\Delta t}$ = water elevation at time $t+\Delta t$

ρ = density of water

1, 2 = subscripts denoting Sections 1 and 2, respectively

These quantities will be used in the derivations given next and in subsequent discussion. The relationship between the channel top width B and area A is $B = dA/dz$.

Mass conservation equation

21. The mass of water entering the channel during a time interval Δt is $\rho Q\Delta t + \rho q\Delta t\Delta y$, and the mass of water leaving the channel reach during the same time interval is $\rho(Q + \partial Q/\partial y\Delta y)\Delta t$. Assuming $\partial Q/\partial y$ and q to be positive, there is a net mass outflow from the reach. The law for conservation of mass requires that the mass inside the reach be reduced because of the net mass outflow during the time Δt, and, consequently, the water surface should fall. The mass of water inside the reach of length Δy is $\rho A\Delta y$, and the rate of decrease of the mass can be expressed as $-\partial/\partial t(\rho A\Delta y) = -\rho\Delta y\ \partial A/\partial t$. The reduction in mass during the interval Δt is $-\rho\Delta y(\partial A/\partial t)\Delta t$. To satisfy conservation of mass, the net mass outflow must be equal to the reduction in mass inside the reach, so that

$$\rho\left(Q + \frac{\partial Q}{\partial y}\Delta y\right)\Delta t - (\rho Q\Delta t + \rho q\Delta t\Delta y) = -\rho\frac{\partial A}{\partial t}\Delta t\Delta y \tag{1}$$

Simplifying, $\partial Q/\partial y = -\partial A/\partial t + q$, or

$$\frac{\partial Q}{\partial y} + \frac{\partial A}{\partial t} - q = 0 \tag{2}$$

22. Equation 2 is the equation of continuity and is the mathematical expression for the law of conservation of mass in open channels.

Momentum equation

23. Conservation of momentum is given by Newton's second law of motion, which states that the rate of change of momentum is equal to the applied force. In Figure 1, the net applied force on the element of volume in the reach Δy is the resultant of the pressure, gravity, shear forces, and form drag on the element. The water depth is h at Section 1 and $h + \partial h/\partial y\Delta y$ at Section 2. The cross-sectional area is A at Section 1 and $A + \partial A/\partial y\Delta y$ at Section 2.

24. The pressure distribution is assumed to be hydrostatic. This assumption is valid if the surface curvature is small and is true of tidal flows. The pressure force at Section 1 acts toward the right, and the pressure force at Section 2 acts toward the left. The net pressure force acts toward the left and is equal to $\rho gA(\partial h/\partial y)\Delta y$.

25. The gravity force is equal to the weight of the fluid inside the element and is equal to $\rho gA\Delta y$. The component of the gravity force in the direction of motion is $-\rho gA\Delta y(\Delta z_b/\Delta y)$.

26. The possible shear forces consist of bottom stress due to friction and eddy viscosity, and the surface stress. The shear produced by the eddy viscosity is believed to be small and can, in concept, be assumed to be incorporated with the term describing the bottom friction stress, which requires specification of an empirical friction coefficient. The main source of the surface stress is the wind. The bottom stress opposes the motion (directed to the left in Figure 1). The direction of the surface stress produced by the wind depends on the wind direction with respect to the channel alignment. If the bottom shear stress is designated by τ_b, the shear force becomes $\tau_b P\Delta y$. If the surface shear stress is designated by τ_s, then the surface shear force would be $\tau_s B\Delta y$.

27. Form drag results from abrupt changes in the flow area and can be represented in the same manner as a shear stress. The effect of the form drag is conveniently expressed as a transition head loss or an expansion-contraction head loss. It is computed as the product of an empirical coefficient of drag and velocity head difference at the cross section where the abrupt change is located. Values of the coefficient of drag are determined empirically. The basic theory and procedure for describing expansion and contraction losses are discussed under the heading "Minor Losses" in fluid mechanics books. The transition head loss is expressed as $gAS_e\Delta y$, where S_e is the rate of head loss with longitudinal distance y and will be discussed in more detail in the following paragraphs.

28. The momentum inside the volume element is ρAv or ρQ. The momentum inflow rate to the volume element is ρQv. The rate of change of convective (spatial) momentum is given as,

$$\frac{\partial}{\partial y}(\rho Q v) = \rho v \frac{\partial Q}{\partial y} + \rho Q \frac{\partial v}{\partial y} \tag{3}$$

29. The total rate of change of momentum is the sum of the local and convective changes $\rho \partial Q/\partial t + \rho v \partial Q/\partial y + \rho Q \partial v/\partial y$, or $\rho \partial Q/\partial t + \rho v \partial Q/\partial y + \rho A v \partial v/\partial y$.

30. Application of Newton's second law to the flow through the element of volume can be expressed by Equation 4,

$$\begin{aligned} -\rho g A \frac{\partial z_b}{\partial y} - \tau_b P + \tau_s B - \rho g A \frac{\partial h}{\partial y} - \rho g A S_e \\ = \rho \frac{\partial Q}{\partial t} + \rho v \frac{\partial Q}{\partial y} + \rho A v \frac{\partial v}{\partial y} \end{aligned} \tag{4}$$

Since $h + z_b = z$, the sum of the two terms $-\partial z_b/\partial y$ and $-\partial h/\partial y$ can be replaced by $-\partial z/\partial y$. By dividing all terms by ρA, the equation simplifies to

$$\frac{1}{A}\frac{\partial Q}{\partial t} + \frac{1}{A}\frac{\partial}{\partial y}\left(\frac{Q^2}{A}\right) = -\tau_b \frac{P}{\rho A} + \tau_s \frac{B}{\rho A} - g S_e - g \frac{\partial z}{\partial y} \tag{5}$$

31. Equation 5 is the mathematical expression for the conservation of momentum. The bottom shear stress term $P\tau_b/\rho A$ is commonly replaced by gS_f, where S_f is called the friction slope. Replacing Q by vA, and using the equation of continuity to replace $\partial A/\partial t$ by $-\partial Q/\partial y + q$, Equation 5 may be rewritten as

$$\frac{\partial v}{\partial t} + v \frac{\partial v}{\partial y} = -gS_f - gS_e + g\tau_s \frac{B}{A} - g \frac{\partial z}{\partial y} \tag{6}$$

Equation 6 is which is the standard version of the conservation of momentum in one direction. Although both forms, Equations 5 and 6, can be used for numerical modeling, Equation 5 is more desirable for application to waterways of irregular shape because use of the discharge Q rather than the velocity v as the independent variable preserves the momentum equation in conservative form.

32. Equations 2 and 5 are known as the one-dimensional shallow-water equations or the one-dimensional long-wave equations. The equations are valid if the assumption of a hydrostatic pressure distribution holds. They are

applicable to tidal flow, flows in lakes and reservoirs, river flow, and wave motion where the wavelength is significantly greater than the water depth (hence the terminology "long-wave equations").

Numerical Solution Method

33. Equations 2 and 5 constitute a system of first-order nonlinear partial differential equations of the hyperbolic type. These equations do not have analytical solutions except for certain special cases.

34. Numerical methods for the solution of the equations of unsteady flow have been known since the time of Massau (1889). These solution methods may be classified as either direct or characteristic. In the direct method, the finite-difference representation is based directly on the primary equations. In the characteristic method, the equations are first transformed into the characteristic form, and this form is then used to develop the finite-difference representation. In the direct method, a fixed mesh of points on the time-space plane is commonly employed to identify grid points, that is to say, times and locations at which solutions are to be obtained. In the characteristic method, solutions may be obtained at the intersection of the characteristic curves on the time-space plane or at fixed points of a rectangular mesh by interpolation.

35. Finite-difference numerical solution schemes used in the direct and characteristic methods may be further classified as being either explicit or implicit. In explicit solution methods, the finite-difference equations are usually reduced to linear algebraic equations by some form of approximation from which the unknowns can be individually isolated explicitly, i.e., evaluated directly. In implicit methods, the finite-difference equations are generally expressed as nonlinear algebraic equations from which the unknowns cannot be isolated. Depending on the manner in which derivatives are replaced by finite differences, whether forward, centered, or backward, a variety of numerical methods can be developed.

36. The fixed-mesh explicit method is the first and well-known numerical method for the solution of the equations of unsteady flow. It was developed by Stoker (1957) and colleagues and applied to river flow problems. The method is subject to a stringent stability condition that imposes a

limiting value on the size of the time step in relation to the space step. The method of characteristics employing a characteristic network was applied to flood flows by Amein (1966) and Fletcher and Hamilton (1967). Baltzer and Lai (1968) applied the fixed-mesh method of characteristics to tidal flows in estuaries. The impetus for the development of an implicit method was the need for accurate and flexible solution methods that could allow use of large time steps, thereby shortening the computation time.

37. Implicit schemes for writing difference equations to represent the partial differential equations and methods for the solution of the resulting difference equations have been introduced by various authors. Thomas (1934) was probably the first to propose an implicit four-point grid. Implicit grid schemes have been proposed by Cunge and Wegner (1964), Preissmann (1971), Isaacson (1966), Lai (1967), Liggett and Woolhiser (1967), Abbott and Ionescu (1967), and others. A double-sweep method is described by Strelkoff (1970). Most of the earlier methods introduced some form of linearization to the finite-difference equations and devised schemes to avoid simultaneous solution of algebraic equations. Isaacson (1966) used a finite-difference scheme centered both in time and space in the study of the dam-break problem. The nonlinear algebraic equations were solved by Newton iteration.

38. Amein (1968) presented an implicit solution method employing centered finite-differences for the numerical simulation of flood flows. The nonlinear algebraic equations were solved by generalization of the Newton iteration method. Although the procedure requires solution of a large system of simultaneous equations, by taking advantage of the sparseness and bandedness of the coefficient matrix, a rapidly convergent and very accurate solution method was developed. The method was extended to natural and irregular channels by Amein and Fang (1970), to power plant transients and reservoirs by Amein and Chu (1975), and to a tidal inlet network by Amein (1975).

39. The two main technical objectives of the present study are to further extend the implicit solution method of Amein (1972, 1975) to realize a practical numerical model for analyzing tidal inlet flows and to demonstrate the validity of the model. Newly added features of the model developed in this study include:

a. Allowing variable bottom elevations and friction coefficients at user-specified locations across channel cross sections.

b. Computation of a variable velocity field across the cross section.

c. Optimization of the computational procedure by employing a banded matrix solver in channel networks.

d. Generalization of external and internal boundary conditions so that a variety of channel networks can be described.

e. Graphic display of the velocity field and stage

40. The model presented in this study, DYNLET1, is very efficient and unconditionally stable, permitting use of large time steps; it allows flexible grid spacing and grid numbering in the lateral and longitudinal directions. The model also provides detailed two-dimensional velocity field information in a system of interconnecting channels (each channel comprising a one-dimensional calculation element) of different orientations. These channels can represent actual channels, such as inlet throats, and bays. Thus, the velocity at locations (called stations) that can be spaced irregularly across the channel as governed by depth, roughness, and other physical processes entering the full shallow-water equation set can be calculated. Locations of stations along the particular cross section can be arbitrary, allowing the velocity and stage at physically important locations of interest to be readily obtained. The only capability lacking in DYNLET1 in comparison to complete two-dimensional models is that flow directions are constrained to be along the specified channel axis.

PART III: DYNLET1 NUMERICAL SOLUTION PROCEDURE

Model Setup

41. Summarizing from the derivation given in the previous chapter and replacing the velocity v by Q/A, the one-dimensional shallow-water equations for application to tidal inlets are

$$\frac{\partial Q}{\partial y} + \frac{\partial A}{\partial t} - q = 0 \tag{7}$$

$$\frac{\partial Q}{\partial t} + \frac{\partial}{\partial y}\left(\frac{Q^2}{A}\right) = -gAS_f + \frac{B\tau_s}{\rho} - gAS_e - gA\frac{\partial z}{\partial y} \tag{8}$$

42. The procedure for developing a numerical model based on Equations 7 and 8 is described in this chapter. The space coordinate y and the time coordinate t are selected as the independent variables; Q and z are selected as the primary dependent variables. Other dependent variables, consisting of A, B, and P, are functions of z, and S_f and S_e are functions of both Q and z. If values of the average velocity v are desired, they are calculated from Q and A. Values of the surface shear stress τ_s are functions of t only. Therefore, the numerical model solves Equations 7 and 8 for values of z and Q as functions of y and t. Once z and Q are known, the other dependent variables can be readily calculated.

43. Application of DYNLET1 will be illustrated for a system of five interconnecting channels meeting at two junctions, as shown in Figure 3. The term channel is used in a broad sense to denote any body of water that conveys flow along its length regardless of its width. More complex systems may have more channels and junctions (locations where channels meet) than shown in Figure 3. Each channel must have a beginning node and an end node. An initial flow direction to define the beginning and end of each channel is assumed as indicated by arrows. A channel may have any number of nodes, the nodes being locations at which cross-sectional data are given or are measured in the field.

44. In Figure 3, Nodes 1, 12, 20, and 26 are external nodes (nodes at which data are introduced to drive the model). Nodes 6, 7, and 13 are

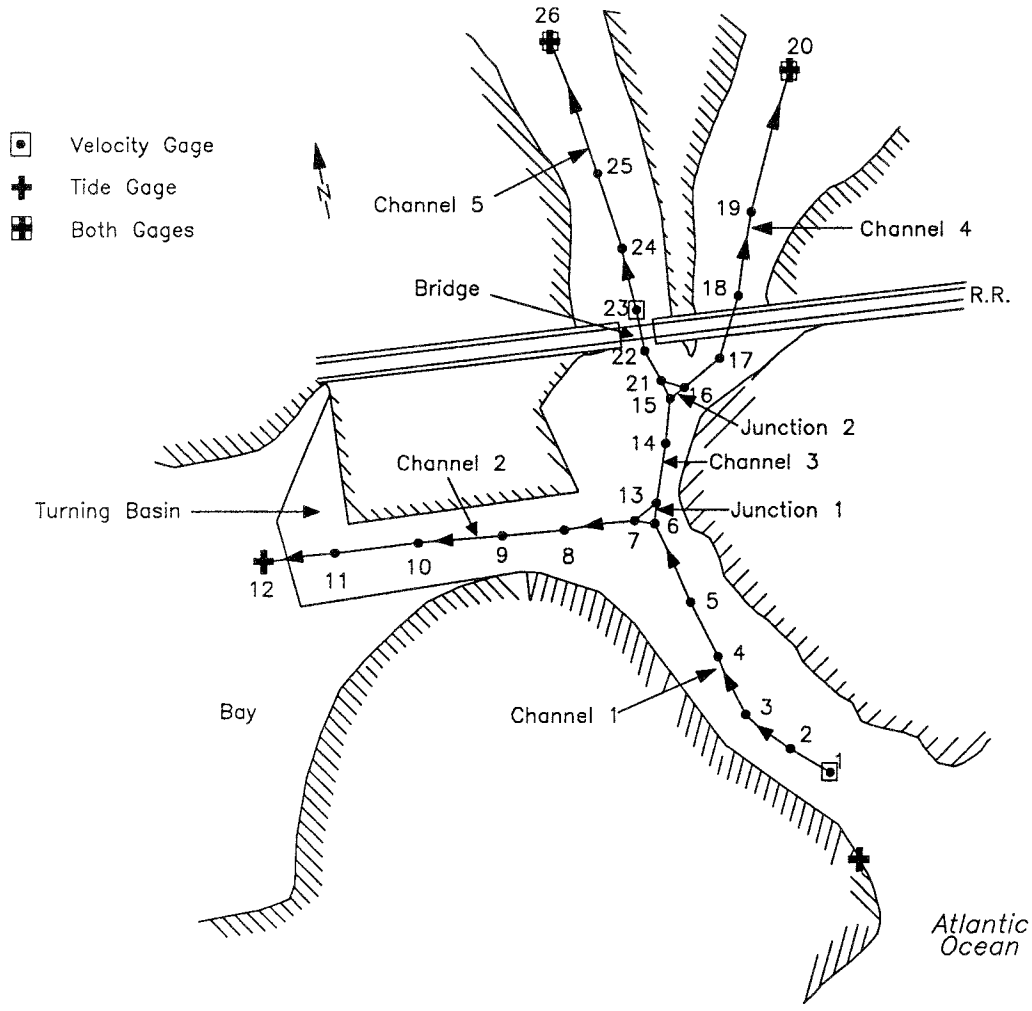

Figure 3. Definition sketch for inlet channel network (modeled after Moorhead Harbor, North Carolina)

junction nodes at Junction 1, and Nodes 15, 16, and 21 are junction nodes at Junction 2. Channel 1 has six nodes beginning at the sea boundary at Node 1 and ending at Junction 1. Channel 2 has six nodes beginning at Node 7 at Junction 1 and ending at Node 12 in the bay. Channel 2 was terminated at Node 12 because a tide gage was located at this node, making it convenient to use as an external boundary condition (a node at which data are introduced to drive the model). Node 7 becomes an internal boundary node because it defines the boundary of Channel 2, but is in the interior of the inlet system. The number of nodes of each channel, and their relationship to the junctions and

boundary nodes, can be readily determined from a sketch such as Figure 3, which needs to be prepared based on physical features, particularly depth changes, changes in channel width, and inferred flow direction.

45. The purpose of DYNLET1 is to determine values of flow properties at all points in each channel. Selecting the flow rate or discharge Q and the water surface elevation z as the basic flow variables, each node has two unknowns, the values of Q and z. If there are N nodes in the inlet system, the total of number of unknowns is $2N$. Therefore, $2N$ equations are needed to determine the values of the $2N$ basic unknowns. These equations are obtained from three sources:

a. Application of the shallow-water equations to the interior points of each channel.

b. External boundary conditions.

c. Junction conditions.

46. It follows that development of a numerical model based on the one-dimensional shallow-water equations for a complex inlet system consisting of interconnecting channels and bays requires three types of information:

a. Identification of interior points.

b. Specification of external boundary conditions.

c. Specification of junction conditions.

Interior points

47. The component of the numerical model involving interior points of each channel is obtained by replacing the partial derivatives in Equations 7 and 8 with finite-difference representations. Using a nonuniform rectangular grid on the y - t plane, as shown in Figure 4, distances along a channel are represented by abscissas, and times are represented by ordinates. Values of a function α and its derivatives at a point $M(i + 1/2,\ j + \theta\Delta t)$ can be written as

$$\alpha(M) = \frac{1}{2}\left[\alpha(i+1, j+1) + \alpha(i, j+1)\right]\theta + \frac{1}{2}\left[\alpha(i+1, j) + \alpha(i, j)\right](1-\theta) \tag{9}$$

$$\frac{\partial\alpha(M)}{\partial t} = \frac{1}{2}\left\{\left[\alpha(i+1, j+1) + \alpha(i, j+1)\right] - \left(\alpha(i+1, j) + \alpha(i, j)\right]\right\}\frac{1}{\Delta t} \tag{10}$$

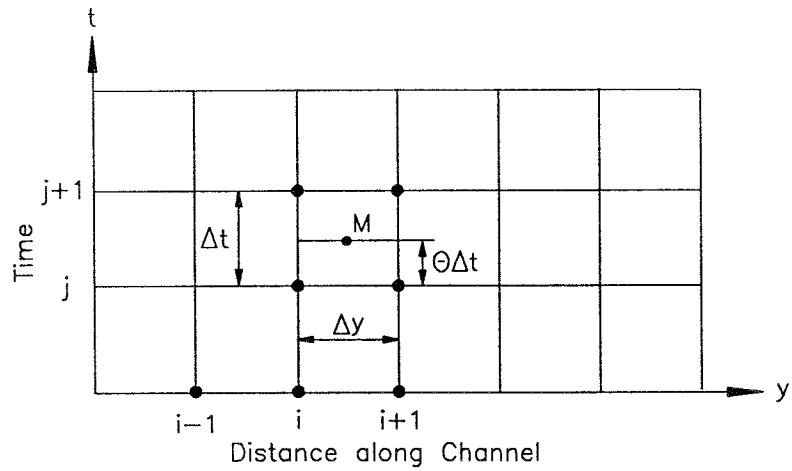

Figure 4. Computation grid on the y - t plane

and

$$\frac{\partial \alpha(M)}{\partial y} = [\alpha(i+1,j+1) - \alpha(i,j+1)]\theta\frac{1}{\Delta y} + [\alpha(i+1,j) - \alpha(i,j)](1-\theta)\frac{1}{\Delta y} \tag{11}$$

where θ is a temporal weighting factor, $\Delta y = y_{i+1} - y_i$, and $\Delta t = t^{j+1} - t^j$.

48. The weighting factor θ determines the type (as explicit or implicit) and stability of the numerical method, and its value ranges from 0 to 1. For $\theta = 0$, the numerical solution scheme is explicit; with $\theta = 0.5$, the numerical solution scheme becomes implicit centered in time; and $\theta = 1$ produces a fully implicit scheme forward differenced in time.

49. If the variables and their derivatives in Equations 6 and 8 are replaced with their equivalent finite-difference representations, then, at each point M contained between sections i and $i+1$ and time steps j and $j+1$, two algebraic equations representing the differential Equations 7 and 8 can be written.

50. The equation of continuity, Equation 7, is replaced by Equation 12, and the finite-difference representation of the equation of conservation of momentum (Equation 8) is written as Equation 13.

$$(Q_{i+1}^{j+1} - Q_i^{j+1})\theta + (Q_{i+1}^{j} - Q_i^{j})(1-\theta) + \frac{\Delta y}{\Delta t}\left[A_{i+1/2}^{j+1} - A_{i+1/2}^{j}\right] - \Delta y\, q_{i+1/2}^{j+1} = 0 \tag{12}$$

$$\begin{aligned}
Q_{i+1/2}^{j+1} - Q_{i+1/2}^{j} &+ \frac{\Delta t}{\Delta y}\left[\frac{(Q_{i+1}^{j+1})^2}{A_{i+1}^{j+1}} - \frac{(Q_i^{j+1})^2}{A_i^{j+1}}\right]\theta \\
&+ \frac{\Delta t}{\Delta y}\left[\frac{(Q_{i+1}^{j})^2}{A_{i+1}^{j}} - \frac{(Q_i^{j})^2}{A_i^{j}}\right](1-\theta) \\
&+ g\frac{\Delta t}{\Delta y} A_{i+1/2}^{j+1}(z_{i+1}^{j+1} - z_i^{j+1})\theta \\
&+ g\frac{\Delta t}{\Delta y} A_{i+1/2}^{j}(z_{i+1}^{j} - z_i^{j})(1-\theta) \\
&+ g\Delta t\, A_{i+\frac{1}{2}}^{j+1} S_{f_{i+\frac{1}{2}}}^{j+1}\theta + g\Delta t\, A_{i+\frac{1}{2}}^{j} S_{f_{i+\frac{1}{2}}}^{j}(1-\theta) \\
&+ g\Delta t\, A_{i+\frac{1}{2}}^{j+1} S_{e_{i+\frac{1}{2}}}^{j+1}\theta + g\Delta t\, A_{i+\frac{1}{2}}^{j} S_{e_{i+\frac{1}{2}}}^{j}(1-\theta) \\
&- g\Delta t\, \tau_{s_{i+\frac{1}{2}}}^{j+1} B_{i+\frac{1}{2}}^{j+1}\theta - g\Delta t\, \tau_{s_{i+\frac{1}{2}}}^{j} B_{i+\frac{1}{2}}(1-\theta) = 0
\end{aligned} \tag{13}$$

51. In the above equations, the value of a variable $\alpha_{(i+1/2)}$ is,

$$\alpha_{i+\frac{1}{2}} = \frac{1}{y_{i+1} - y_i}\int_{y_i}^{y_{i+1}} \alpha(y,t)\,dy \tag{14}$$

where α represents any of the variables τ_b, τ_s, A, Q, etc. A good approximation for $\alpha_{(i+1/2)}$ is

$$\alpha_{i+\frac{1}{2}} \approx \frac{1}{2}(\alpha_i + \alpha_{i+1}) \tag{15}$$

52. In Equations 12 and 13, all variables with superscripts j are known, whereas all variables with superscript $(j+1)$ are unknown. However, all the unknowns are not independent because the water cross-sectional area and the top width of the channel are functions of the water surface elevation at grid points $(i,j+1)$ and $(i+1,j+1)$. It should also be noted that the distance increment Δy and the time increment Δt need not be constants in the solution scheme and in DYNLET1.

53. Equations 12 and 13 constitute a system of two nonlinear algebraic equations in four unknowns: $z(i,j+1)$, $z(i+1,j)$, $Q(i,j+1)$, and $Q(i+1,j+1)$. By themselves, these two equations are not sufficient to evaluate all unknowns at points $(i,j+1)$ and $(i+1,j+1)$. Let $N1$ be the number of nodes in Channel 1. However, the unknowns are common to any two neighboring cells. Because there are $N1-1$ cells between rows j and $j+1$ in Channel 1, two equations such as Equations 12 and 13 can be written for each cell. The combination of all cells provide $2(N1-1)$ equations for the evaluation of $2N1$ unknowns. For a single channel, two additional equations are needed to determine all the unknowns, and they are provided by the external boundary conditions. For networks consisting of interconnecting channels, each individual channel will lack two additional equations. The additional equations are provided by external boundary conditions where the channel meets the bay or the sea, and by junction conditions where two or more channels meet.

External boundary conditions

54. In the inlet system shown in Figure 3, Node 1 of Channel 1 is an external boundary node because it is not connected to another channel. End nodes of Channels 4 and 5 are also external boundaries. If the water surface elevation at an external boundary is known as a function of time, then

$$z_{ib}^{j+1} - (z')_{ib}^{j+1} = 0 \tag{16}$$

where $(z')_{ib}^{j+1}$ is the known water surface elevation at the external boundary node ib at time step $j+1$, and Equation 16 becomes available as one of the supplementary equations. If the discharge is available at the external boundary ib, then

$$Q_{ib}^{j+1} - (Q')_{ib}^{j+1} = 0 \tag{17}$$

where $(Q')_{ib}^{j+1}$ is the known discharge at the external boundary ib at time step $j+1$, and Equation 17 becomes available as an alternative supplementary equation provided by the external boundary.

55. Other types of permitted boundary conditions providing the necessary equations could be an equation expressing the discharge as a function of water surface elevation, as in a weir or jetty, or an analytical expression specifying water surface elevation or velocity as functions of time. In a single channel, for any physical situation two supplementary equations such as

Equations 16 and 17 can be obtained. For channel networks, the boundary equations for all channels are assembled together with the equations for the interior points and for junctions.

Junction conditions

56. A junction is created if two or more channels meet. A two-channel junction is not necessary because the two channels may combine into a single channel. Therefore, attention will be focused on three-channel confluence or a three-node junction. In Figure 3, the end node of Channel 1 and the beginning nodes of Channel 2 and Channel 3 constitute a junction. A three-node junction provides three equations for the inlet system on the basis of conservation of mass and continuity of the water surface.

57. Conservation of mass equation applied at Junction 1 in Figure 3 can be written as Equation 18,

$$Q_1 - Q_2 - Q_3 = 0 \tag{18}$$

where

Q_1 = flow rate at Node 1

Q_2 = flow rate at Node 2

Q_3 = flow rate at Node 3

58. In general, at a junction with nodes k, l, and m, conservation of mass may be written as

$$(Q_k^{j+1} + Q_l^{j+1} + Q_m^{j+1}) = 0 \tag{19}$$

59. An independent boundary condition at the junction may be obtained from the continuity of the water surface. This condition can be expressed as,

$$z_1 = z_2 = z_3 \tag{20}$$

60. In general, for a junction with node numbers k, l, and m, the continuity of the water surface may be expressed as

$$\begin{aligned} z_k^{j+1} - z_l^{j+1} &= 0 \\ z_k^{j+1} - z_m^{j+1} &= 0 \end{aligned} \tag{21}$$

Solution of the Finite-Difference Equations

61. The finite-difference equations based on the shallow-water equations as given by the system of Equations 12 and 13, together with the boundary conditions given by Equations 16 and 17 and the junction conditions given by Equations 19 and 21, constitute a system of *2N* nonlinear algebraic equations in *2N* unknowns, where *N* is the total number of nodes. In this system of equations, the values of the variables at time step t^j are known and may be treated as constants. The unknowns consist of all the variables with superscript *(j+1)*. Because the number of equations is equal to the number of unknowns, the system is determinate.

62. For convenience, let the entire system of finite-difference equations, consisting of the external boundary conditions, interior nodes, and junction conditions, be represented by the system of Equations 22.

$$
\begin{aligned}
F_1 \; (z_1^{j+1}, Q_1^{j+1}, z_2^{j+1}, Q_2^{j+1}) &= 0 \\
F_2 \; (z_1^{j+1}, Q_1^{j+1}, z_2^{j+1}, Q_2^{j+1}) &= 0 \\
\\
F_{2i-1} \; (z_i^{j+1}, Q_i^{j+1}, z_{i+1}^{j+1}, Q_{i+1}^{j+1}) &= 0 \\
F_{2i} \; (z_i^{j+1}, Q_i^{j+1}, z_{i+1}^{j+1}, Q_{i+1}^{j+1}) &= 0 \\
\\
F_{2N-1} \; (z_{2N-1}^{j+1}, Q_{2N-1}^{j+1}, z_{2N}^{j+1}, Q_{2N}^{j+1}) &= 0 \\
F_{2N} \; (z_{2N-1}^{j+1}, Q_{2N-1}^{j+1}, z_{2N}^{j+1}, Q_{2N}^{j+1}) &= 0
\end{aligned}
\tag{22}
$$

63. Routine methods for the solution of nonlinear systems do not exist. For the present model, the generalized Newton iteration method is applied to solve the nonlinear equations. The equation system involves *2N* unknowns, but each equation contains a maximum of four unknowns, which can be of great advantage in devising efficient computational schemes.

64. Let R^k_{2i-1} and R^k_{2i} be the residual at the kth cycle of the system of Equations 12 and 13 corresponding to F_{2i-1} and F_{2i}. Then, according to the generalized Newton iteration method, the residuals and partial derivatives are

related by the system of Equations 23, with all the partial derivatives evaluated at the kth iteration cycle,

$$\frac{\partial F_1}{\partial z_1} dz_1 + \frac{\partial F_1}{\partial Q_1} dQ_1 + \frac{\partial F_1}{\partial z_2} dz_2 + \frac{\partial F_1}{\partial Q_2} dQ_2 = -R_1^k$$

$$\frac{\partial F_2}{\partial z_1} dz_1 + \frac{\partial F_2}{\partial Q_1} dQ_1 + \frac{\partial F_2}{\partial z_2} dz_2 + \frac{\partial F_2}{\partial Q_2} dQ_2 = -R_2^k$$

$$\frac{\partial F_{2i-1}}{\partial z_i} dz_i + \frac{\partial F_{2i-1}}{\partial Q_i} dQ_i + \frac{\partial F_{2i-1}}{\partial z_{i+1}} dz_{i+1} + \frac{\partial F_{2i-1}}{\partial Q_{i+1}} dQ_{i+1} = -R_{2i-1}^k$$

$$\frac{\partial F_{2i}}{\partial z_i} dz_i + \frac{\partial F_{2i}}{\partial Q_i} dQ_i + \frac{\partial F_{2i}}{\partial z_{i+1}} dz_{i+1} + \frac{\partial F_{2i}}{\partial Q_{i+1}} dQ_{i+1} = -R_{2i}^k \tag{23}$$

$$\frac{\partial F_{2N-1}}{\partial z_{N-1}} dz_{N-1} + \frac{\partial F_{2N-1}}{\partial Q_{N-1}} dQ_{N-1} + \frac{\partial F_{2N-1}}{\partial z_N} dz_N + \frac{\partial F_{2N-1}}{\partial Q_N} dQ_N = -R_{2N-1}^k$$

$$\frac{\partial F_{2N}}{\partial z_N} dz_N + \frac{\partial F_{2N}}{\partial Q_N} dQ_N = -R_{2N}^k$$

The values of dz_1, dQ_1,.., dz_i, dQ_i,..., dz_N, dQ_N are defined in the system of Equations 24,

$$dz_1 = z_1^{k+1} - z_1^k$$
$$dQ_1 = Q_1^{k+1} - Q_1^k$$

$$dz_i = z_i^{k+1} - z_i^k$$
$$dQ_i = Q_i^{k+1} - Q_i^k \tag{24}$$

$$dz_N = z_N^{k+1} - z_N^k$$
$$dQ_N = Q_N^{k+1} - Q_N^k$$

The solution of the system of Equations 22, which consists of the equations for interior points, together with the equations arising from the external boundary conditions and junctions, will provide values of z_1^{k+1}, Q_1^{k+1},..., z_i^{k+1}, Q_i^{k+1},...,z_N^{k+1}, i.e., values of the variables at the kth iteration cycle. The procedure can be repeated as many times as required until the difference between the values of any variable in two consecutive iteration cycles falls

below a specified tolerance value. The values of the variables found in the terminal iteration cycle will be taken as the values of the variables for the time step $j+1$, and the computation will be advanced to time step $j+2$.

65. A significant feature of the system of Equations 22 is that the matrix of coefficients has a maximum of four non-zero elements in any row, because each equation involves at most four of the $2N$ unknowns. For a single channel, the non-zero elements are banded around the main diagonal, giving a band width of five. For multiple channels, the matrix band width is greater and depends on the node numbering scheme. Nevertheless, the matrix will be sparse and banded around the main diagonal. Band width can and should be minimized by numbering nodes to minimize the differences between any two junction node numbers. This property of the linear system can be used to great advantage in devising an efficient solution method, and such a method has been implemented in DYNLET1.

66. Application of the Newton iteration procedure requires evaluation of the coefficients of the linear system. The coefficients are the values of the partial derivatives of the function F at each cycle of iteration. The evaluation of the partial derivatives of the nonlinear algebraic system will be considered in three parts: interior points, external boundary conditions, and junction conditions.

Interior equations

67. The finite-difference equations arising from application of the shallow-water equations to a channel segment located between nodes i and $i+1$ will be numbered F_{2i-1} and F_{2i}, and are given as:

$$\begin{aligned} F_{2i-1}(z_i^k,\ Q_i^k,\ z_{i+1}^k,\ Q_{1+i}^k) &= R_{2i-1}^k \\ F_{2i}(z_i^k,\ Q_i^k,\ z_{i+1}^k,\ Q_{i+1}^k) &= R_{2i}^k \end{aligned} \tag{25}$$

$$\begin{aligned} &F_{2i-1}\ (z_i, Q_i, z_{i+1}, Q_{i+1}) \\ &\quad = (Q_{i+1} - Q_i)\theta + \frac{\Delta y}{\Delta t} A_{i+\frac{1}{2}} + C_1 - q_i^{j+1}\Delta y \end{aligned} \tag{26}$$

$$
\begin{aligned}
&F_{2i}(z_i,\ Q_i,\ z_{i+1},\ Q_{i+1}) \\
&= (Q_{i+\frac{1}{2}}) + \theta\ \frac{\Delta t}{\Delta y}\left[\frac{(Q_{i+1})^2}{A_{i+1}} - \frac{(Q_i)^2}{A_i}\right] \\
&\quad - g\frac{\Delta t}{\Delta y}\ A_{i+\frac{1}{2}}(z_{i+1} - z_i)\theta \\
&-g\Delta t\left[A_{i+\frac{1}{2}}\left(S_{f_{i+\frac{1}{2}}} + S_{e_{i+\frac{1}{2}}}\right) - \tau_{s_{i+\frac{1}{2}}}B_{i+\frac{1}{2}}\right]\theta + C_2
\end{aligned}
\tag{27}
$$

The function F_{2i-1} is the finite-difference representation of the equation of continuity, given as Equation 12, and F_{2i} is the finite-difference representation of the equation for conservation of momentum, given as Equation 13. Therefore, from Equations 12 and 13 the values of F_{2i-1} and F_{2i} are given as Equations 26 and 27, where C_1 and C_2 are constants whose values depend on the values of the variables on row t^j. In Equations 26 and 27, the superscripts have been omitted because all subscripted variables now belong to row t^{j+1}. The partial derivatives of Equations 26 and 27 with respect to the independent variables are given below:

$$\frac{\partial F_{2i-1}}{\partial z_i} = \frac{1}{2}\ \frac{\Delta y}{\Delta t}\ B_i \tag{28}$$

$$\frac{\partial F_{2i-1}}{\partial z_{i+1}} = \frac{1}{2}\frac{\Delta y}{\Delta t}B_{i+1} \tag{29}$$

$$\frac{\partial F_{2i-1}}{\partial Q_i} = -\ \theta \tag{30}$$

$$\frac{\partial F_{2i-1}}{\partial Q_{i+1}} = \theta \tag{31}$$

$$\frac{\partial F_{2i}}{\partial z_i} = \frac{\Delta t}{\Delta y}\left(\frac{Q_i}{A_i}\right)^2 B_i\theta$$

$$- g\,\frac{\Delta t}{\Delta y}\,A_{i+\frac{1}{2}}\theta$$

$$+ \frac{g}{2}\,\frac{\Delta t}{\Delta y}\,(z_{i+1} - z_i)\,B_i\theta$$

$$+ g\Delta t\theta\,\frac{\partial\left(A_{i+\frac{1}{2}}S_{f_{i+\frac{1}{2}}}\right)}{\partial z_i} + g\Delta t\theta\,\frac{\partial\left(A_{i-\frac{1}{2}}S_{e_{i-\frac{1}{2}}}\right)}{\partial z_i} \tag{32}$$

$$-g\Delta t\tau_{s_{i+\frac{1}{2}}}\frac{\partial B_i}{\partial z_i}\theta$$

$$\frac{\partial F_{2i}}{\partial z_{i+1}} = -\frac{\Delta t}{\Delta y}\left(\frac{Q_{i+1}}{A_{i+1}}\right)^2 B_{i+1}\theta + g\frac{\Delta t}{\Delta y}A_{i+\frac{1}{2}}\theta$$

$$+ \frac{g}{2}\,\frac{\Delta t}{\Delta y}\,(z_{i+1} - z_i)\,B_{i+1}\theta$$

$$+ g\Delta t\,\frac{\partial\left(A_{i+\frac{1}{2}}S_{f_{i+\frac{1}{2}}}\right)}{\partial z_{i+1}}\theta + g\Delta t\,\frac{\partial\left(A_{i+\frac{1}{2}}S_{e_{i+\frac{1}{2}}}\right)}{\partial z_{i+1}}\theta \tag{33}$$

$$- \frac{g}{2}\,\Delta t\tau_{s_{i+\frac{1}{2}}}\frac{\partial B_{i+1}}{\partial z_{i+1}}\theta$$

$$\frac{\partial F_{2i}}{\partial Q_i} = \frac{1}{2} - 2\,\frac{\Delta t}{\Delta y}\,\frac{Q_i}{A_i}\,\theta + g\,\frac{\Delta t}{2}\,A_{i+\frac{1}{2}}\left(\frac{\partial S_{f_i}}{\partial Q_i} + \frac{\partial S_{e_i}}{\partial Q_i}\right)\theta \tag{34}$$

$$\frac{\partial F_{2i}}{\partial Q_{i+1}} = \frac{1}{2} + 2\,\frac{\Delta t}{\Delta y}\,\frac{Q_{i+1}}{A_{i+1}}\,\theta + g\,\frac{\Delta t}{2}\,A_{i+\frac{1}{2}}\left(\frac{\partial S_{f_{i+1}}}{\partial Q_{i+1}} + \frac{\partial S_{e_i}}{\partial Q_{i+1}}\right)\theta \tag{35}$$

External boundaries

68. If the external boundary is given as the value of the water surface elevation at the beginning node of a channel, Equation 16 applies. The boundary Equation 16 is denoted F_{2i-1}, and its partial derivative is given as,

$$\frac{\partial F_{2i-1}}{\partial z_i} = 1 \tag{36}$$

where i is the boundary node number.

69. If the external boundary is given as the value of the flow rate at the end node i of a channel, the corresponding boundary equation is Equation 17, which is denoted as F_{2i}, and its partial derivative is given as

$$\frac{\partial F_{2i}}{\partial Q_i} = 1 \tag{37}$$

Junction conditions

70. The junction conditions for a three-node junction are given by Equations 19 and 21. Assuming junction node k to be the end node of a channel and junctions l and m to be the beginning nodes of a channel, then the three junction equations are numbered as given in the system of Equations 38,

$$\begin{aligned} F_{2k} &= Q_k - Q_l - Q_m \\ F_{2k-1} &= z_k - z_l \\ F_{2m-1} &= z_m - z_k \end{aligned} \tag{38}$$

71. The partial derivatives of the junction equations are given in the system of Equations 39.

$$\begin{aligned} \frac{\partial F_{2k}}{\partial Q_k} &= 1 \\ \frac{\partial F_{2k}}{\partial Q_l} &= -1 \\ \frac{\partial F_{2k}}{\partial Q_m} &= -1 \\ \frac{\partial F_{2l-1}}{\partial z_k} &= 1 \\ \frac{\partial F_{2l-1}}{\partial z_l} &= -1 \\ \frac{\partial F_{2m-1}}{\partial z_m} &= 1 \\ \frac{\partial F_{2m-1}}{\partial z_k} &= -1 \end{aligned} \tag{39}$$

Evaluation of shear stress terms

72. In the preceding sections, the friction slope was represented as S_f, and the surface shear stress was designated as τ_s. The most commonly used relation for computation of the bottom shear stress is Manning's formula. According to this formula, if a channel of complex shape, consisting of subareas with different roughnesses and depths, is subdivided into M elements, the volume flow rate in the channel is given by Equation 40,

$$Q = K\sqrt{S_f} \tag{40}$$

where

$$K = C\sum_{j=1}^{j=M}\frac{1}{n_j}\,A_j\,R_{h_j}^{2/3} \tag{41}$$

73. In Equation 41, K is known as the conveyance, A_j is the area of element i, R_{hj} is the hydraulic radius of element j, and n_j is the Manning's friction factor of element j. If the composite channel is subdivided into a number of nearly rectangular subchannels, the hydraulic radius of each subchannel would be practically the same as the depth in the subchannel, and the depth in the element can be used as the hydraulic radius.

74. Once the friction formula is selected, the values of the friction slope and its derivatives with respect to the independent variables can be calculated. Using Manning's formula as the friction formula, the value of the friction slope and its derivatives at node i in the numerical model are given in Equations 42 to 44,

$$S_{f_i} = \left(\frac{Q_i}{K_i}\right)^2 \tag{42}$$

$$\frac{\partial S_{f_i}}{\partial z_i} = \frac{Q_i^2}{K_i^3}\,\frac{\partial K_i}{\partial z_i} \tag{43}$$

$$\frac{\partial S_{f_i}}{\partial Q_i} = \frac{2Q_i}{K_i^2} \tag{44}$$

Evaluation of surface shear stress

75. The main source of the surface shear stress is the wind. The shear stress at the water surface produced by the wind is usually computed using the turbulent shear stress formula given as Equation 45, where C_D is the drag coefficient, ρ_a is the density of air, and V_w is the wind speed.

$$\tau_s = C_D \rho_a \frac{V_w^2}{2} \tag{45}$$

A typical value of the drag coefficient is 2×10^{-3} (Hsu 1988).

Evaluation of transition losses

76. Transition loss is the energy loss accompanying sharp expansions or contractions of the flow area and may be expressed as Equation 46, where S_e is the rate of loss with longitudinal distance y, and K_e is an empirical form-drag coefficient. The partial derivatives of the transition loss term with respect to the independent variables are needed in Equations 33 and 34. These derivatives are computed from Equation 46.

$$gAS_e = gAK_e \frac{\partial}{\partial y}\left(\frac{v^2}{2g}\right) \tag{46}$$

A value of $K_e = 0.5$ is recommended as an initial estimate, and K_e should never exceed 1.

77. In DYNLET1, values of the transition loss term S_e between nodes i and $i+1$ and its derivatives with respect to the independent variables are given in Equations 47 to 49,

$$S_{e_i} = K_{e_i}\left|\frac{Q_{i+1}^2}{A_{i+1}^2} - \frac{Q_i^2}{A_i^2}\right|\frac{1}{2g} \tag{47}$$

$$\frac{\partial S_{e_i}}{\partial z_i} = K_{e_i} \frac{Q_i^2 B_i}{gA_i^3} \tag{48}$$

$$\frac{\partial S_{e_i}}{\partial Q_i} = -K_{e_i} \frac{Q_i}{gA_i^2} \tag{49}$$

Evaluation of the cross section velocity field

78. Equation 41 is used to compute the discharge and velocity in each subchannel. The discharge in each subchannel is proportional to the conveyance of the subchannel. Assuming that the cross section has been subdivided into M subchannels and the discharge through the cross section has been calculated, then the discharge dQ_j through subchannel j is calculated by

$$dQ_j = \frac{\frac{1}{n_j} A_j R_{hj}^{\frac{2}{3}}}{K} \tag{50}$$

The average velocity v_j through the subchannel j is computed as

$$v_j = \frac{dQ_j}{A_j} \tag{51}$$

In the present configuration, DYNLET1 can accommodate 50 subchannels in a given cross section.

PART IV: DYNLET1

79. This chapter describes the general structure and operation of the user interface of DYNLET1 and preparations that must be made prior to running the model. DYNLET1 also generates graphs for display on the monitor, for storing in graphics files, and for printing. The graphical display contains plots of cross sections, plots comparing computed and measured velocities and volume flow rates, and plots comparing measured and computed water surface elevations. These plots are not intended to be true report quality graphics; rather, they are provided to facilitate interpretation of the calculations and measurements. Unless otherwise stated, plots shown in this report involving use of DYNLET1 were generated by the modeling system. In the following, focus is on the input and output files comprising the interface.

Preparation to Run DYNLET1

Coordinate system and grid

80. From the characteristics of the flow system, the various channels to comprise the system must be identified. If more than two channels meet or a channel branches into two forks, a junction must be identified. Appropriate locations for the channel cross sections can be determined from a hydrographic map. The distance between any two cross sections is arbitrary, but cross sections should be placed at locations where channel properties (width, depth, etc.) change significantly to represent the flow in regions of physical importance. Cross sections are identified by nodes, a node being a grid point on the chart representing the cross section passing through that grid point. Once locations of the cross sections are known, the number of nodes N, that is, the number of cross sections comprising the inlet system, is defined.

81. For numbering of nodes, an initial flow direction must be assumed to determine where a channel begins and ends. The selection of flow direction is arbitrary, but once it is chosen, it cannot be changed during run time. It is convenient, although not necessary, to assume the initial direction of the flow to be from the sea toward land and to number the nodes in increasing order away from the sea.

82. Nodes in a channel may be numbered starting from any number, provided one of the channels begins with the number *1* and there are no missing numbers. The largest node number will then equal the total number of nodes. Nodes in a channel must be numbered consecutively starting at the beginning node and ending in the end node of the channel. It is standard practice to label the seaward node as node number *1*.

83. System geometry is denoted by x- and y-coordinates. The x-coordinate identifies positions across the channel cross section, and the y-coordinate identifies distances in the longitudinal direction, that is, in the direction of flow. Variable distances x and y provide a realistic representation of the system; for example, closely spaced nodal points are used where significant changes take place in geometric properties. The value of y along a channel increases from the beginning to the end node, and the starting value of y is arbitrary. It is convenient for graphic display, but not necessary, to measure distance from the sea boundary.

General control parameters

84. General control parameters are values controlling operation of DYNLET1 and consist of:

a. Initial time.

b. Termination time.

c. Tolerance values for iteration convergence.

d. Temporal weighting coefficient.

e. Presence of wind.

f. Computation time step.

g. Number of iteration steps.

h. External boundaries.

i. Internal boundaries.

The general control parameters are given in the following.

85. Initial time. An initial time *T0*, conveniently taken as the chronological time of the modeled sequence in decimal hours, must be specified.

86. Termination time. A termination time *Tfin*, also in units of decimal hours, must be specified. The model halts when the termination time is reached. *Tfin* must be greater than *T0*.

87. Tolerance values for iteration convergence. Tolerance values for elevation and discharge determine the number of iterations required for the solution to converge to a certain degree of accuracy. These values should be chosen based on consideration of the inlet geometry. If the cross sections are highly irregular, the computation may not converge in a reasonable number of steps, or not at all if the tolerance values are too small. In this case, DYNLET1 will stop and a message to this effect will be printed on the screen. If the tolerance values are large, the model will finish rapidly, but the accuracy of the solution is lowered. Tolerance values of 0.02 to 0.05 ft* for elevation and 50 to 200 cfs for discharge are reasonable estimates for most inlets.

88. Temporal weighting coefficient. The weighting coefficient θ can vary between 0.5 and 1.0 to define an implicit solution scheme. A weighting coefficient of 0.0 will transform the numerical procedure into an explicit method. However, DYNLET1 has not been tested for weighting coefficients less than 0.5. A value $\theta = 1.0$ is recommended to start a simulation series, and this value is generally recommended for simulations of field conditions. Numerical tests for idealized and severe situations have shown that the value of $\theta = 1.0$ may introduce some damping, whereas $\theta = 0.5$ may introduce oscillations. The damping effect is negligible in realistic tidal flows.

89. Presence of wind. Inclusion of wind in the simulation is regulated by the wind index, which can be either 0 or 1. A value of 0 instructs the model to omit wind shear, but for a wind index of 1, the program needs a coefficient of wind drag to be used in the calculation of surface shear. The drag coefficient, wind speed, and wind direction are specified in data input files.

90. Computation time step. Numerical tests (e.g., Price 1974) of numerical models of the shallow-water wave equations have shown that solution accuracy depends on the size of the computation step. In natural channels,

---

* A table of factors for converting non-SI units of measurement to SI (metric) units is presented on page 4.

comparison with field observations (e.g., Amein and Chu 1975) has demonstrated that the time step can be selected in accordance with the resolution of the available field data. For example, if boundary condition data are provided at hourly intervals, time steps of 1 or 0.5 hr are adequate. The use of small time steps does not improve accuracy of the solution because the resolution in the field data controls the final answer. Because the numerical procedure used in DYNLET1 is implicit, the computation is unconditionally stable, and large time steps are possible. DYNLET1 overrides the time step if it is larger than the interval between two consecutive time-dependent data inputs.

91. A computation time step of the same magnitude as the interval between data inputs is satisfactory. Numerical accuracy is not seriously affected by the time-step size, because accuracy also depends on the tolerance value. For tidal inlets, a computation time step of 1,800 sec is recommended unless the input values are specified at shorter intervals or more frequent outputs are desired.

92. Number of iteration steps. The number of iteration steps executed by the model to reach convergence depends on the tolerance values selected for the variables. For natural channels, convergence is usually attained within three to five iterations. Additional iterations may be required at start-up, where cross-sectional properties vary sharply between cross sections or if there are rapid changes in water surface elevation and flow rate with time. A limit of 20 iteration steps is recommended. If the solution does not converge within a reasonable number of iterations, one of the following situations may be the cause:

a. The time step may be too large for the problem.

b. The tolerance values may be too small for the given physical situation.

c. There is an error in cross-sectional geometrical data, in the friction coefficients, or in the transition loss coefficients.

d. The model fails because it is applied to a physical situation violating the assumptions underlying its development.

93. External boundary conditions. External boundary forcing and the boundary type must be identified. Presently, DYNLET1 accepts four types of external boundary conditions:

a. Type 1. Values of water surface elevation as a function of time are tabulated in the input file.

b. Type 2. Values of velocity as a function of time are tabulated in the input file.

c. Type 3. An equation relating initial bay area, initial elevation in the bay, and elevation in the channel is specified at the boundary.

d. Type 4. Values of discharge as a function of time are tabulated in the input file.

e. Type 5. The water surface elevation as a function of time is described by a formula, e.g., a sine wave. A sine wave requires two parameters, the wave amplitude and the wave period.

94. For every external boundary node, a tabulation of time-dependent input data is needed. Tabulated values are ignored if the boundary type is Type 5, that is, if a formula describes the water surface elevation as a function of time. For boundary Types 1 and 2, values of water surface elevation and velocity as functions of time must be tabulated.

95. In boundary Type 3, an equation involving two parameters is used to relate the flow rate in the inlet channel to the bay water elevation. The parameters are given as values of the variables DESC1 and DESC2 (for example, DESC1 as the bay area and DESC2 as the difference in water surface elevation between the channel and the bay). In many applications involving rivers, discharge data will be available, and this situation is described by a Type 4 boundary condition. In boundary Type 5, values of wave amplitude and wave period are entered as DESC1 and DESC2.

96. Internal boundaries. Internal boundaries are specified at junctions. However, DYNLET1 handles this automatically. The model determines how the junction nodes are located with respect to the channels and applies the conservation of mass and momentum at the nodes.

Nodal parameters

97. Nodal parameters are values of variables assigned to an entire channel cross section and consist of:

a. Reference elevation.

b. Lateral inflow rate.

c. Channel alignment angle.

d. Transition loss coefficients.

e. Initial values of water surface elevation.

f. Initial values of volume flow rate.

98. Reference elevation. The reference elevation z_b is the horizontal datum for specifying water surface elevation and channel geometry. Mean sea level (MSL), mean low water (MLW), National Geodetic Vertical Datum (NGVD), or any other suitable horizontal datum can be chosen as the reference elevation. If MSL is selected as the reference elevation, the water surface elevation z would be the difference in elevation between the water surface and the mean sea level. The aforementioned tidal datums are the most commonly used in practical engineering studies of inlets.

99. Lateral inflow rate. The lateral inflow rate q is the rate at which water enters or leaves the channel at a cross section from the channel banks or bottom by seepage, or enters or leaves the water surface by evaporation or precipitation. Flow from a minor tributary stream can be represented by specifying values of lateral inflow. An examination of the flow records at the two ends of a channel reach can be used to evaluate lateral inflow rate. In the present version of DYNLET1, q can be represented as a different constant value at each node.

100. Channel alignment angles. The channel alignment angle is defined as the angle that the channel axis makes with a reference axis. The reference axis may be, for example, the bottom edge of the hydrographic map for the inlet. The angle is measured counterclockwise from the reference axis and is given in degrees. Values of channel alignment angle must be specified at each node.

101. Transition loss coefficient. The value of the transition loss coefficient K_e, the coefficient assigned to describe turbulent losses caused by flow expansion and contraction, must be specified at all nodes. If these losses are to be omitted, K_e must be set to zero. Such losses must be accounted for to accurately represent turbulent losses produced by sharp channel contractions and expansions, bridge pilings, culverts, etc. A cross section that produces flow contraction during ebb flow will produce flow expansion during flood flow. The maximum values for the contraction coefficient is 0.5, and the maximum value for the expansion coefficient is 1.0. Values of 0.5 for both contraction and expansion coefficients are recommended as initial values in model calibration. For modeling the flow around important structures, such as bridges, it may be necessary to calibrate these coefficients with field data.

102. Initial values of water surface elevation. Values of the water surface elevation must be given at every node at the initial time. These values are obtained from field measurements. For a cold start, a horizontal water surface may be prescribed, best taken as the average measured value if available.

103. Initial values of volume flow rate. Initial values of volume flow rates (discharges) at all nodes must be specified. These values are taken from field measurements. For a cold start, the initial discharges may be set to zero.

Cross-section data

104. Cross-section data provide information on the shape of the inlet and the boundary or perimeter roughness. Cross section data consist of the inlet geometry (bottom elevation, z_b) and bottom friction coefficient (n) at the station of each node.

105. Inlet geometry. Geometric data for the cross section must be obtained from maps or field surveys. The data are recorded as "distances" and "elevations," where distance is an offset from the left bank and elevation is the bottom elevation referred to the reference elevation discussed in paragraph 98.

106. Bottom friction coefficient. Manning's coefficient of friction n is specified at every cross-section data point. These values are estimates obtained from previous studies, experience, and judgment. Textbooks such as Chow (1959) provide guidelines for selecting values of n according to the physical conditions. Typically, a value $n = 0.02$ is used for sand. This value may be increased to 0.025 if the boundary consists of coarse sand. If the inlet channel contains vegetation, an initial value of 0.035 is recommended. Values of the friction coefficient are specified at every data point in the cross section so that in a wide cross section consisting of part sandy bottom and part vegetation, different friction coefficients can be assigned to the sandy and the vegetated parts. Adjustment of the value of n at selected locations is the main calibration procedure for DYNLET1.

Input Files

107. The model DYNLET1 uses four input files, named START.DAT, SECTION.DAT, EXTER.DAT, and PARAM.DAT, and it generates five output files as shown in Figure 5. Examples of input files are given in Appendices A and B for the two examples presented in Parts V and VI. In this section the input files are discussed.

START.DAT

108. As many as 100 comment lines can be placed at the beginning or header of the START.DAT file. Comment lines are identified by an asterisk in Column 1. Titles, identifications, notes, and miscellaneous useful information can be entered in these lines. After the header, the main file consists of data groups, and each data group consists of one or more data sets. A data set consists of a single identifier title line followed by lines of data. As many lines of data as needed may be used. All data are input in free format (irrespective of number of digits or characters, location on line, or spacing

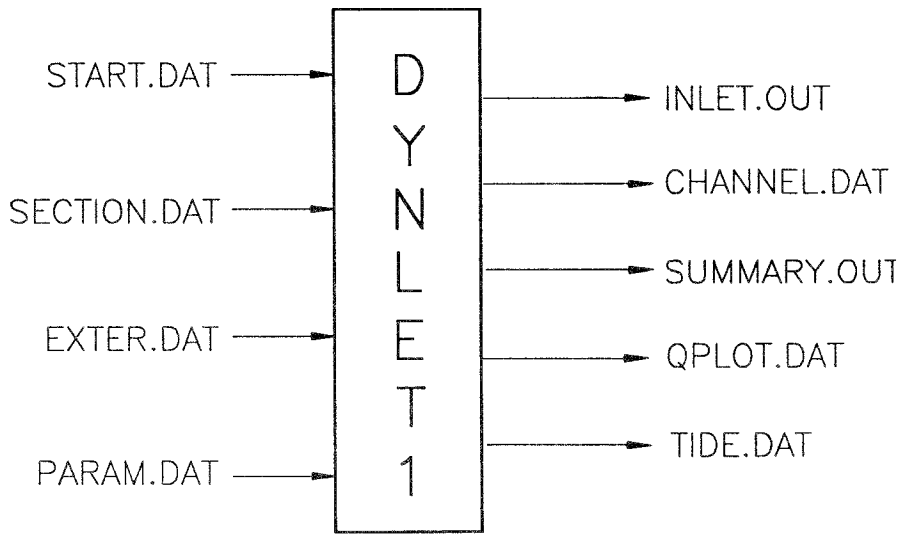

Figure 5. DYNLET1 input and output file structure

between entries on a line), and there is no requirement on the number of items that may be placed on a line.

109. Group A. General parameters

Set A.1: Initial Time, Final Time, Tolerance Value for Elevation in iteration solution convergence, Tolerance Value for Discharge in iteration solution convergence, Weighting Coefficient, Number of Nodes, Wind Index. (Wind Index is a flag for inclusion of wind stress. If Wind Index is 0, wind effects are not considered in the model.)

Data: TO Tfin Zeps Qeps Theta N Iwind

Set A.2: Units

Data: ENGLISH or SI

Set A.3: Units of distance

Data: Feet, Miles, Meters, or Km

110. Group B. Computational Parameters

Set B.1: Computational time step in sec

Data: DTCOM

Set B.2: Maximum number of iterations

Data: ITERN

(If the computations do not converge after the specified number of iterations, the model will stop. A default value of 20 is recommended.)

Set B.3: Number of printout (display) times

Data: NP

Set B.4: Print out times in hours

Data: NPR (list of values of the times)

Set B.5: Number of nodes at which output is desired

Data: NOUTN (one value)

Set B.6: Output nodes

Data: (list of NOUTN values of nodes)

111. Group C. Channel and junction parameters

Set C.1: Number of channels, Number of junctions, Number of external boundary points

Data: NC NJ NBP

Set C.2: Channel number, Beginning node, End node

Data: (list of three numbers)

Set C.3: Junction number, Number of nodes at the junction, Node numbers

Data: (list of numbers)

Set C.4: External boundary point (beginning with 1 and ending with the total number of external boundary points), Node number of the external boundary point, Type of boundary, Optional parameters (DESC1, DESC2) if boundary Type 3 or 4 is selected

Data: (list of numbers)

112. Group D. Nodal parameters

Set D.1: Distances at nodes along the axis of the channel, in the order Node 1 to Node N

Data: DIST (list of N values)

Set D.2: Values of lateral inflow rate at each node

Data: QL (list of N values)

Set D.3: Values of Reference Elevation

Data: Z_b (list of N values)

Set D.4: Values of Channel Alignment Angles (in degrees)

Data: (list of N values)

Set D.5: Transition Loss Coefficients

Data: Ke (list of N values)

Set D.6: Values of Initial water surface elevations

Data: Zin (list of N values)

Set D.7: Values of Initial Discharge

Data: Qin (list of N values)

SECTION.DAT

113. This input file contains detailed information on cross-section geometry and boundary resistance. The cross-section geometry is defined by data points identifying the channel boundary, and each data point is described by pairs of values of distance and elevation. The boundary resistance is defined by the value of the coefficient of friction at each data point. The input data format is described in the following.

114. Group E. Cross-section parameters (Note: The total number of Group E data values is equal to the number of nodes, N.)

Set E.1: Node number, Number of elevation points at the cross section; optional comments

Data: Node Number, NumElev

Set E.2: Distance and Elevation pairs

Data: (NumElev pairs of values)

Set E.3: Manning's Coefficient of Friction

Data: (NumElev values)

EXTER.DAT

115. This file contains time-dependent boundary data for each external boundary node, tabulated as a function of time. Time-dependent data consist of values of velocity or water surface elevation at external boundaries. If wind effects are to be included in the computations, the values of wind speed and direction as a function of time are provided here. Details of the data requirement are described as follows.

116. Group F. Time-dependent data

Set F.1: Index (a counter), Time (hour), values of elevation, discharge, or velocity at external boundary nodes, values of wind speed and direction when IWind has been assigned a value of 1

Data: (list of values)

PARAM.DAT

117. This file specifies nodes and parameters for output files that will be used by auxiliary programs. The auxiliary programs produce graphs and tables for comparing computed outputs to field data, for displays, and for other purposes. Similar to the START.DAT file, the PARAM.DAT file also classifies data into groups of data sets, each data set consisting of a title line identifying the data set, followed by one or more lines of data.

118. Group G. Velocity output is given in this group. The number of Group-G data sets equals the number of nodes (cross-sections) at which output is desired.

Set G.1: Number of velocity measurements (gages) with field data

Data: NumVelG (one value)

If NumVelG is greater than zero continue to G.3

Set G.2: Number of nodes at which output of computed velocity is required

Data: VoutN (one value)

Set G.3: Number of field stations at the velocity gage

Data: NumVelGSt (one value)

If NumVelG is zero, continue to G.5

Set G.4: Names of field stations at the velocity gage NumVelG

Data: (list of names)

Set G.5: Node Number

Data: VelNode (one value)

Set G.6: Number of velocity output stations in this cross section

Data: (one value)

Set G.7: Station numbers for velocity output along the cross section

Data: (list of numbers)

The above procedure for Group G is repeated VoutN times for data Sets G.2 to G.7. If field data are available, the values of VoutN and NumVelG must be the same.

119. Group H. Stage (water surface elevation) is given in this group. The number of Group-H data sets equals the number of nodes (cross sections) at which output is desired.

Set H.1: Number of nodes where elevation output is required

Data: EoutN (one value)

Set H.2: Node number

Data: (one value)

Set H.3: Number of points in the cross section to be plotted

Data: NumEel (one value)

Set H.4: Stations on the cross section where elevation output is desired

Data: (list of NumEel values)

Set H.5: Is a field data set (measurements) available for this node?

Data: "Y" or "N"

If YN = Y, then continue to Set H.6

Set H.6: Number of measurement gages in the cross section

Data: NumGage (one value)

Set H.7: Names of gages

Data: (NumGage alphanumeric words(s))

The above process for Group H is repeated EoutN times for data Sets H.2 to H.7.

temporal acceleration, and pressure gradient at nodes. All values are normalized with respect to the bottom stress so that the strengths of the terms relative to that of the friction term can be evaluated.

QPLOT.DAT

123. This file contains the volume flow rate (discharge) as a function of time at the nodes specified in PARAM.DAT. The file is used by:

a. Program QPLOT to make graphic displays comparing the computed discharge with the measured discharge.

b. Program QPRN to send graphs of the discharge on a printer.

c. Program VPAS to make graphic displays comparing the computed output of velocity at gaging stations with measured velocities.

d. Program VPRN to output graphs of velocity on a printer.

TIDE.DAT

124. This file contains the calculated water surface elevation as a function of time at the nodes specified in PARAM.DAT. The file is used by program HPAS to make graphic displays comparing the computed output of water

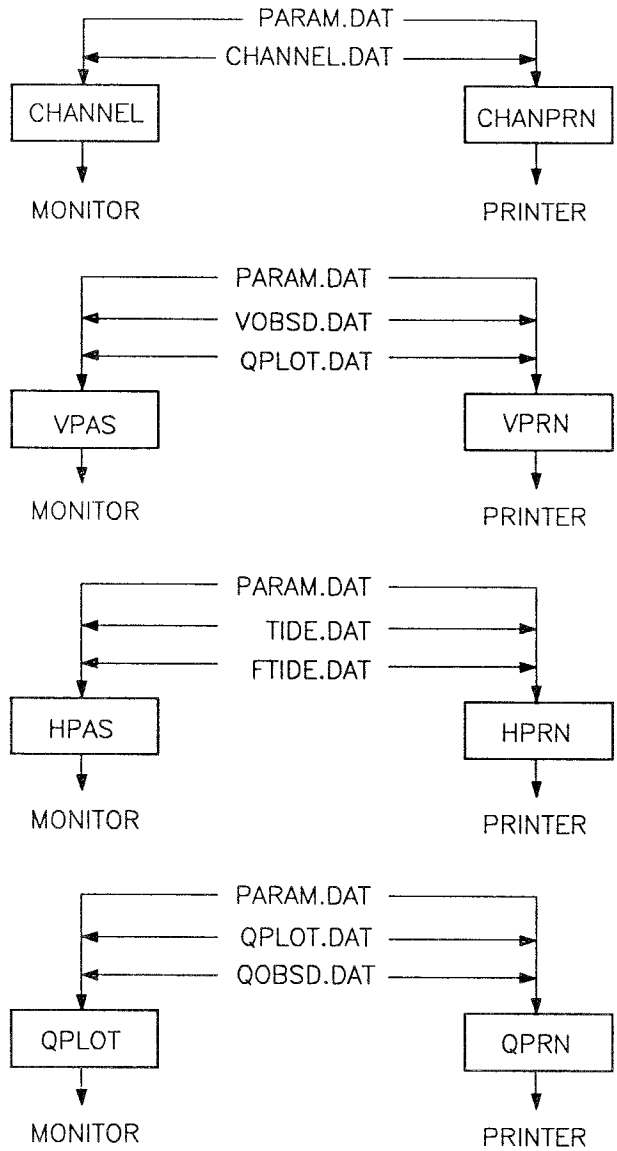

Figure 6. Auxiliary program input and output file structure

surface elevation with measured values. The file is also used by the program HPRN to print graphs for comparing computed and measured water surface elevations.

Auxiliary Programs

125. Several optional special-purpose programs have been developed for characterizing and visualizing the inlet hydrodynamics generated by DYNLET1. Some of the programs compare field measurements with computed values. The auxiliary programs must, therefore, also have input and output files. There are two sources for the input files: files containing field data and files generated by DYNLET1 to provide computed values. Care must be exercised that the number of time steps and the number and location of the nodes in the generated output files match the times and locations in the field data files. Descriptions of the auxiliary programs and their input-output files are given next (see also Figure 6).

CHANNEL and CHANPRN

126. The program CHANNEL determines point-by-point velocities across the channel and displays cross-section geometry and velocities on the monitor. CHANPRN functions similarly by sending user-specified plots to the printer.

Input File: CHANNEL.DAT

Output File: CHANNEL.OUT

QPLOT and QPRN

127. The program QPLOT plots, on the monitor, the computed discharge as a function of time at selected nodes prescribed in PARAM.DAT. If a file named QOBSD.DAT, containing measured values of discharge is available, the program graphs the measured values on the same plot. QPRN functions similarly by sending user-specified plots to a printer.

Input Files: QPLOT.DAT; QOBSD.DAT (measured flow rates)

VPAS and VPRN

128. The program VPAS computes velocities, as a function of time across the channel cross section, at designated points specified in file PARAM.DAT and plots them on the monitor. If a file named VOBSD.DAT containing measured values of velocity is available, the program graphs the measured values on the

same plots. VPRN functions similarly by sending user-specified plots to a printer.

Input Files: CHANNEL.DAT; PARAM.DAT; VOBSD.DAT (measured velocities)

HPAS and HPRN

129. The program HPAS plots water surface elevations as a function of time at nodes specified in file PARAM.DAT against measured values on the screen. If a file named FTIDE.DAT containing measured values of water surface elevation is available, the program graphs the measured values on the same plot. HPRN functions similarly by sending user-specified plots to a printer.

Input Files: TIDE.DAT; PARAM.DAT; FTIDE.DAT (measured tidal elevation)

PART V: EXAMPLE APPLICATION 1: MASONBORO INLET, NORTH CAROLINA

130. The purposes of Parts V and VI, each describing a case study, are to verify DYNLET1 and demonstrate how the model is applied by means of realistic examples. The case study in this chapter, Masonboro Inlet, North Carolina, consists of two tasks: application of DYNLET1 and comparison of results with measurements, and review of simple inlet hydrodynamics models developed in the General Investigation of Tidal Inlets (GITI) program.

131. Masonboro Inlet was the subject of intensive study under the GITI Program (Harris and Bodine 1977) conducted by the USACE and involved both physical and numerical modeling of tidal flow. Three numerical models, a lumped-parameter model (a lumped-parameter model combines major parameters into a single variable), a one-dimensional explicit finite-difference model, and an explicit two-dimensional finite-difference model were evaluated. The finite-difference models (Reid and Bodine 1968, Chen and Hembree 1977) will not be discussed here because they are considered old technology compared with present-day one- and two-dimensional modeling capabilities.

132. The data employed as the test case were field measurements made in September 1969. Masonboro Inlet was also studied under the Sea Grant Program by Amein (1975) employing field data collected in 1974, using a predecessor model to DYNLET1.

Masonboro Inlet

133. The basic features of Masonboro Inlet are shown in Figure 7. The entrance to the inlet from the sea is protected by a jetty. During flood tide, the flow enters Banks Channel to the east, Masonboro Channel to the west, and Shinn Creek to the north. Thus, the system consists of a network of channels, and there is no actual bay.

134. All previous modeling efforts have had difficulty using the September 1969 tidal elevations in the interior inlet channels for boundary conditions. There is an apparent discrepancy in the data; for example, the water level in some channels is consistently lower than the sea during part of the ebb cycle. The source of the discrepancy could be unquantified wind effects, shifts in the reference datum, or some other (unknown) reason.

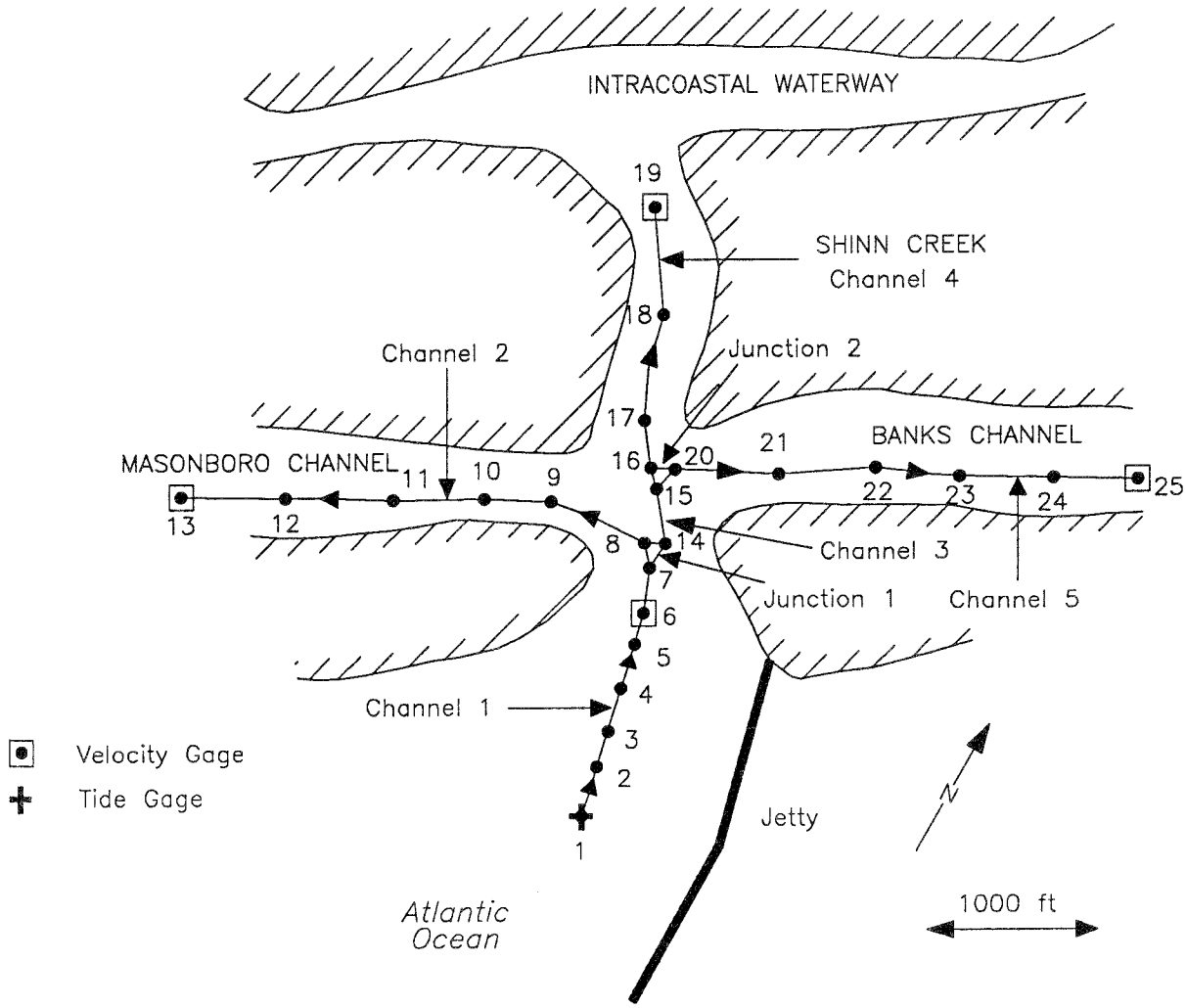

Figure 7. Schematic for Masonboro Inlet model

Modeling efforts that required these water surface elevations as boundary conditions had to make adjustments by manipulating the data or replacing the data by average values from all gages. In the present study, this ambiguity did not enter because the water surface elevation data in the channels were not used to supply boundary conditions, as discussed below.

DYNLET1

135. This section is concerned with the computation of tidal flow through Masonboro Inlet using DYNLET1. An attempt is made to compare the results with results obtained during the GITI studies, and also to perform a comparative analysis of terms in the basic equations by analyzing their relative importance.

DYNLET1 representation

136. Masonboro Inlet is represented in the model by 25 cross sections or nodes in five channels (Figure 7). The channels are numbered from 1 to 5, and there are two junctions numbered 1 and 2. The channels and their cross sections (node numbers) are listed in Table 1.

137. Channels 1, 2, and 3 meet at Junction 1. Channel 2 is a short channel extending from the confluence of the main inlet and Masonboro Channel to the confluence of Banks Channel and Shinn Creek. Junction 1 consists of Nodes 7, 8, and 14, and Junction 2 consists of Nodes 15, 16 and 20.

138. The cross-sectional geometrical data were taken from hydrographic maps, and MLW was used as the reference datum. Values of Manning's coefficient of friction were specified at every cross-section data point. These

Table 1

Channel Cross Sections, Masonboro Inlet

Channel Number	Channel Cross Section From	To
1	1	7
2	8	13
3	14	15
4	17	19
5	20	25

values are reasonable estimates from previous studies and also calibration parameters. As initial values, 0.02 was used everywhere for deeper channels and the inlet throat with sand bottoms, and 0.04 was used everywhere in the interior channel cross-sections with rough boundaries expected because of vegetation. Sensitivity testing showed that these initial values provided adequate results for the purpose of this example; therefore, they were not optimized.

139. At the sea boundary, Node 1, measured values of water surface elevation were specified as a function of time (Type-1 boundary condition). This boundary condition was also successfully applied at all external boundary nodes in Masonboro Inlet employing the 1974 data (Amein 1975).

140. At the end nodes located in Masonboro Channel, Shinn Creek, and Banks Channel (Nodes 13, 19, and 25), Type-2 boundary conditions of zero velocity were applied under the assumption that the discharge would be negligible far from the inlet (on the order of 20,000 to 40,000 ft). This is a fictitious boundary condition, and for most accurate results, values for these distances should be determined in model calibration. This boundary condition produces correct values and is a very reasonable method given the absence of a well-defined bay or well-defined boundary. Sensitivity of model results can be investigated by changing the distance from the inlet, but, in the present example, the initially specified distances were maintained because the calculated results were sufficiently accurate.

141. A third boundary type, Type 3, may also be used at the external boundaries. This boundary was employed in the lumped-parameter models of GITI. The boundary condition Type 3 requires values of bay area, the bank slope of the bay, and an empirical coefficient called the flood repletion coefficient (Seelig, Harris, and Herchenroder 1977). In the case of Masonboro Inlet, the bay area would be a fictitious number presumably based on the tidal prism. This type of boundary condition may be specified at Nodes 13, 19, and 25 inside Masonboro Channel, Shinn Creek, and Banks Channel. A number of trials with DYNLET1 using this method showed that the "bay area" is actually a calibration parameter, and good results could be obtained with this method if an appropriate fictitious bay area was specified. The Type-3 results are not discussed further here.

142. Total time required to set up DYNLET1 for modeling Masonboro Inlet was approximately 40 person hours. Cross-section elevation data were read from available plots and maps (12 to 37 points per cross section), as were other data such as the time-dependent water elevation boundary condition. Approximately 1 day was required to run the model several times, graph and output results, and conclude that the model was accurately calculating tidal flow velocity, stage, and discharge.

143. A 16-hr run with an 1,800-sec (30 min) time step for Masonboro Inlet, consisting of five channels, two junctions, and 25 nodes took 57 sec (Pascal-language version of the model) and 50 sec (C-language version) on a 386-based 25-MHz processor with a math coprocessor. On a 486-based 25-MHz processor, the run times were less than half the preceding values.

DYNLET1 calculation results

144. Using the cross-sections obtained from hydrographic survey maps and the tidal elevation and velocity measurements for the interval 09:00 to 18:00 Eastern Standard Time, 12 September 1969, with the boundary conditions specified in the input file, the flow at Masonboro Inlet was modeled using DYNLET1. (All input and output data for the Masonboro Inlet example are given in Appendix A.)

145. The model can produce output in several formats. For comparison with measured values, average velocities were computed at several points in the cross-sections at Nodes 6, 13, 19, and 25, corresponding to velocity gaging stations in the inlet throat, Masonboro Channel, Shinn Creek, and Banks Channel, respectively. Comparisons of the computed and measured velocities at the inlet throat (Node 6) are given in Figures 8 and 9 for Gages 2C and 2S respectively, and additional velocity plots are given in Appendix A. Computed velocities are shown as solid lines, and measured velocities are shown as dashed lines. Because the exact correspondence between the data points in the cross section and the location of the gaging station is not known, it is expected that one or more of the model calculation points shown would represent the gaging station. Considering the uncertainties in modeling this complex natural environment, DYNLET1 performed well in reproducing magnitudes, ranges, and phases of the velocities with use of only the two original estimates of the bottom friction coefficient. It should also be noted that accurate and comprehensive field measurements are very difficult to obtain,

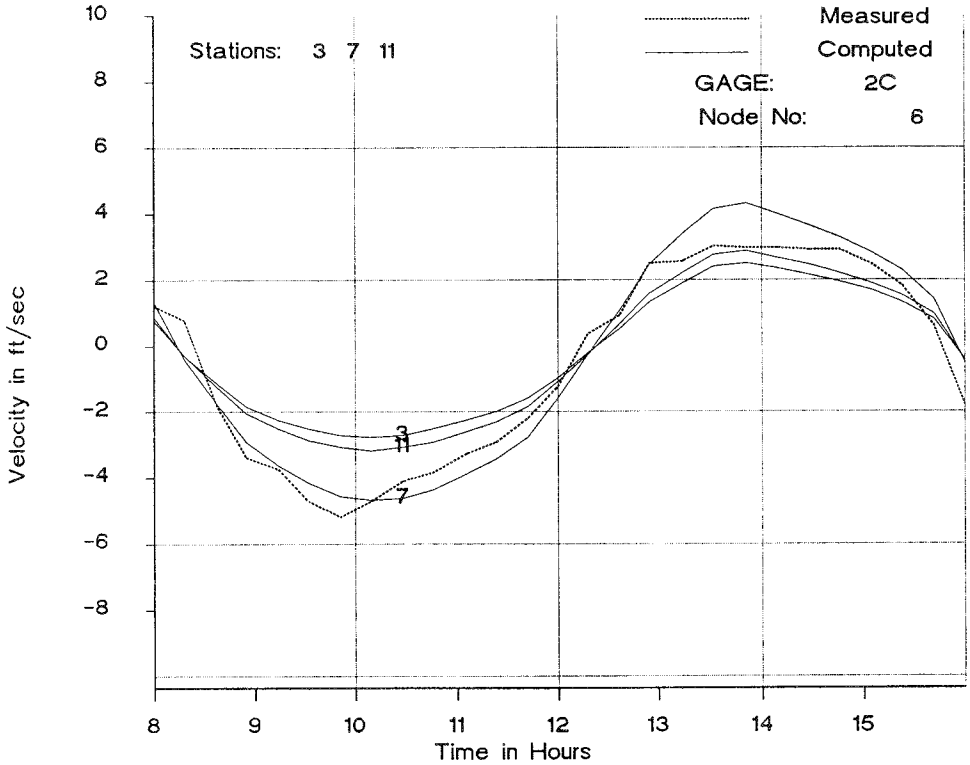

Figure 8. Computed and measured velocities (Gage 2C), Masonboro Inlet

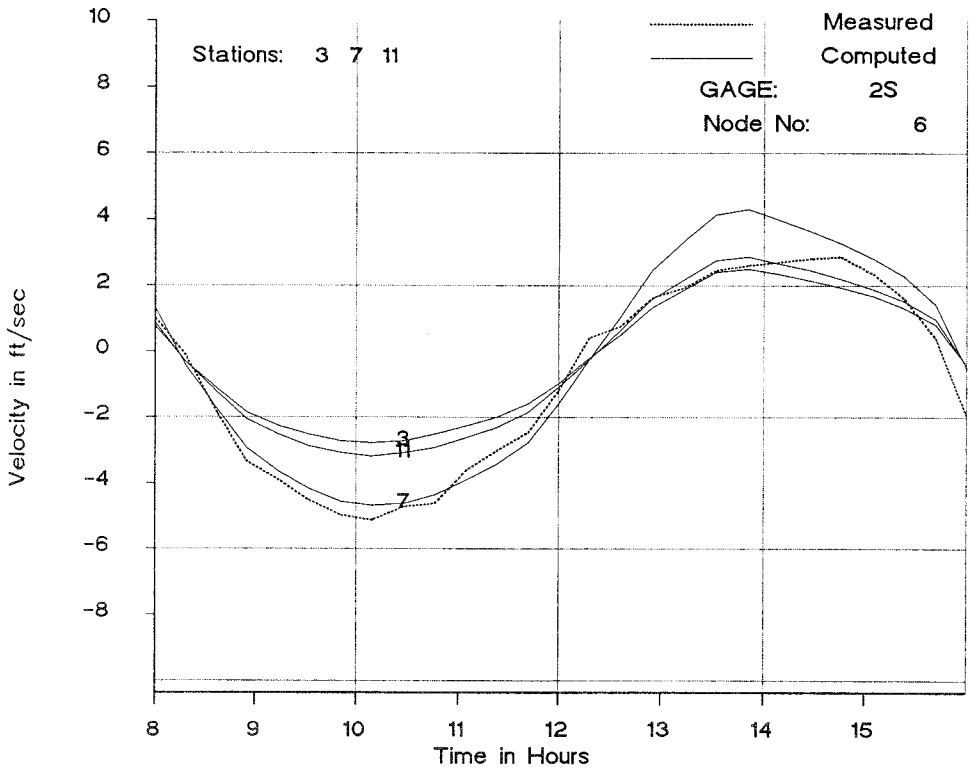

Figure 9. Computed and measured velocities (Gage 2S), Masonboro Inlet

and examination of the field records indicates that the total measured ebb and flood flows at some gaging stations are not balanced. This discrepancy in the field data may act to reduce agreement between measurements and model.

146. The model also provides discharges at all nodes. Comparison of the computed and measured discharges at the inlet throat (Node 6) is given in Figure 10. Measured discharges were computed manually by the USACE District, Wilmington, from the measured velocities, and some error may be expected owing to estimation of effective channel cross section. Figure 10 indicates that DYNLET1 gave a maximum (flood) flow of 48,031 cfs at the inlet throat, whereas the maximum flood flow from measured velocities at gaging stations was estimated at 42,129 cfs. Similarly, the maximum ebb flow was computed as -42,613 cfs, and the estimated value from the measurements was -44,225 cfs.

147. The plot of the cross section at Node 1, the sea boundary, is shown in Figure 11 as an example of how DYNLET1 processes cross-sectional data. Data points describing the horizontal locations and elevations of the channel bottom divide the cross section into subchannels, and the average

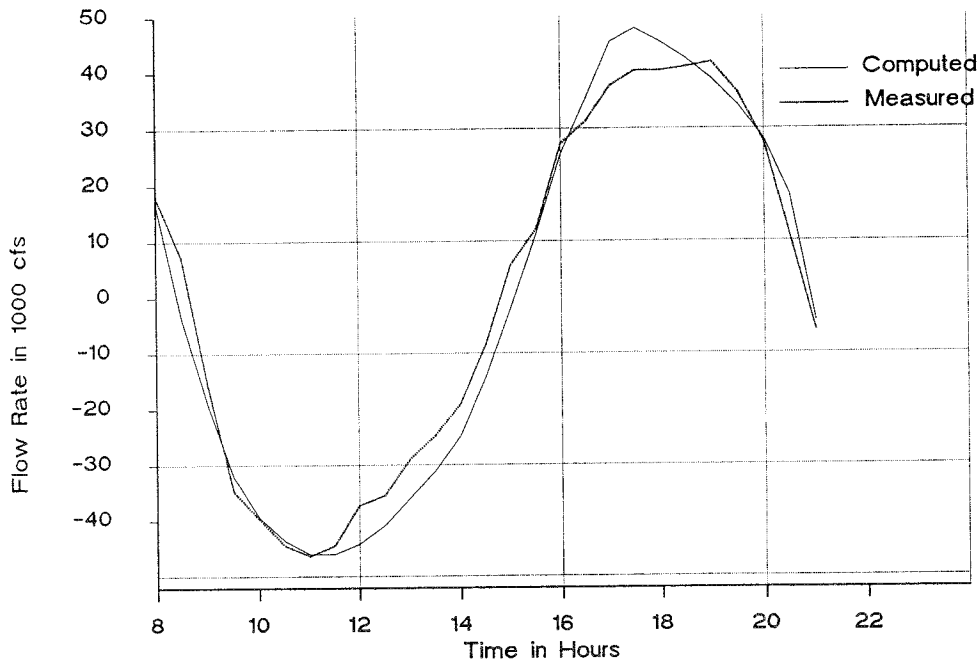

Figure 10. Computed and measured discharges, Masonboro Inlet

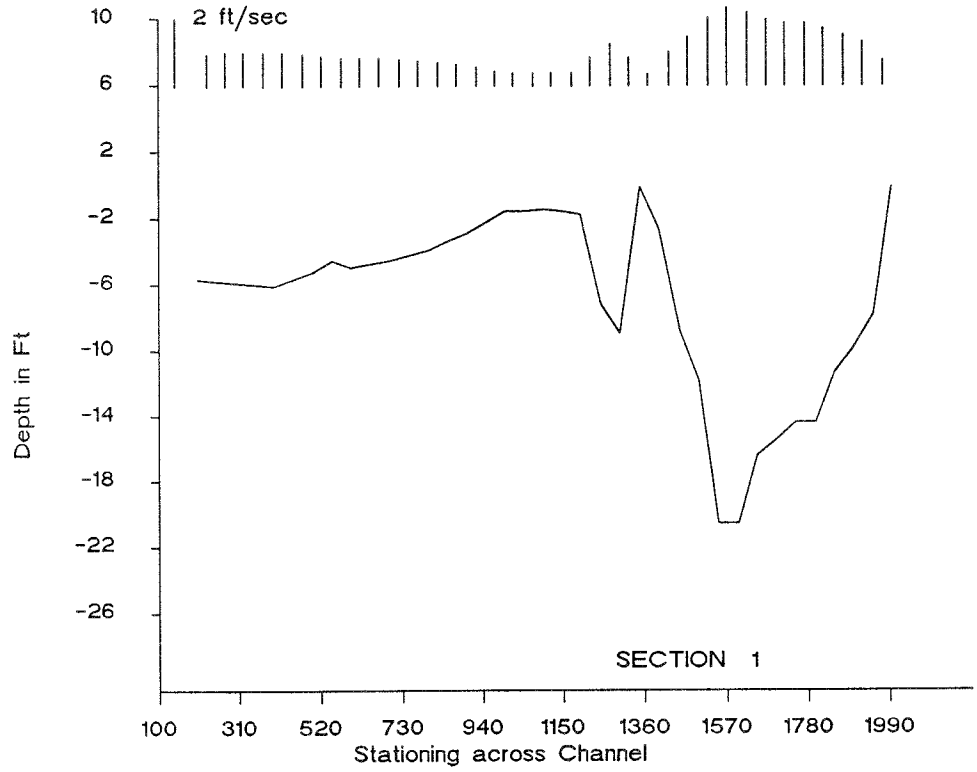

Figure 11. Cross section through Node 1, Masonboro Inlet

velocity is computed in each subchannel. Vertical bars at the top of the figure represent relative magnitudes of average velocities in subchannels.

GITI Models for Masonboro Inlet

148. As part of the GITI studies, Masonboro Inlet was a test case for evaluation of physical and numerical models. Data collected on 12 September 1969 were used to calibrate the models, and data collected in July 1974 were to be used for verification; however, the hydrography changed between the two dates, and the same cross sections could not be used for verification. Detailed analyses of the outputs from these models are given by Harris and Bodine (1977); Masch, Brandes, and Reagan (1977); and McTamany (1982). All models, except for the lumped-parameter model of Seelig, Harris, and Herchenroder (1977), which will be referred to as the GITI Lumped-Parameter Model (GLPM), appear to be special-purpose models specifically designed to describe Masonboro Inlet. As such, they may be considered outdated and

nonoperational. A modified version of the lumped-parameter model has been incorporated as the Automated Coastal Engineering System (ACES) (Leenknecht, Szuwalski, and Sherlock 1990) model, hereafter referred to as the ACES Lumped-Parameter Model (ALPM). However, the input data structure of the ALPM model is different from its predecessor model, and many modifications have been introduced so that the ALPM can no longer be considered to be the same as the GLPM, although it is in the same class. It was found in this review that in all GITI model studies of Masonboro Inlet, the field data, particularly the water surface elevations at tide gages, were adjusted to obtain calibration.

149. It should be noted that the major parameter determining the magnitude of flow in the GLPM is the bay area. By computing the bay area from the tidal range, tidal duration, and tidal prism, as has been done in the Masonboro Inlet case, the procedure, in effect, provides the solution as input to the model.

GLPM

150. The GLPM is described in GITI Report 14 (Seelig, Harris, and Herchenroder 1977). This model is a lumped-parameter model and can be traced to a simple, physically appealing one-dimensional quasi-steady state analytical model introduced by Keulegan (1967). The solution of Keulegan was based on a channel of constant cross-section and constant friction factor. However, the GLPM goes beyond Keulegan's simple analytical model and uses a composite channel made up of subchannels of variable width and length.

151. Application of the GLPM model to Masonboro Inlet using the September 1969 data is of interest. Comparisons of the cross sections as given in Seelig, Harris, and Herchenroder (1977) with the cross sections obtained from hydrographic maps from the USACE District, Wilmington, show that the natural cross section was simulated by four rectangular subchannels. The maximum (flood) flow was computed as 55,000 cfs at the inlet throat by Seelig, Harris, and Herchenroder, to be compared with the maximum flood flow of 42,000 cfs estimated from measured velocities at gaging stations.

152. The data used by Seelig, Harris, and Herchenroder (1977) was modified in an attempt to find an approximate estimate of the flow. Therefore, direct comparison of results with the DYNLET1 model cannot be made.

Model of Huval and Wintergerst (1977)

153. This is also a numerical lumped-parameter model inspired by Keulegan's (1967) analytical model and is described in Appendix 4 of GITI Report 6 (Huval and Wintergerst 1977). The basic concepts are similar to the GLPM. In application to Masonboro Inlet, the inlet hydrodynamic system was represented by five cross sections, starting with Cross Section 1 at the seaward end of the jetty and ending at Cross Section 5 located approximately 500 ft inland of the inlet throat. The bay boundary condition was imposed at Cross Section 5. A bay area of 1.9×10^8 ft^2 was derived from the tidal prism. No attempt was made to simulate conditions along Masonboro Channel, Banks Channel, and Shinn Creek. A Manning's friction coefficient of 0.027 was used throughout as compared with a value of 0.037 in the application by Seelig, Harris, and Herchenroder (1977). The model was calibrated with the September 1969 data and applied to predict conditions in November 1964 (prior to jetty construction) and July 1966 (modified inlet and jetty condition). This model does not appear to have been verified with the 1974 data. The maximum flood and ebb tides computed by the model were 57,000 and -53,000 cfs, compared with estimated measured values of 42,000 and -42,000 cfs. The reasons for the systematic overestimations are not known.

Evaluation of Flow Parameters from DYNLET1

154. DYNLET1 is based on the complete hydrodynamic equations in one dimension (along the direction of the main flow), and the numerical implementation does not require modification or simplification of the governing equations. Analytical models or simple numerical models developed in the past depended on linearization or other simplifications to solve the equations. Such modifications were necessary in the precomputer era. The most common procedures adopted were elimination of the temporal acceleration term, elimination or linearization of the convective acceleration term, and linearization of the bottom friction stress term. For example, the ALPM incorporates simplifications of the governing equations, with the temporal acceleration neglected, the convective acceleration and the pressure head computed in a gross sense (between the ends of the inlet), and the bottom friction stress considered to be the predominant governing physical mechanism.

155. There are justifications for using simple analytical and numerical models, such as ease of application and saving of computer costs or speed. A stronger case can be made for the simple models on engineering projects if the eliminated terms do not greatly affect final results.

156. To evaluate the relative strengths of the various terms in the hydrodynamic equations, values of the temporal acceleration, the convective acceleration and the pressure gradient as given from DYNLET1 were computed for Masonboro Inlet. These terms, normalized by the bottom friction stress term, are given in Table 2 for Cross Sections 2 to 6. This table was taken directly from the auxiliary program SUMMARY.OUT. If a value is much smaller than one, the term could be neglected in justification of a simpler solution scheme.

157. The temporal acceleration term is large at the first hour because flow at the internal nodes of the model are in transit to proper values from their initial condition (constant discharge in each channel as given by the data at the related measured channel node, and constant water surface elevation, the initial level of the sea). Its strength relative to the bottom friction is also large when the flow reverses (for example, between hours 14.5 and 15), but this is also partly an artifact of the bottom friction stress approaching zero when the velocity approaches zero. The pressure term behaves similarly. Both the temporal acceleration and pressure terms are small relative to the bottom friction term when the flow is slowly changing.

158. The convective acceleration term is relatively large and constant from section to section, but is particularly large where the cross-sectional area changes significantly (for example, going from Node 5 at the sea to Node 6 at the inlet throat).

159. It is clear from Table 2 that elimination or gross simplification of any of the forcing terms governing the tidal flow could cause significant local errors in calculations at specific points at different times for an inlet such as Masonboro.

Table 2

Comparison of Relative Strengths of Various Terms, Masonboro Inlet

Time hr	Sec.	Sea El ft	Bay El ft	Q cfs	Tempor. Accel./ Bot. Stress	Convec. Accel./ Bot. Stress	Pressure/ Bot. Stress
8.0	2	4.50	4.40	-5518	-7.05	-0.09	7.48
8.0	3	4.50	4.40	-5469	-6.98	0.20	7.46
8.0	4	4.50	4.40	-5424	-7.96	-0.20	8.46
8.0	5	4.50	4.40	-5392	-11.67	5.95	11.26
8.0	6	4.50	4.40	-5380	-14.16	0.24	14.88
8.5	2	4.20	4.40	-17548	-0.82	-0.10	1.34
8.5	3	4.20	4.40	-17403	-0.81	0.21	1.10
8.5	4	4.20	4.40	-17267	-0.91	-0.23	1.59
8.5	5	4.20	4.40	-17171	-1.33	6.07	-0.97
8.5	6	4.20	4.40	-17136	-1.60	0.32	2.15
9.0	2	4.00	4.40	-22760	-0.23	-0.09	0.76
9.0	3	4.00	4.40	-22661	-0.22	0.23	0.51
9.0	4	4.00	4.40	-22567	-0.25	-0.24	0.97
9.0	5	4.00	4.40	-22499	-0.37	6.19	-2.14
9.0	6	4.00	4.40	-22475	-0.44	0.40	0.95
9.5	2	3.50	4.40	-30944	-0.06	-0.11	0.67
9.5	3	3.50	4.40	-30836	-0.07	0.25	0.39
9.5	4	3.50	4.40	-30729	-0.09	-0.30	0.94
9.5	5	3.50	4.40	-30650	-0.15	6.41	-2.48
9.5	6	3.50	4.40	-30620	-0.17	0.56	0.66
10.0	2	3.00	4.40	-35748	-0.11	-0.15	0.82
10.0	3	3.00	4.40	-35508	-0.11	0.25	0.46
10.0	4	3.00	4.40	-35284	-0.12	-0.39	1.12
10.0	5	3.00	4.40	-35126	-0.16	6.61	-2.51
10.0	6	3.00	4.40	-35069	-0.18	0.73	0.65
10.5	2	2.40	4.40	-39574	-0.09	-0.19	0.92
10.5	3	2.40	4.40	-39285	-0.09	0.27	0.49
10.5	4	2.40	4.40	-39014	-0.10	-0.50	1.32
10.5	5	2.40	4.40	-38823	-0.13	6.86	-2.62
10.5	6	2.40	4.40	-38753	-0.14	0.99	0.56
11.0	2	1.75	4.40	-42372	-0.08	-0.25	1.08
11.0	3	1.75	4.40	-42059	-0.08	0.29	0.54
11.0	4	1.75	4.40	-41768	-0.08	-0.67	1.61
11.0	5	1.75	4.40	-41562	-0.11	7.13	-2.71
11.0	6	1.75	4.40	-41486	-0.11	1.36	0.46

(Continued)

(Sheet 1 of 4)

Table 2 (Continued)

Time hr	Sec.	Sea El ft	Bay El ft	Q cfs	Tempor. Accel./ Bot. Stress	Convec. Accel./ Bot. Stress	Pressure/ Bot. Stress
11.5	2	1.20	4.40	-42614	-0.05	-0.31	1.22
11.5	3	1.20	4.40	-42347	-0.04	0.32	0.57
11.5	4	1.20	4.40	-42096	-0.05	-0.84	1.89
11.5	5	1.20	4.40	-41919	-0.05	7.35	-2.81
11.5	6	1.20	4.40	-41854	-0.05	1.78	0.29
12.0	2	0.75	4.40	-40940	-0.01	-0.37	1.37
12.0	3	0.75	4.40	-40719	-0.01	0.34	0.61
12.0	4	0.75	4.40	-40511	-0.01	-1.02	2.19
12.0	5	0.75	4.40	-40362	-0.00	7.52	-2.88
12.0	6	0.75	4.40	-40308	0.01	2.20	0.13
12.5	2	0.45	4.40	-37356	0.04	-0.41	1.44
12.5	3	0.45	4.40	-37203	0.04	0.37	0.61
12.5	4	0.45	4.40	-37057	0.05	-1.16	2.39
12.5	5	0.45	4.40	-36951	0.07	7.63	-2.96
12.5	6	0.45	4.40	-36912	0.09	2.57	-0.06
13.0	2	0.30	4.40	-32223	0.13	-0.42	1.41
13.0	3	0.30	4.40	-32141	0.12	0.40	0.55
13.0	4	0.30	4.40	-32059	0.14	-1.24	2.45
13.0	5	0.30	4.40	-31997	0.19	7.68	-3.09
13.0	6	0.30	4.40	-31974	0.22	2.82	-0.27
13.5	2	0.15	4.40	-27369	0.18	-0.45	1.44
13.5	3	0.15	4.40	-27289	0.17	0.41	0.53
13.5	4	0.15	4.40	-27211	0.19	-1.33	2.57
13.5	5	0.15	4.40	-27153	0.27	7.71	-3.15
13.5	6	0.15	4.40	-27131	0.31	3.05	-0.43
14.0	2	0.20	4.40	-20510	0.54	-0.39	1.01
14.0	3	0.20	4.40	-20524	0.50	0.45	0.18
14.0	4	0.20	4.40	-20533	0.55	-1.28	2.18
14.0	5	0.20	4.40	-20536	0.72	7.74	-3.66
14.0	6	0.20	4.40	-20536	0.79	3.09	-0.98
14.5	2	0.50	4.40	-9799	3.75	-0.22	-2.42
14.5	3	0.50	4.40	-9937	3.42	0.54	-2.89
14.5	4	0.50	4.40	-10062	3.66	-1.04	-1.14
14.5	5	0.50	4.40	-10148	4.74	7.79	-8.21
14.5	6	0.50	4.40	-10178	5.15	2.90	-5.72

(Continued)

(Sheet 2 of 4)

Table 2 (Continued)

Time hr	Sec.	Sea El ft	Bay El ft	Q cfs	Tempor. Accel./ Bot. Stress	Convec. Accel./ Bot. Stress	Pressure/ Bot. Stress
15.0	2	0.75	4.40	1152	256.67	-1.03	-252.00
15.0	3	0.75	4.40	1030	307.01	-0.44	-316.08
15.0	4	0.75	4.40	916	433.44	-1.74	-411.02
15.0	5	0.75	4.40	835	704.60	6.13	-801.74
15.0	6	0.75	4.40	805	842.61	0.96	-915.07
15.5	2	1.00	4.40	11981	2.20	-0.33	-2.75
15.5	3	1.00	4.40	11859	2.15	0.33	-3.46
15.5	4	1.00	4.40	11745	2.45	-0.95	-2.51
15.5	5	1.00	4.40	11664	3.40	7.42	-15.84
15.5	6	1.00	4.40	11635	3.85	2.14	-8.56
16.0	2	1.60	4.40	25897	0.53	-0.26	-1.04
16.0	3	1.60	4.40	25607	0.52	0.31	-1.64
16.0	4	1.60	4.40	25337	0.59	-0.74	-0.76
16.0	5	1.60	4.40	25147	0.83	7.28	-12.64
16.0	6	1.60	4.40	25079	0.96	1.70	-4.65
16.5	2	2.20	4.40	35112	0.15	-0.19	-0.63
16.5	3	2.20	4.40	34818	0.15	0.30	-1.18
16.5	4	2.20	4.40	34545	0.18	-0.57	-0.39
16.5	5	2.20	4.40	34346	0.26	7.13	-11.70
16.5	6	2.20	4.40	34276	0.32	1.34	-3.31
17.0	2	3.00	4.40	44846	0.08	-0.14	-0.49
17.0	3	3.00	4.40	44456	0.08	0.27	-0.97
17.0	4	3.00	4.40	44090	0.09	-0.41	-0.32
17.0	5	3.00	4.40	43831	0.14	6.85	-11.06
17.0	6	3.00	4.40	43738	0.18	0.93	-2.43
17.5	2	3.40	4.40	46225	-0.00	-0.11	-0.39
17.5	3	3.40	4.40	46025	-0.00	0.27	-0.86
17.5	4	3.40	4.40	45835	0.00	-0.32	-0.25
17.5	5	3.40	4.40	45698	0.01	6.70	-10.65
17.5	6	3.40	4.40	45649	0.02	0.76	-1.96
18.0	2	3.60	4.40	43046	-0.05	-0.09	-0.34
18.0	3	3.60	4.40	42944	-0.05	0.27	-0.79
18.0	4	3.60	4.40	42844	-0.05	-0.29	-0.20
18.0	5	3.60	4.40	42771	-0.07	6.58	-10.36
18.0	6	3.60	4.40	42744	-0.08	0.66	-1.68

(Continued)

(Sheet 3 of 4)

Table 2 (Concluded)

Time hr	Sec.	Sea El ft	Bay El ft	Q cfs	Tempor. Accel./ Bot. Stress	Convec. Accel./ Bot. Stress	Pressure/ Bot. Stress
18.5	2	3.85	4.40	39644	-0.06	-0.09	-0.31
18.5	3	3.85	4.40	39519	-0.06	0.25	-0.73
18.5	4	3.85	4.40	39398	-0.07	-0.26	-0.18
18.5	5	3.85	4.40	39310	-0.09	6.42	-10.08
18.5	6	3.85	4.40	39276	-0.11	0.54	-1.43
19.0	2	4.10	4.40	35894	-0.08	-0.08	-0.28
19.0	3	4.10	4.40	35769	-0.07	0.24	-0.68
19.0	4	4.10	4.40	35648	-0.08	-0.23	-0.16
19.0	5	4.10	4.40	35561	-0.12	6.28	-9.81
19.0	6	4.10	4.40	35528	-0.14	0.44	-1.21
19.5	2	4.30	4.40	31567	-0.10	-0.08	-0.24
19.5	3	4.30	4.40	31466	-0.10	0.23	-0.63
19.5	4	4.30	4.40	31369	-0.11	-0.21	-0.13
19.5	5	4.30	4.40	31299	-0.16	6.16	-9.57
19.5	6	4.30	4.40	31272	-0.19	0.36	-1.03
20.0	2	4.40	4.40	25789	-0.19	-0.07	-0.15
20.0	3	4.40	4.40	25737	-0.18	0.23	-0.54
20.0	4	4.40	4.40	25686	-0.20	-0.19	-0.05
20.0	5	4.40	4.40	25649	-0.29	6.09	-9.30
20.0	6	4.40	4.40	25634	-0.35	0.33	-0.80
20.5	2	4.35	4.40	17084	-0.60	-0.06	0.25
20.5	3	4.35	4.40	17106	-0.58	0.25	-0.14
20.5	4	4.35	4.40	17124	-0.65	-0.19	0.39
20.5	5	4.35	4.40	17135	-0.94	6.10	-8.55
20.5	6	4.35	4.40	17138	-1.14	0.34	-0.03
21.0	2	3.90	4.40	-2866	-50.00	-0.36	50.21
21.0	3	3.90	4.40	-2650	-56.52	-0.06	58.57
21.0	4	3.90	4.40	-2450	-73.83	-0.53	73.35
21.0	5	3.90	4.40	-2309	-119.53	5.64	138.03
21.0	6	3.90	4.40	-2258	-150.20	-0.05	153.22

(Sheet 4 of 4)

PART VI: EXAMPLE APPLICATION 2: INDIAN RIVER INLET, DELAWARE

160. This chapter presents an example calculation demonstrating the applicability of DYNLET1 in tidal flow studies involving a bay (in this case, two bays) and a narrow inlet throat at Indian River Inlet, Delaware.

Indian River Inlet

161. Indian River Inlet is located approximately half-way between Cape Henlopen at the entrance to Delaware Bay and the State line of Maryland. It is the only inlet in the State of Delaware (Figure 12) and the only opening to the Atlantic Ocean for Indian River Bay and Rehoboth Bay. Both bays are shallow, with an average depth of approximately 7 ft (Anders, Lillycrop, and Gebert 1990). Historically, this inlet was an ephemeral feature that intermittently opened to expose Rehoboth and Indian River Bays to the Atlantic Ocean. During flood tide, the flow goes through the main channel, under the State Highway 14 bridge that spans the inlet, and then splits into Rehoboth Bay and Indian River Bay. Thus, the system consists of a well-defined main channel and two bays.

162. Between 1938 and 1940, the USACE constructed two rubble-mound jetties that stabilized the inlet, thereby maintaining water quality and allowing free navigation between the bays and the ocean. The jetties are 500 ft apart, and two sets of pilings from the Highway 14 bridge are located in the inlet channel. Upon construction of the jetties, the navigation channel was 200 ft wide and 14 ft deep.

163. The coastal area around Indian River Inlet has experienced three problems of engineering significance (Anders, Lillycrop, and Gebert 1990): scour in the inlet, particularly at the tip of the north jetty and adjacent to the pilings of the bridge along Delaware Highway 14; erosion of the shoreline interior to the inlet; and erosion of the beach to the north of the jetties (with corresponding accretion on the beach south of the jetties). The last two-listed problems have been substantially mitigated and are effectively under control, with the interior shorelines now protected by bulkheads and revetments, and the imbalance in longshore sand transport at the jetties appears to be corrected by a successful sand bypassing operation (Clausner

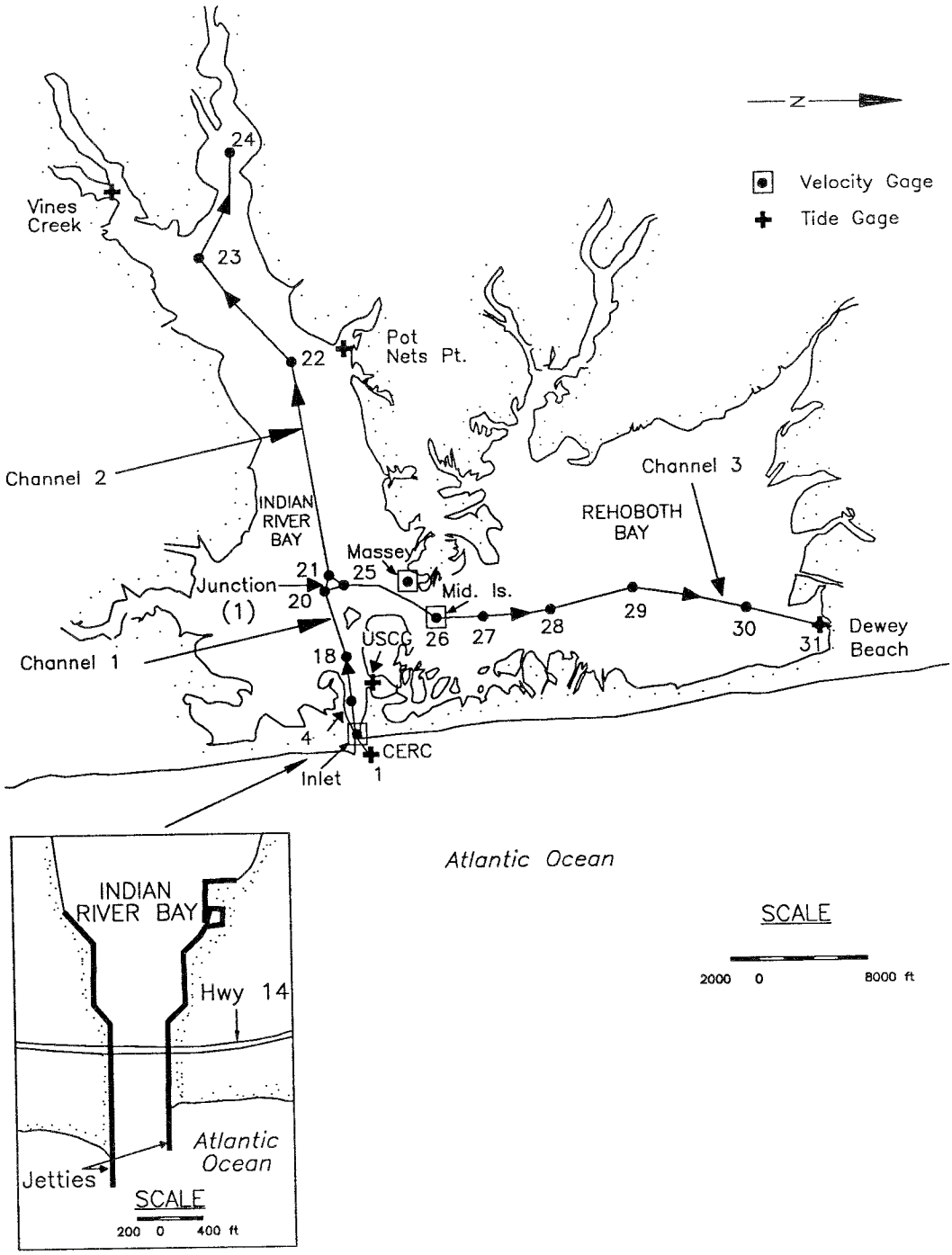

Figure 12. Schematic plan for Indian River Inlet

1990; Clausner, Patterson, and Rambo 1990).

164. The problem of scour in the inlet, however, still remains and is the subject of ongoing studies. In 1940, the channel depth was approximately 20 ft. At present (December 1990) the inlet throat averages over 40 ft in depth and contains three large scour holes. One scour hole, located near the tip of the jetty, has caused loss of part of the north jetty. The other two scour holes are in the vicinity of the bridge pilings where the depth reaches more than 80 ft along certain sections.

165. One of the basic questions to be answered is why the rate of scour increased in the period 1974 to the present as compared with the time 1934 to 1974. Several factors are under evaluation, such as different layers of material composing the underlying sedimentary structure, changes in jetty configuration, and mining of the flood-tidal shoal. Whatever the cause, the capability to quantitatively predict tidal flow through the inlet is required to arrive at a process-and-response understanding of the sediment transport regime at the site. To this end, the Coastal Engineering Research Center (CERC), in support of the USACE District, Philadelphia, collected tidal velocity data for conducting a comprehensive two-dimensional hydrodynamic numerical modeling effort.

166. The Indian River Inlet channel is relatively narrow and long, and the tidal flow in it is expected to be well described by a one-dimensional hydrodynamic model. Also, current velocity data taken in the shallow natural channels connecting Rehoboth and Indian River Bays, as well as tidal elevation measurements made in the bays at intermediate and far distances from the inlet, make the site highly suited for testing both the accuracy of a one-dimensional model and its capability to represent boundary conditions in complex bays represented by multiple channels.

167. In the present study, tidal flow and elevation data obtained for the more extensive hydrodynamic modeling effort presently in progress at CERC were used to examine the predictive capability of DYNLET1. A description of the data collection effort, associated hydrodynamic modeling, and results pertaining to the aforementioned scour problem can be found in McGehee and Lillycrop (1989) and Anders, Lillycrop, and Gebert (1990). The measurements processed for use in the ongoing two-dimensional modeling effort were used directly in the present study without modification.

DYNLET1

Model setup

168. The Indian River Inlet System is represented in DYNLET1 by 31 cross sections distributed in three channels. The channels are numbered from 1 to 3 and there is a single junction numbered 1, as shown in Figure 12. The channels and their cross sections are listed in Table 3.

169. The assumed initial flow direction is from the sea toward the bays. Cross Section 1, represented as Node 1, is taken at the location of the CERC tide gage. Channel 1 extends from the sea through the inlet throat to Indian River Bay. Channel 2 simulates Indian River Bay, and Channel 3 simulates Rehoboth Bay. Mid Island lies within Channel 3. Channels 1, 2, and 3 meet at Junction 1, the only junction in the model. Junction 1 consists of Nodes 20, 21, and 25.

170. The required cross-sectional geometric data were taken from hydrographic maps obtained from the USACE District, Philadelphia, dated 3 March 1989. The data are recorded as distances and elevations, where distance is an offset from the left bank, and elevation is with respect to the bottom with the MLW datum as the reference level.

171. Manning's coefficient of friction was initially specified at every cross-section point as 0.03 and as a first estimate. After a few trial runs, the value was changed to 0.045 in Cross Sections 5 through 12, which encompass the bridge area. This decision was made by examining plots of calculated velocity and observation of large bed irregularity on the hydrographic charts

Table 3

Channel Cross Sections, Indian River

Channel Number	Channel Cross Section From	To
1	1	20
2	21	24
3	25	31

in this area. No other changes in bottom friction values were necessary to achieve reasonable agreement between model calculations and measurements.

172. Two types of boundary conditions were used at the external boundaries. The Type-1 condition, values of water surface elevation specified as a function of time, was used at Node 1, the sea boundary, and provided the forcing for tidal flow. Therefore, at Node 1, the model expects a table of values of water surface elevation as a function of time. This table is supplied in the input data file EXTER.DAT (Appendix B).

173. The Type-2 boundary condition, discharge as a function of time, is applied at Nodes 25 and 31, which represent the end nodes in Indian River and Rehoboth Bays. Since neither the discharge nor water surface elevations were recorded at these boundaries, a zero discharge was used as the boundary condition. This is a good assumption because the magnitude of velocity at these locations would be very small because of the large bay areas.

174. At Cross Sections 4, 5, and 6 the transition loss coefficient was initially set to 0.5 and then revised after the first few model runs to 0.4 to simulate head losses at the pilings of the highway bridge and constriction of the channel in general. In models not having the capability to simulate transition head loss, a larger value of the bottom friction coefficient would have to be used; however, increased bottom friction often results in an underestimate of velocity.

175. In the present study, tidal elevations available for hours 39 through 63 of a 63-hr-long measurement record were used in the calculations and comparisons. Locations of cross sections and the single junction were determined by inspection of the hydrographic survey charts, and needed depths were read from the charts, visually interpolating and extrapolating readings, as necessary. Total time required to set up DYNLET1 for modeling Indian River Inlet was approximately 50 person hours, extra time being required to check the depth survey readings. Approximately 1 day was required to run the model, graph and output results, make some slight changes for calibration, as discussed in the following paragraphs, and conclude that the model was accurately simulating tidal flow velocity, stage, and discharge.

176. Execution time for the simulated 63-hr period with a time step of 1,800 sec (30 min) for Indian River Inlet (consisting of three channels, one junction, and 31 nodes) took 187 sec (Pascal-language version of the program)

and 180 sec (C-language version) on a 386-based 25-MHz processor with a math coprocessor. On a 486-based 25-MHz processor, the run times were less than half the preceding values.

Results

177. DYNLET1 provides calculation results of stage, velocity, and discharge at any cross section (Part IV). From examination of survey maps, the velocity gaging stations INLET3 and MIDIS3 were located inside cross sections at Nodes 4 and 26, respectively, and the tide gages US Coast Guard (USCG), Pot Nets Point, Vines, Massey Ditch, and Dewey Beach were located inside cross sections at Nodes 12, 22, 23, 26, and 28, respectively (Figure 12). These were used in the comparisons. The number "3" on the station names INLET3 and MIDIS3 denotes the third velocity gage in a string of three. Velocity gage station MIDIS3 was located in a narrow strait between islands, thereby connecting two large water masses in the double back-bay area in a region not too distant from where the tidal flow must turn relatively sharply toward or away from the inner inlet throat. Measurements at Gage MIDIS3 therefore provide a severe test of any model.

178. For comparison with measured velocities, calculated values at several stations at Nodes 4 and 26, corresponding to the locations of Gage INLET3 and MIDIS3, are plotted on Figures 13 and 14.

Additional plots are given in Appendix B. Because the location of the gage sites could not be identified with a particular station on the cross sections, it is expected that one or more of the computed plots would represent model results at or near the location of the gage. Computed values are plotted as solid lines, and the measured values are plotted as dashed lines. These figures indicate that DYNLET1 reproduced the ranges, magnitudes, and phases of the average velocities with almost no adjustment of the bottom friction coefficient, as described previously.

179. For comparison of computed and measured stages, values of water surface elevation at several data points at Nodes 12, 22, 23, 25, and 28, corresponding to the location of tide gages USCG, Pot Nets, Vines, Massey, and Dewey, were plotted. Two of these, one at Gage USCG and one at Gage Dewey, are shown on Figures 15 and 16. The remainder of the plots are contained in Appendix B. The agreement between the computed and measured values ranges from good to excellent at all gages except Massey. There is poor agreement

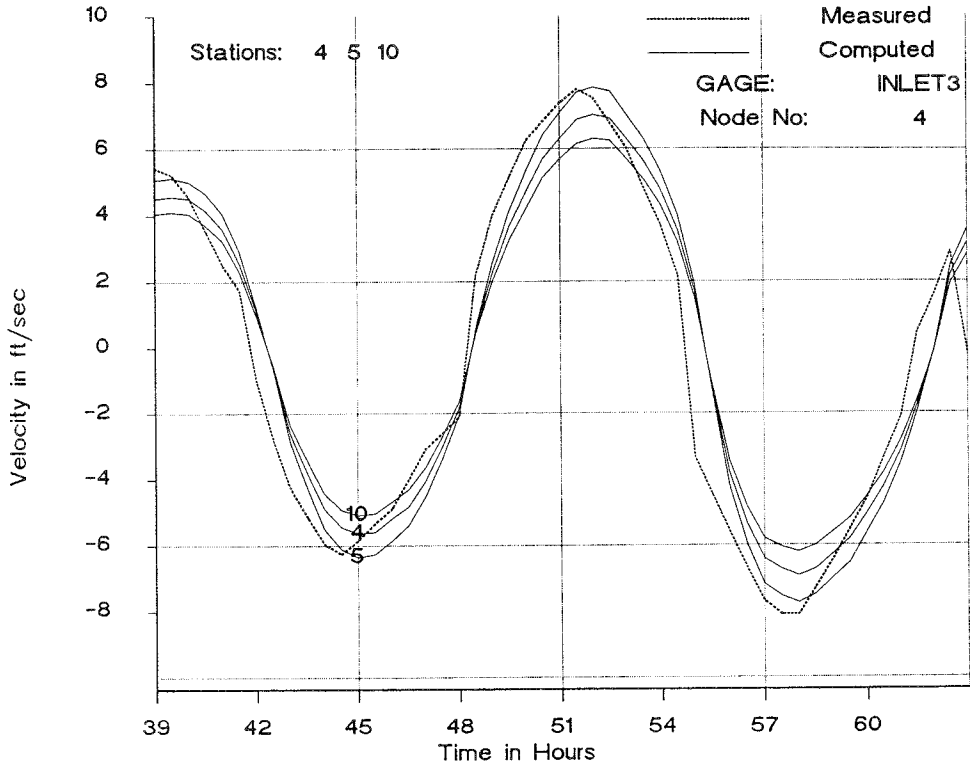

Figure 13. Computed and measured velocities (Gage INLET3), Indian River, using DYNLET1

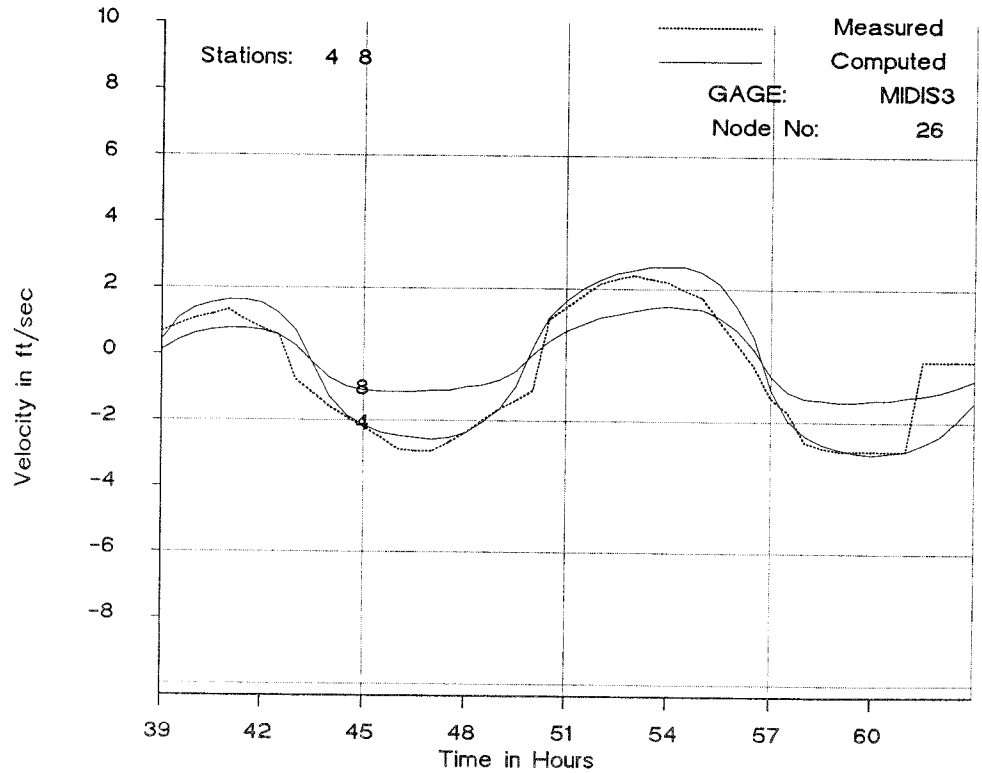

Figure 14. Computed and measured velocities (Gage MIDIS3), Indian River, using DYNLET1

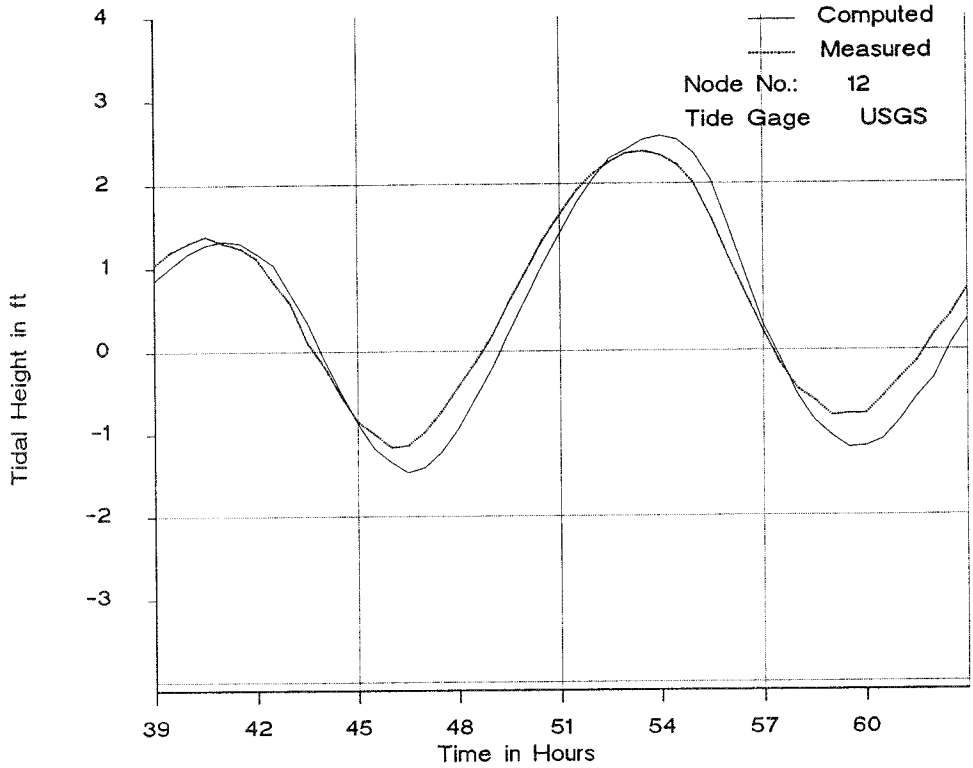

Figure 15. Computed and measured stage (Gage USCG), Indian River, using DYNLET1

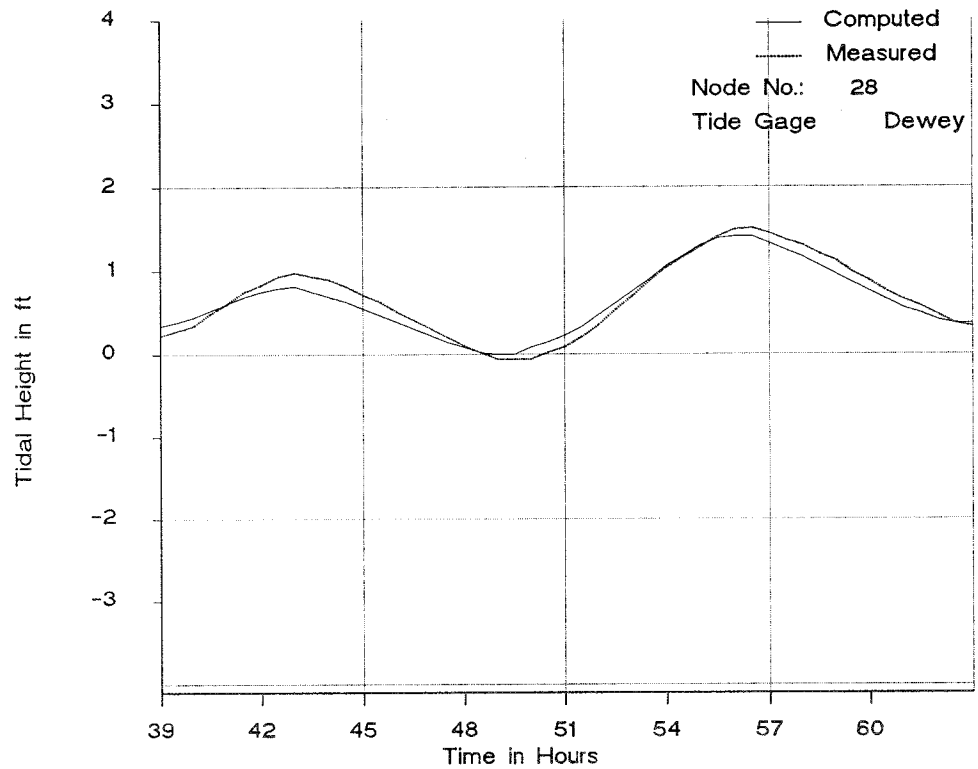

Figure 16. Computed and measured stage (Gage Dewey), Indian River, using DYNLET1

between the computed and measured values at Massey, and there is inconsistency in the measured data between Massey and the other gages. The cause of the discrepancy could be a difference in the base elevation at the Massey gage (believed to be the probable cause), river discharge, wind, or some unknown flow situation taking place at Massey.

180. Comparison of computed and measured stages indicates that the computed stage at Gage USCG is sensitive to the friction and transition loss coefficients in the inlet. Gage USCG is located in a small harbor, which may account for the slight discrepancy between computed and measured stages there. Significant energy losses occur at the bridge pilings, indicating that the transition-loss term describes a vital physical process in this narrow channel further constricted by the bridge pilings.

181. Examination of the stage records in Rehoboth and Indian River Bays indicates considerable differences in water surface elevations at different locations in the bays. The water surface is not fluctuating simultaneously in the bays, indicating significant dynamic action in the double bay system. There is thus a kind of long-period wave in this big bay system that cannot be properly described by a lumped-parameter model that assumes the water level rises equally over an equivalent bay area. Comparison of measured and computed values indicates that DYNLET1 has correctly reproduced the dynamic fluctuations in water surface elevations in the two bays. Comparison of computed and measured discharges cannot be made because measured volume flow rates were not available.

PART VII: SUMMARY AND CONCLUSION

182. This report introduces a numerical model called DYNLET1, developed for project-level reconnaissance studies of inlet hydrodynamics. The model simulates tidal flow based on an implicit finite-difference representation of the one-dimensional shallow-water equations. It computes water surface elevations and average velocities as a function of time in tidal inlets ranging in configuration from single channels connecting a bay to the sea to complex inlet systems consisting of interconnected channels with and without bays.

183. The numerical scheme replaces partial derivatives in the complete governing momentum and continuity equations by finite differences, leading to a system of nonlinear algebraic equations solved by iteration. By taking advantage of bandedness of the equation systems, an efficient computation scheme can be employed. The numerical solution procedure is unconditionally stable, and large time steps consistent with the resolution of the input data can be used.

184. General types of boundary conditions are easily implemented and include the velocity, discharge, and water surface elevation. The model has great flexibility in data input; data can be input in free format, cross-sectional properties can be entered with varying distance intervals, and time-dependent boundary data can be entered with variable time intervals. The data can be submitted through batch files, or the model can generate an input file using an interactive screen entry system under development and not described here. Other features of use to the practicing engineer are the generation of graphs of various types for display on the monitor or for obtaining hard copy.

185. Application of the model was illustrated through two case studies. One study site was Masonboro Inlet, North Carolina, for which an extensive set of field data for model testing is available. DYNLET1 successfully reproduced the magnitudes and phases of average velocities and volume flow rates for this situation involving five channels and no bay.

186. The other study site was Indian River Inlet, Delaware, for which a set of extensive field data for model testing is also available. The numerical model successfully reproduced the magnitudes and phases of average velocities and water surface elevations for the inlet system consisting of two large bays and a narrow inlet throat perturbed by bridge pilings. This example also

demonstrated that DYNLET1 can accurately represent the dynamics of water movement in a shallow bay. This report also contains a short review of other work on tidal inlets that involved simple models.

187. The ease of use, accuracy, and efficiency of DYNLET1 satisfies the objective of this study in providing a reconnaissance-level model for use by planners and engineers. The main resource required is a modern desk-top computer, and preparations to perform quantitative tidal flow studies with the model can be completed in a matter of 1 or 2 weeks, with actual model run duration typically on the order of minutes.

188. The major theoretical limitation of the one-dimensional tidal flow model DYNLET1 is restriction of flow along the inlet or channel axes. This condition is expected to be satisfied at most inlet throats, and, in fact, the model provided accurate results in two tidal flow field case studies with converging flows and multiple channels, including a situation with two side bay areas. Thus this rigorous one-dimensional model appears to be robust beyond the apparent theoretical limitation. The actual range of validity of the model has yet to be explored empirically and should be the subject of further study.

REFERENCES

Abbott, M. B., and Ionescu, F. 1967. "On the Numerical Computation of Nearly Horizontal Flows," Journal of Hydraulic Research, Vol 5, pp 98-117.

Amein, M. 1966. "Numerical Flood Routing by Characteristics," Water Resources Research, Vol 1, pp 123-130.

_____. 1968. "An Implicit Method for Numerical Flood Routing," Water Resources Research, Vol 4, No. 4, pp 719-726.

_____. 1972. "Numerical Simulation of Unsteady Flows in Rivers and Reservoirs," Technical Report COM-73-10674, prepared for National Oceanic and Atmospheric Administration, National Weather Service, National Technical Information Service.

_____. 1975. "Computation of Flow Through Masonboro Inlet, N.C.," Journal of the Waterways, Harbors and Coastal Engineering Division, American Society of Civil Engineers, Vol 1, No. WW1, pp 93-108.

Amein, M., and Chu, H. L. 1975. "Numerical Modeling of Unsteady Flow in Rivers and Reservoirs," Journal of the Hydraulics Division, American Society of Civil Engineers, Vol 101, No. HY6, pp 717-731.

Amein, M., and Fang, C. S. 1970. "Implicit Flood Routing in Natural Channels," Journal of the Hydraulics Division, American Society of Civil Engineers, Vol 96, No. HY1, pp 2481-2500.

Anders, F. J., Lillycrop, J. W., and Gebert, J. 1990. "Effects of Natural and Man-Made Changes at Indian River Inlet, Delaware," Proceedings, Third Annual National Beach Preservation Technology Conference, Florida Shore and Beach Preservation Association, Tallahassee, Florida, pp 280-294.

Baltzer, R. A., and Lai, C. 1968. "Computer Simulations of Unsteady Flows in Waterways," Journal of the Hydraulics Division, American Society of Civil Engineers, Vol 94, No. HY4, pp 1083-1117.

Butler, H. L. 1980. "Evolution of a Numerical Model for Simulating Long-Period Behavior in Ocean-Estuarine Systems," Estuarine and Wetland Processes with Emphasis on Modeling, Marine Science Series, Vol 11, Plenum Press, New York.

_____. 1982. "Numerical Modeling of Inlet-Estuary Systems," Proceedings of Applying Research to Hydraulic Practice, American Society of Civil Engineers, pp 715-726.

Chow, V. T. 1959. Open Channel Hydraulics, McGraw-Hill Book Co., Inc., New York.

Chen, R. M., and Hembree, L. A. 1977. "Numerical Simulation of Hydrodynamics," Appendix 3 in GITI Report 6, "Comparison of Numerical and Physical Hydraulic Models, Masonboro Inlet, North Carolina," Coastal Engineering Research Center, Fort Belvoir, VA.

Cialone, M. A. "Coastal Modeling System: User's Manual," Instruction Report in preparation, US Army Engineer Waterways Experiment Station, Coastal Engineering Research Center, Vicksburg, MS.

Clausner, J. E. 1990. "Jet Pump Sand Bypassing at Indian River Inlet, Delaware," in Proceedings, 23rd Annual Dredging Seminar, Center for Dredging Studies, Texas A&M University, College Station, TX.

Clausner, J. E., Patterson, D. K., and Rambo, G. 1990. "Fixed Sand Bypassing Plants, An Update," Proceedings, Third Annual National Beach Preservation Technology Conference, Florida Shore and Beach Preservation Association, Tallahassee, Florida, pp 249-264.

Cunge, J. A., and Wegner, M. 1964. "Integration Numerique des Equations d'Ecoulement de Barre de Saint Venant par un Schema Implicite de Differences Finies," La Houille Blanche, No. 1, pp 33-39.

Fletcher, A. G., and Hamilton, W. S. 1967. "Flood Routing in an Irregular Channel," Journal of the Engineering Mechanics Division, American Society of Civil Engineers, Vol 93, No. EM3, pp 45-62.

French, R. H. 1984. Open Channel Flow, McGraw-Hill Book Co., New York.

Harris, D. L., and Bodine, B. R. 1977. "Comparison of Numerical and Physical Hydraulic Models, Masonboro Inlet, North Carolina," GITI Report 6, Coastal Engineering Research Center, Fort Belvoir, VA.

Hsu, S. A. 1988. Coastal Meteorology, Academic Press, New York.

Huval, C. J., and Wintergerst, G. L. 1977. "Simplified Numerical (Lumped Parameter) Simulation," Appendix 4 in GITI Report 6, "Comparison of Numerical and Physical Hydraulic Models, Masonboro Inlet, North Carolina," Coastal Engineering Research Center, Fort Belvoir, VA.

Ippen, A. T., ed. 1966. Coastline and Estuary Hydrodynamics, McGraw-Hill Book Co., New York.

Isaacson, E. 1966. "Fluid Dynamical Calculations," Numerical Solution of Partial Differential Equations, Academic Press, New York, pp 35-49.

Johnson, B. H., Kim, K. W., Sheng, Y. P., and Heath, R. E. 1989. "Development of a Three-Dimensional Hydrodynamic Model of Chesapeake Bay," Proceedings of Conference on Estuarine and Coastal Modeling, American Society of Civil Engineers.

Keulegan, G. H. 1967. "Tidal Flow in Entrances - Water Level Fluctuations of Basins in Communication with Seas," T.B. No. 14, Committee on Tidal Hydraulics, US Army Engineer Waterways Experiment Station, Vicksburg, MS.

Kim, K. W., Johnson, B. H., and Sheng, Y. P. 1989. "Modeling a Wind-Mixing and Fall Turnover Event on Chesapeake Bay," Proceedings of Conference on Estuarine and Coastal Modeling, American Society of Civil Engineers.

Lai, C. 1967. "Computation of Transient Flows in Rivers and Estuaries by the Multiple Reach Implicit Method," Geological Survey Professional Paper 575-B, US Government Printing Office, Washington, DC.

Leenknecht, D. A., Szuwalski, A., and Sherlock, A. 1990. "Automated Coastal Engineering System, User's Guide," US Army Engineer Waterways Experiment Station, Coastal Engineering Research Center, Vicksburg, MS.

Liggett, J. A., and Woolhiser, D. A. 1967. "Difference Solution of the Shallow Water Equations," Journal of the Engineering Mechanics Division, American Society of Civil Engineers, Vol 94, No. EM2, pp 39-71.

Masch, F. D., Brandes, R. J., and Reagan, J. D. 1977. "Numerical Simulation of Hydrodynamics (WRE)," Appendix 2 in GITI Report 6, "Comparison of Numerical and Physical Hydraulic Models, Masonboro Inlet, North Carolina," Coastal Engineering Research Center, Fort Belvoir, VA.

Massau, J. 1889. "Memoire sur l'Integration Graphique des Equations aux Derivations Partielles," Ann. Ingenieurs Sortis de Gand, No. 12, pp 185-444.

McGehee, D. D., and Lillycrop, W. J. 1989. "Indian River Inlet Field Management Program," Proceedings of Oceans '89, Institute of Electrical and Electronics Engineers, pp 1.81-1.83.

McTamany, J. E. 1982. "Evaluation of Physical and Numerical Hydraulic Models, Masonboro Inlet, North Carolina," GITI Report 22, Coastal Engineering Research Center, Fort Belvoir, VA.

Preissmann, A. 1971. "Modeles pour le calcul del la Propagation des Crues," La Houille Blanche, Vol 3, pp 219-224.

Price, R. K. 1974. "Comparison of Four Numerical Methods for Flood Routing," Journal of the Hydraulics Division, American Society of Civil Engineers, Vol 100, No. HY7, pp 879-899.

Reid, R. O., and Bodine, B. R. 1968. "Numerical Model for Storm Surges in Galveston Bay," Journal of the Waterways and Harbors Division, American Society of Civil Engineers, Vol 94, No. WW1, pp 33-57.

Roesner, L. A., Aldrich, J. A., and Dickinson, R. E. 1989. "Storm Water Management Model User's Manual, Version 4: Extran Addendum," Environmental Research Laboratory, US Environmental Protection Agency, Athens, GA.

Seelig, W. N., Harris, D. L., and Herchenroder, B. E. 1977. "A Spatially Integrated Numerical Model of Inlet Hydraulics," GITI Report 14, Coastal Engineering Research Center, Fort Belvoir, VA.

Stoker, J. J. 1957. Water Waves, Intersciences Publishers, New York.

Strelkoff, T. 1970. "Numerical Solution of the Saint-Venant Equations," Journal of the Hydraulics Division, American Society of Civil Engineers, Vol 96, No. HY1, pp 223-252.

APPENDIX A: FILES FOR MASONBORO INLET

This appendix contains input and output files for the Masonboro Inlet, North Carolina, case study presented in Part V of the main text of this report. Files pertaining to both DYNLET1 and ACES-INLET are included. Plots of DYNLET1 calculations supplementing Part V are given at the end of this appendix.

START FILE

```
*********************************************************************
*                PROGRAM DYNLET1
*********************************************************************
*        MASONBORO INLET SYSTEM
*      CASE 2 (MAS69C2)
*      IMPLICIT NETWORK INLET MODEL
*         Banded Matrix  Implicit  Model
*     5 channels and 2 junctions
*    Station 6 corresponds to Throat Range 2
*    Station 18   corresponds to SHINN  CREEK Range 3
*    Station 12  corresponds to MASONBORO CHANNEL Range 5
*    Station 24  corresponds to BANKS CREEK   Range 4
*    Station 1   corresponds to SEA  Range 1
*          1   6    JETTY
*   FIELD DATA BY THE US ARMY CORPS OF ENGINEERS
*    ~
*********************************************************************
A     Computational Parameters
*********************************************************************
A.1  TO    Tfin yeps Qeps theta N IWIND
  6.00 21.00 0.05 50.0  1.0 25    0
A.2  units
ENGLISH
A.3 UNIT OF DISTANCE
FEET
*********************************************************************
B    Channel,Junction and External Boundary Nodes
*********************************************************************
B.1      NC  NJ   NB
         5  2    4
B.2   Channel No  Start at  End at
         1         1         7
         2         8        13
         3        14        15
         4        16        19
         5        20        25
B.3  Junction Number    How Many Nodes      Node numbers of Junction
      1                        3          7       8       14
      2                        3         15      16       20
B.4  Boundary Point   Node Number     Id    desc1   desc2
           1            19          2
           2            13          2
           3            25          2
           4             1          1
*******************************************************
C       Computational Parameters
*******************************************************
C.1         Computation Time Step in sec
    1800.0
```

```
C.2  Itern
      50
C.3  Number of Printout( Display) Times NP
  27
C.4    Print Times in Hours
  8.0  8.5  9.00   9.50   10.00          10.5   11.0  11.5  12.0 12.5
 13.0 13.5  14.0   14.5   15.0           15.5   16.0  16.5  17.0 17.5
 18.0 18.5  19.0  19.5    20.0           20.5   21.0
C.5    Number of Stations at which output is desired NoutN
 30
C.6     Output Stations
 1  6   18  23  12        1    2  3  4   5            6  7   8   9  10
11 12   13  14  15       16   17 18 19  20           21 22  23  24  25
*********************************************************************
D            Node Parameters
*********************************************************************
D.1    Values Of Distances at Channel Nodes: Node 1 to N
      0.0        500.0    1000.0   1500.0   1900.0
   2100.0       2600.0    2600.0   3100.0   3600.0
   4100.0       6200.0   70000.0   2600.0   2850.00
   2850.0       3650.0    4450.0 110000.0   2600.0
   3300.0       4100.0    4900.0   6100.0   90000.0
D.2    x-coordinate of left bank
-3000.0  -2500.0     -2000.0     -2000.0   -2000.0  -2000.0 -2000.0  -2000.0
-2200.0  -2400.0     -2600.0     -2800.0   -3000.0  -2000.0 -2000.0  -2000.0
-2000.0  -2000.0     -2000.0        0.0     200.0    400.0   600.0    -800.0
 -1000.0
D.3      y coordinate of the left bank
    0.0      500.0     1000.0     1500.0    1900.0     2100.0   2600.0  2600.0
 2600.0     2600.0     2600.0     2600.0    2600.0     2600.0   2850.0  2850.0

 3650.0     4452.0     5000.0     2850.0    2850.0     2850.0   2850.0  2850.0
 2850.0
D.4    Values of Lateral Inflow QL at each Node
 0.0  0.0 0.0 0.0 0.0        0.0 0.0 0.0 0.0 0.0
 0.0  0.0 0.0 0.0 0.0        0.0 0.0 0.0 0.0 0.0
 0.0  0.0 0.0 0.0 0.0
D.5     Values of Reference Elevation Z
 0.0  0.0 0.0 0.0 0.0        0.0 0.0 0.0 0.0 0.0
 0.0  0.0 0.0 0.0 0.0        0.0 0.0 0.0 0.0 0.0
 0.0  0.0 0.0 0.0 0.0
D.6    Values of Channel Alignment Angles
   90.0   90.0   90.0   90.0   90.0         90.0  90.0   0.0   0.0    0.0
    0.0    0.0    0.0   90.0   90.0         90.0  90.0  90.0  90.0 180.
  180.0  180.0  180.0  180.0  180.0
D.7  Transition Loss  Coefficients
 0.5  0.5 0.5 0.5 0.5        0.5 0.5 0.5 0.5 0.5
 0.5  0.5 0.5 0.5 0.5        0.5 0.5 0.5 0.5 0.5
 0.5  0.5 0.5 0.5 0.5
D.8  Values of Initial w.s. elev  YIN
    3.30  3.30   3.30   3.30    3.30   3.30   3.30   3.30   3.30  3.30
    3.30  3.30   3.30   3.30    3.30   3.30   3.30   3.30   3.30  3.30
```

```
    3.30  3.30   3.30   3.30    3.30
D.9    Values of Initial Discharge   QIN
  25000.0   25000.0  25000.0  25000.0  25000.0    25000.0  25000.0
  5000.0     5000.0   5000.0   5000.0   5000.0     5000.0
 24000.0    25000.0
  8000.0   8000.0   8000.0     8000.0
 12000.0    12000.0  12000.0  12000.0  12000.0    12000.0
```

SECTION

```
**********************************************************************
E        Cross Section  Geometry and Friction Coefficients, Masonboro Inlet
**********************************************************************
E.1   NODE   NUMBER    Number of Elevation Points 1S at J=27,1C at J=30,1N at
J=34
    1        37
E.2  Stations and Elevations
 200.0  -5.40  250.0  -5.5  300.0   -5.6   350.0  -5.70  400.0  -5.8
 450.0  -5.40  500.0  -5.0  550.0   -4.3   600.0  -4.70  650.0  -4.5
 700.0  -4.30  750.0  -4.0  800.0   -3.70  850.0  -3.20  900.0  -2.7
 950.0  -2.10 1000.0  -1.4 1050.0   -1.40 1100.0  -1.30 1150.0  -1.4
1200.0  -1.60 1250.0  -6.9 1300.0   -8.60 1350.0   0.0  1400.0  -2.50
1450.0  -8.50 1500.0 -11.5 1550.0  -20.0  1600.0 -20.0  1650.0 -16.0
1700.0 -15.0  1750.0 -14.0 1800.0  -14.0  1850.0 -11.0  1900.0  -9.50
1950.0  -7.50 2000.0   0.0
E.3  Manning's Coefficient of Friction
  0.0200 0.0200 0.0200 0.0200 0.0200 0.0200 0.0200 0.0200 0.0200 0.0200
  0.0200 0.0200 0.0200 0.0200 0.0200 0.0200 0.0200 0.0200 0.0200 0.0200
  0.0200 0.0200 0.0200 0.0200 0.0200 0.0200 0.0200 0.0200 0.0200 0.0200
  0.0200 0.0200 0.0200 0.0200 0.0200 0.0200 0.0200
E.1  NODE    NUMBER    Number of Elevation Points
    2        37
E.2  Stations and Elevations
  150.0   -0.0   200.0   -1.20  250.0  -1.70  300.0  -2.20  350.0  -2.70
  400.0   -3.30  450.0   -3.10  500.0  -2.90  550.0  -2.60  600.0  -2.30
  650.0   -1.80  700.0   -1.30  750.0  -0.80  800.0  -0.0   850.0  -0.50
  900.0   -1.0   950.0   -0.70 1000.0  -0.30 1050.0  -0.80 1100.0  -1.20
 1150.0   -3.0  1200.0   -4.70 1250.0 -14.30 1300.0 -19.50 1350.0 -20.60
 1400.0  -19.50 1450.0  -18.80 1500.0 -18.30 1550.0 -15.10 1600.0 -14.30
 1650.0  -13.50 1700.0  -12.70 1750.0 -10.70 1800.0  -8.70 1850.0  -8.90
 1900.0   -9.10 1950.0   -9.30
E.3  Manning's Coefficient of Friction
  0.0200 0.0200 0.0200 0.0200 0.0200 0.0200 0.0200 0.0200 0.0200 0.0200
  0.0200 0.0200 0.0200 0.0200 0.0200 0.0200 0.0200 0.0200 0.0200 0.0200
  0.0200 0.0200 0.0200 0.0200 0.0200 0.0200 0.0200 0.0200 0.0200 0.0200
  0.0200 0.0200 0.0200 0.0200 0.0200 0.0200 0.0200
```

```
E.1  NODE     NUMBER     Number of Elevation Points
   3          37
E.2  Stations and Elevations
 150.0    5.0    200.0   -2.6    250.0   -2.50  300.0   -2.40  350.0   -2.20
 400.0   -2.10   450.0   -1.9    500.0   -1.40  550.0   -0.90  600.0   -0.40
 650.0   -0.60   700.0   -0.8    750.0   -0.90  800.0   -1.0   850.0   -1.40
 900.0   -1.70   950.0   -2.10 1000.0   -2.40 1050.0   -6.10 1100.0   -9.80
1150.0  -11.60 1200.0  -13.4   1250.0  -15.60 1300.0  -17.70 1350.0  -17.60
 1400.0  -17.60 1450.0  -15.7 1500.0  -13.80 1550.0  -15.0  1600.0  -16.20
 1650.0  -13.40 1700.0  -10.5 1750.0   -9.50 1800.0   -8.40 1850.0   -8.30
 1900.0   -8.20 1950.0   -8.10
E.3  Manning's Coefficient of Friction
  0.0200 0.0200 0.0200 0.0200 0.0200 0.0200 0.0200 0.0200 0.0200 0.0200
  0.0200 0.0200 0.0200 0.0200 0.0200 0.0200 0.0200 0.0200 0.0200 0.0200
  0.0200 0.0200 0.0200 0.0200 0.0200 0.0200 0.0200 0.0200 0.0200 0.0200
  0.0200 0.0200 0.0200 0.0200 0.0200 0.0200 0.0200
E.1  NODE     NUMBER     Number of Elevation Points
   4          35
E.2  Stations and Elevations
 150.0    5.0    200.0  -3.10  250.0  -3.40  300.0  -3.70   350.0   -4.10
 400.0  -4.40   450.0  -3.30  500.0  -2.20  550.0  -1.10   600.0   -0.10
 650.0  -0.10   700.0  -0.10  750.0  -0.10  800.0  -0.20   850.0   -0.50
 900.0  -0.90   950.0  -6.10 1000.0  -11.30 1050.0 -15.90 1100.0  -20.40
1150.0  -25.40 1200.0 -20.0 1250.0  -16.80 1300.0 -14.80 1350.0  -15.40
1400.0  -16.0 1450.0  -14.20 1500.0  -12.30 1550.0  -9.80 1600.0  -7.20
 1650.0  -5.70 1700.0   -4.10 1750.0   -3.40 1800.0  -2.70 1850.0   5.0
E.3  Manning's Coefficient of Friction
  0.0200 0.0200 0.0200 0.0200 0.0200 0.0200 0.0200 0.0200 0.0200 0.0200
  0.0200 0.0200 0.0200 0.0200 0.0200 0.0200 0.0200 0.0200 0.0200 0.0200
  0.0200 0.0200 0.0200 0.0200 0.0200 0.0200 0.0200 0.0200 0.0200 0.0200
  0.0200 0.0200 0.0200 0.0200 0.0200
E.1  NODE     NUMBER     Number of Elevation Points
   5          29
E.2  Stations and Elevations
 200.0   -0.0    250.0   -1.10  300.0  -2.10  350.0  -3.30  400.0  -4.40
 450.0  -3.90    500.0   -3.40  550.0  -2.90  600.0   -2.90  650.0  -2.90
 700.0  -2.8     750.0   -2.8   800.0  -24.20  850.0  -24.2   900.0  -24.3
 950.0  -24.40   1000.0 -20.0   1050.0 -18.0   1100.0  -17.60  1150.0  -16.90
 1200.0  -16.1 1250.0  -14.3 1300.0 -12.50 1350.0 -10.7 1400.0  -8.90
 1450.0  -6.7 1500.0   -4.5 1550.0  -2.20   1600.0  -0.0
E.3  Manning's Coefficient of Friction
  0.0200 0.0200 0.0200 0.0200 0.0200 0.0200 0.0200 0.0200 0.0200 0.0200
  0.0200 0.0200 0.0200 0.0200 0.0200 0.0200 0.0200 0.0200 0.0200 0.0200
  0.0200 0.0200 0.0200 0.0200 0.0200 0.0200 0.0200 0.0200 0.0200
E.1  NODE     NUMBER     Number of Elevation Points 2S at J=4,2C at J=7,2N at
J=11
   6          20
E.2  Stations and Elevations
   0.0   -0.0    50.0   -4.30  100.0   -6.50  150.0  -15.0  200.0  -22.0
 250.0  -27.50  300.0  -28.0  350.0  -25.50  400.0  -24.0  450.0  -21.0
 500.0  -15.40  550.0  -12.0  600.0   -8.50  650.0   -6.0  700.0   -5.50
 750.0   -4.0  800.0   -2.0  850.0     5.0  900.0    5.0  950.0    5.0
```

```
E.3  Manning's Coefficient of Friction
  0.0200 0.0200 0.0200 0.0200 0.0200 0.0200 0.0200 0.0200 0.0200 0.0200
  0.0200 0.0200 0.0200 0.0200 0.0200 0.0200 0.0200 0.0200 0.0200 0.0200
E.1  NODE     NUMBER     Number of Elevation Points
    7         30
E.2  Stations and Elevations
   0.0     5.0    50.0     5.0  100.0     5.0  150.0     5.0  200.0     5.0
 250.0     5.0   300.0     5.0  350.0    -0.0  400.0    -4.8  450.0    -4.7
 500.0    -4.60  550.0    -4.5  600.0    -4.3  650.0    -4.2  700.0    -3.9
 750.0    -3.60  800.0    -3.2  850.0    -3.3  900.0    -3.4  950.0   -10.0
1000.0   -22.2  1050.0   -19.1 1100.0   -15.9 1150.0   -15.5 1200.0   -15.1
1250.0   -13.8  1300.0   -12.4 1350.0   -11.4 1400.0   -10.3 1450.0    -0.0
E.3  Manning's Coefficient of Friction
  0.0200 0.0200 0.0200 0.0200 0.0200 0.0200 0.0200 0.0200 0.0200 0.020
  0.0200 0.0200 0.0200 0.0200 0.0200 0.0200 0.0200 0.0200 0.0200 0.020
  0.0200 0.0200 0.0200 0.0200 0.0200 0.0200 0.0200 0.0200 0.0200 0.020
E.1  NODE     NUMBER     Number of Elevation Points
    8         30
E.2  Stations and Elevations
   0.0     5.0    50.0     5.0  100.0     5.0  150.0     5.0  200.0     5.0
 250.0     5.0   300.0     5.0  350.0    -0.0  400.0    -4.8  450.0    -4.7
 500.0    -4.6   550.0    -4.5  600.0    -4.3  650.0    -4.2  700.0    -3.9
 750.0    -3.6   800.0    -3.2  850.0    -3.3  900.0    -3.4  950.0   -10.0
1000.0   -22.2  1050.0   -19.1 1100.0   -15.9 1150.0   -15.5 1200.0   -15.1
1250.0   -13.8  1300.0   -12.4 1350.0   -11.4 1400.0   -10.3 1450.0    -0.0
E.3  Manning's Coefficient of Friction
  0.0200 0.0200 0.0200 0.0200 0.0200 0.0200 0.0200 0.0200 0.0200 0.0200
  0.0200 0.0200 0.0200 0.0200 0.0200 0.0200 0.0200 0.0200 0.0200 0.0200
  0.0200 0.0200 0.0200 0.0200 0.0200 0.0200 0.0200 0.0200 0.0200 0.0200
E.1  NODE     NUMBER     Number of Elevation Points
    9         20
E.2  Stations and Elevations
   0.0     5.0    50.0     5.0  100.0     5.0  150.0     5.0  200.0    -3.2
 250.0    -4.7   300.0    -6.4  350.0    -5.6  400.0    -5.3  450.0    -4.7
 500.0    -4.2   550.0    -3.8  600.0    -3.5  650.0    -5.8  700.0    -8.1
 750.0    -8.6   800.0    -9.0  850.0    -5.0  900.0    -1.0  950.0    -0.0
E.3  Manning's Coefficient of Friction
  0.0375  0.0375  0.0375  0.0375  0.0375  0.0375  0.0375  0.0375  0.0375
0.0375
  0.0375  0.0375  0.0375  0.0375  0.0375  0.0375  0.0375  0.0375  0.0375
0.0375
E.1  NODE     NUMBER     Number of Elevation Points
   10         20
E.2  Stations and Elevations
   0.0     5.0    50.0     5.0  100.0    -5.0  150.0    -5.0  200.0    -5.0
 250.0    -5.5   300.0    -6.0  350.0    -5.4  400.0    -4.8  450.0    -4.2
 500.0    -3.5   550.0     5.0  600.0     5.0  650.0     5.0  700.0     5.0
 750.0     5.0   800.0     5.0  850.0     5.0  900.0     5.0  950.0     5.0
E.3  Manning's Coefficient of Friction
  0.035  0.035  0.035  0.035  0.035  0.035  0.035  0.035  0.035  0.035
  0.035  0.035  0.035  0.035  0.035  0.035  0.035  0.035  0.035  0.035
```

```
E.1  NODE     NUMBER     Number of Elevation Points
   11         20
E.2  Stations and Elevations
   0.0     5.0    50.0    -0.0  100.0    -5.0  150.0    -5.0  200.0    -5.0
 250.0    -5.50  300.0    -6.0  350.0    -5.4  400.0    -4.8  450.0    -4.2
 500.0    -3.50  550.0    -0.0  600.0     5.0  650.0     5.0  700.0     5.0
 750.0     5.0   800.0     5.0  850.0     5.0  900.0     5.0  950.0     5.0
E.3  Manning's Coefficient of Friction
  0.035  0.035  0.035  0.035  0.035  0.035  0.035  0.035  0.035  0.035
  0.035  0.035  0.035  0.035  0.035  0.035  0.035  0.035  0.035  0.035
E.1  NODE     NUMBER     Number of Elevation Points 5E at J=4, 5C at J=6, 5W at
J=11
   12         20
E.2  Stations and Elevations
   0.0     5.0    50.0    -0.0  100.0    -5.0  150.0    -7.0  200.0    -7.0
 250.0    -7.0   300.0    -7.0  350.0    -7.0  400.0    -4.8  450.0    -5.0
 500.0    -5.0   550.0    -2.5  600.0     0.0  650.0     5.0  700.0     5.0
 750.0     5.0   800.0     5.0  850.0     5.0  900.0     5.0  950.0     5.0
E.3  Manning's Coefficient of Friction
  0.035  0.035  0.035  0.035  0.035  0.035  0.035  0.035  0.035  0.035
  0.035  0.035  0.035  0.035  0.035  0.035  0.035  0.035  0.035  0.035
E.1  NODE     NUMBER     Number of Elevation Points
   13         13
E.2  Stations and Elevations
   0.0   -40.0    50.0   -40.0  100.0   -40.0  150.0   -45.0  200.0   -40.0
 250.0   -40.0   300.0   -40.0  350.0   -40.4  400.0   -40.8  450.0   -40.0
 500.0   -40.0   550.0   -40.0  600.0   -40.0
E.3  Manning's Coefficient of Friction
  0.0350 0.0350 0.0350 0.0350 0.0350 0.0350 0.0350 0.0350 0.0350 0.035
  0.0350 0.0350 0.035
E.1  NODE     NUMBER     Number of Elevation Points
   14         20
E.2  Stations and Elevations
   0.0    -4.6    50.0    -4.50  100.0    -4.30  150.0    -4.20  200.0    -3.9
 250.0    -3.6   300.0    -3.20  350.0    -3.30  400.0    -3.40  450.0   -10.0
 500.0   -22.2   550.0   -19.10  600.0   -15.90  650.0   -15.50  700.0   -15.1
 750.0   -13.8   800.0   -12.40  850.0   -11.40  900.0   -10.30  950.0    -0.0
E.3  Manning's Coefficient of Friction
  0.0350 0.0350 0.0350 0.0350 0.0350 0.0350 0.0350 0.0350 0.0350 0.035
  0.0350 0.0350 0.0350 0.0350 0.0350 0.0350 0.0350 0.0350 0.0350 0.035
E.1  NODE     NUMBER     Number of Elevation Points
   15         23
E.2  Stations and Elevations
   0.0     5.0    50.0    -0.0  100.0    -5.0  150.0    -5.0  200.0    -6.80
 250.0    -8.5   300.0    -9.0  350.0    -9.5  400.0   -11.3  450.0   -13.10
 500.0   -14.1   550.0   -15.1  600.0   -16.1  650.0   -12.8  700.0    -9.50
 750.0    -8.6   800.0    -8.2  850.0    -7.8  900.0    -7.4  950.0    -7.0
1000.0    -6.4  1050.0    -6.1 1100.0    -8.6
E.3  Manning's Coefficient of Friction
  0.0350 0.0350 0.0350 0.0350 0.0350 0.0350 0.0350 0.0350 0.0350 0.035
  0.0350 0.0350 0.0350 0.0350 0.0350 0.0350 0.0350 0.0350 0.0350 0.035
  0.0350 0.0350 0.035
```

```
E.1  NODE     NUMBER     Number of Elevation Points
   16         23
E.2  Stations and Elevations
   0.0     5.0    50.0    -0.0  100.0    -5.0  150.0    -5.0  200.0    -6.80
 250.0    -8.50  300.0   -9.0  350.0    -9.5  400.0   -11.3  450.0   -13.10
 500.0   -14.10  550.0 -15.1  600.0   -16.1  650.0   -12.8  700.0    -9.5
 750.0    -8.60  800.0   -8.2  850.0    -7.8  900.0    -7.4  950.0    -7.0
1000.0    -6.40 1050.0   -6.1 1100.0    -8.6
E.3  Manning's Coefficient of Friction
  0.0350 0.0350 0.0350 0.0350 0.0350 0.0350 0.0350 0.0350 0.0350 0.035
  0.0350 0.0350 0.0350 0.0350 0.0350 0.0350 0.0350 0.0350 0.0350 0.035
  0.0350 0.0350 0.035
E.1  NODE     NUMBER     Number of Elevation Points
   17         13
E.2  Stations and Elevations
   0.0     5.0    50.0     5.0  100.0     5.0  150.0    -0.0  200.0   -10.40
 250.0   -12.2  300.0   -14.1  350.0   -15.9  400.0   -17.3  450.0   -17.0
 500.0   -16.60  550.0    -0.0  600.0     5.0
E.3  Manning's Coefficient of Friction
  0.035  0.035  0.035  0.035  0.035  0.035  0.035  0.035  0.035  0.035
  0.035  0.035  0.035
E.1  NODE     NUMBER     Number of Elevation Points
   18         13
E.2  Stations and Elevations
   0.0     5.0    50.0     5.0  100.0     5.0  150.0    -0.0  200.0   -10.40
 250.0   -12.2   300.0   -14.1  350.0   -15.9  400.0   -17.3  450.   -17.0
 500.0   -16.6  550.0    -0.0  600.0     5.0
E.3  Manning's Coefficient of Friction
  0.035  0.035  0.035  0.035  0.035  0.035  0.035  0.035  0.035  0.035
  0.035  0.035  0.035
E.1  NODE     NUMBER     Number of Elevation Points
   19         13
E.2  Stations and Elevations
   0.0   -40.0    50.0   -40.0  100.0   -40.0  150.0   -40.0  200.0   -40.0
 250.0   -40.0  300.0   -40.1  350.0   -40.9  400.0   -40.3  450.0   -40.0
 500.0   -40.6  550.0   -40.0  600.0   -40.0
E.3  Manning's Coefficient of Friction
  0.035  0.035  0.035  0.035  0.035  0.035  0.035  0.035  0.035  0.035
  0.035  0.035  0.035
E.1  NODE     NUMBER     Number of Elevation Points
   20         23
E.2  Stations and Elevations
   0.0     5.0    50.0    -0.0  100.0    -5.0  150.0    -5.0  200.0    -6.80
 250.0    -8.5  300.0   -9.0  350.0    -9.5  400.0   -11.3  450.0   -13.10
 500.0   -14.1  550.0   -15.1  600.0   -16.1  650.0   -12.8  700.0    -9.50
 750.0    -8.6  800.0   -8.2  850.0    -7.8  900.0    -7.4  950.0    -7.0
1000.0    -6.4 1050.0   -6.1 1100.0    -8.6
E.3  Manning's Coefficient of Friction
  0.0350 0.0350 0.0350 0.0350 0.0350 0.0350 0.0350 0.0350 0.0350 0.035
  0.0350 0.0350 0.0350 0.0350 0.0350 0.0350 0.0350 0.0350 0.0350 0.035
  0.0350 0.0350  0.0350
```

```
E.1  NODE     NUMBER     Number of Elevation Points
   21         12
E.2  Stations and Elevations
   0.0    5.0    50.0   -5.0  100.0   -6.8  150.0   -8.6  200.0   -9.3
 250.0  -10.0   300.0  -11.6  350.0  -13.2  400.0   -9.10 450.0   -5.0
 500.0   -0.0   550.0    5.0
E.3  Manning's Coefficient of Friction
  0.035  0.035  0.035  0.035  0.035  0.035  0.035  0.035  0.035  0.035
  0.035  0.035
E.1  NODE     NUMBER     Number of Elevation Points
   22         12
E.2  Stations and Elevations
   0.0    5.0    50.0   -5.0  100.0   -6.8  150.0   -8.6  200.0   -9.30
 250.0  -10.0   300.0  -11.6  350.0  -13.2  400.0   -9.1  450.0   -5.0
 500.0   -0.0   550.0    5.0
E.3  Manning's Coefficient of Friction
  0.035  0.035  0.035  0.035  0.035  0.035  0.035  0.035  0.035  0.035
  0.035  0.035
E.1  NODE     NUMBER     Number of Elevation Points
   23         20
E.2   Stations and Elevations
   0.0    5.0    50.0   -5.0  100.0  -10.0  150.0  -15.0  200.0  -12.0
 250.0  -20.5   300.0   -9.5  350.0  -19.5  400.0  -16.0  450.0  -19.50
 500.0  -19.0   550.0  -12.5  600.0   -5.0  650.0   -9.0  700.0   -8.0
 750.0   -7.0   800.0   -7.0  850.0   -2.0  900.0   -0.50  950.0    5.0
E.3  Manning's Coefficient of Friction
  0.035  0.035  0.035  0.035  0.035  0.035  0.035  0.035  0.035  0.035
  0.035  0.035  0.035  0.035  0.035  0.035  0.035  0.035  0.035  0.035
E.1  NODE     NUMBER     Number of Elevation Points  4E at J=9,
   24         20
E.2   Stations and Elevations
   0.0    5.0    50.0    5.0  100.0   -5.0  150.0   -5.0  200.0   -5.0
 250.0   -5.0   300.0   -5.0  350.0   -7.50  400.0  -10.0  450.0  -12.0
 500.0  -13.90  550.0  -10.0  600.0  -10.0  650.0  -10.0  700.0  -10.0
 750.0  -10.0   800.0  -10.0  850.0  -10.0  900.0  -10.0  950.0    5.0
E.3  Manning's Coefficient of Friction
  0.035  0.035  0.035  0.035  0.035  0.035  0.035  0.035  0.035  0.035
  0.035  0.035  0.035  0.035  0.035  0.035  0.035  0.035  0.035  0.035
E.1  NODE     NUMBER     Number of Elevation Points
   25         20
E.2   Stations and Elevations
   0.0  -40.0    50.0  -40.0  100.0  -40.0  150.0  -40.0  200.0  -40.0
 250.0  -40.0   300.0  -40.0  350.0  -40.0  400.0  -40.0  450.0  -40.0
 500.0  -40.9   550.0  -40.0  600.0  -40.0  650.0  -40.0  700.0 -40.0
 750.0  -40.0   800.0  -40.0  850.0  -40.0  900.0  -40.0  950.0  -40.0
E.3  Manning's Coefficient of Friction
  0.035  0.035  0.035  0.035  0.035  0.035  0.035  0.035  0.035  0.035
  0.035  0.035  0.035  0.035  0.035  0.035  0.035  0.035  0.035  0.035
```

****
F Time-Dependent Data, Masonboro Inlet
****

F.1	index	time	Ust(1,L)	Ust(2,L)	Ust(3,L)	Ust(4,L)
1	6.5	3.30	4.20	4.20	4.6	
1	7.0	4.0	4.20	4.20	4.6	
1	7.5	4.20	4.20	4.20	4.6	
2	8.0	4.4	4.4	4.4	4.5	
3	8.5	4.12	4.12	4.12	4.20	
4	9.0	4.0	4.0	4.0	4.0	
5	9.25	3.95	3.95	3.95	3.6	
5	9.50	3.70	3.7	3.70	3.50	
6	10.00	3.40	3.40	3.40	3.00	
7	10.50	2.90	2.90	2.90	2.40	
8	11.00	2.40	2.40	2.45	1.75	
9	11.50	2.00	2.00	2.00	1.20	
10	12.00	1.60	1.60	1.60	0.75	
11	12.50	1.20	1.20	1.20	0.45	
12	13.00	1.00	1.00	1.00	0.30	
13	13.50	0.65	0.65	0.65	0.15	
14	14.00	0.70	0.70	0.70	0.20	
14	14.50	0.70	0.70	0.70	0.50	
15	15.00	0.80	0.80	0.80	0.75	
16	15.50	1.00	1.00	1.00	1.00	
17	16.00	1.6	1.60	1.60	1.60	
18	16.50	2.10	2.10	2.10	2.20	
19	17.00	2.75	2.75	2.75	3.00	
20	17.50	3.00	3.00	3.00	3.40	
21	18.00	3.35	3.35	3.35	3.60	
21	18.50	3.65	3.65	3.65	3.85	
23	19.00	3.90	3.90	3.90	4.10	
24	19.50	4.10	4.10	4.10	4.30	
25	20.00	4.30	4.30	4.30	4.40	
26	20.50	4.30	4.30	4.30	4.35	
27	21.00	4.10	4.10	4.10	3.90	
28	21.50	3.87	3.87	3.87	3.78	
29	22.00	3.65	3.65	3.65	3.65	
30	23.00	3.43	3.05	3.05	2.50	

PARAM (Masonboro Inlet)

```
Number of Current Gages in the Field
5
Number of  Stations at the Current Gage
3
LOCATIONS OF VELOCITY OUTPUTS: RANGE 1
 1S        1C        1N
Computed Velocity Cross Section Number
1
Number of  velocity outputs          Stations numbers
5                                     26  27  30 31 33  35
Number of  Stations at the Current Gage
3
LOCATIONS OF VELOCITY OUTPUTS: RANGE 2
  2S       2C        2N
Computed Velocity Cross Section Number
6
Number of Velocity Output Locations   Station Numbers
6                                       4 5  7 8  11 12
Number of  Stations at the Current Gage
3
LOCATIONS OF VELOCITY OUTPUTS: RANGE 3
  3S      3C        3N
Computed Velocity Cross Section Number
18
Number of Velocity Output Locations   Station Numbers
4                                 4  8   10   11
Number of  Stations at the Current Gage
3
LOCATIONS OF VELOCITY OUTPUTS: RANGE 4
  4E       4C       4W
Computed Velocity Cross Section Number
24
Number of Velocity Output Locations   Station Numbers
3                                     5  9  15
Number of  Stations at the Current Gage
3
LOCATIONS OF VELOCITY OUTPUTS: RANGE 5
  5E      5C      5W
Computed Velocity Cross Section Number
12
Number of Velocity Output Locations   Station Numbers
3                                    4  6  7 9 11
Number of Tide Gages
5
Identification of Tide Gages
Range1  Range2   Range3  Range4 Range5
1       6          18      24    12
```

VOBSD.DAT

FILE FOR MASONBORO INLET
(VALUES OF MEASURED VELOCITIES AT GAGING STATIONS)

V(1S) Time hour	V(1C) velocity (ft/s)	V(1N) (ft/s)	(ft/s)
8	0	-0.07	0
8.5	0.5	-0.55	-0.6
9	-1.42	-1.67	-1.28
9.5	-2.72	-2.84	-2.1
10	-3.61	-3.61	-2.6
10.5	-3.6	-3.69	-2.63
11	-3.93	-4.26	-3.2
11.5	-4.4	-4.85	-3.7
12	-3.7	-4.31	-3.44
12.5	-3.58	-4.24	-3.25
13	-2.84	-4.25	-3.02
13.5	-2.54	-3.42	-2.91
14	-2	-2.74	-2.19
14.5	-0.95	-1.55	-1.18
15	0.23	0.15	-0.1
15.5	1.2	1.05	0.95
16	1.7	1.75	1.3
16.5	1.88	2.05	1.31
17	1.94	2.04	1.35
17.5	1.85	1.95	1.3
18	1.85	1.7	1.25
18.5	1.48	1.5	1.27
19	1.52	1.49	0.98
19.5	1.33	1.18	0.75
20	0.95	0.95	0.45
20.5	-0.15	0.3	-0.15
21	-0.97	0	0

V(2S) Time (hrs)	V(2C) Velocity (ft/s)	V(2N) (ft/s)	(ft/s)
8	1.2	1.4	1.16
8.5	0.06	0.95	0.56
9	-1.64	-1.6	0.20
9.5	-3.12	-3.17	-0.78
10	-3.64	-3.5	-1.11
10.5	-4.28	-4.47	-0.70
11	-4.71	-4.9	-0.40
11.5	-4.86	-4.48	-0.55
12	-4.47	-3.84	-0.10
12.5	-4.37	-3.6	-0.16
13	-3.37	-3.05	-0.25
13.5	-2.79	-2.72	-0.15
14	-2.23	-2	-0.15

14.5	-0.99	-1.05	0.35
15	0.6	0.55	0.55
15.5	0.91	1.1	1.15
16	1.81	2.63	2.15
16.5	2.1	2.7	2.56
17	2.6	3.15	2.85
17.5	2.74	3.11	3.05
18	2.87	3.1	2.75
18.5	2.94	3.05	2.72
19	3	3.05	2.72
19.5	2.5	2.61	2.40
20	1.78	1.97	1.95
20.5	0.6	0.805	0.97
21	-1.74	-1.59	0.34

Time (hr)	V(5E) Velocity (ft/s)	V(5C) Velocity (ft/s)	V(5W) Velocity (ft/s)
8	1.1	0.9	1
8.5	0.5	0.5	0.4
9	-0.4	-0.5	-0.4
9.5	-1.4	-1.5	-1.5
10	-1.7	-1.9	-1.8
10.5	-1.8	-2.2	-1.8
11	-2	-2.2	-1.9
11.5	-1.9	-2.2	-1.9
12	-2	-2.2	-1.9
12.5	-1.9	-2.1	-1.7
13	-1.6	-1.8	-1.5
13.5	-0.4	-1.5	-1.3
14	-1.2	-1.2	-1
14.5	-0.7	-0.5	-0.5
15	0.3	0.3	0.2
15.5	0.8	1	0.8
16	1.1	1.4	1.3
16.5	1.4	1.5	1.5
17	1.75	1.8	1.9
17.5	1.6	2.1	2
18	1.8	1.8	2
18.5	1.75	1.8	2.1
19	1.75	1.7	2
19.5	0.5	1.6	1.7
20	0.4	0.5	1.5
20.5	0.8	0.5	0.5
21	-0.5	-0.5	0

Time (hr)	V(3S) Velocity (ft/s)	V(3C) Velocity (ft/s)	V(3N) Velocity (ft/s)
8	1	1.04	1.45
8.5	0.5	0.5	0.52
9	-0.5	-0.55	-0.56
9.5	-0.2	-1.45	-1.54
10	-0.2	-1.84	-2.16

10.5	0.1	-2.08	-2.42
11	-0.25	-2.59	-2.82
11.5	0.9	-2.47	-2.86
12	0.5	-2.3	-2.78
12.5	-0.4	-1.94	-2.46
13	0.2	-1.83	-2.1
13.5	-0.4	-1.1	-1.85
14	0.5	-1.12	-1.42
14.5	0.22	-0.69	-0.95
15	0.9	-0.32	0
15.5	0.4	0.45	0.57
16	0.85	1	1.21
16.5	1.58	1.8	1.93
17	1.77	2.2	2.3
17.5	2.02	2.39	2.31
18	1.53	2.26	2.35
18.5	1.74	2.14	2.27
19	1.82	1.95	2.26
19.5	1.55	1.59	2.1
20	1.18	1.16	1.68
20.5	0.45	0.52	0.45
21	-0.4	-0.47	-0.5

Time (hr)	V(4E)	V(4C)	V(4W)
	Velocity		
8	1.08	0.71	-0.33
8.5	-0.03	0.2	-0.48
9	-0.6	-0.63	-0.56
9.5	-1.17	-1.15	-0.5
10	-1.57	-1.4	-0.35
10.5	-1.52	-1.3	-0.42
11	-1.8	-1.36	-0.48
11.5	-2.03	-1.66	-0.47
12	-1.82	-1.45	-0.38
12.5	-1.6	-1.33	-0.16
13	-1.32	-1.05	-0.17
13.5	-1.38	-0.97	-0.02
14	-0.69	-0.74	-0.14
14.5	-0.4	-0.04	-0.03
15	0.45	0.25	0.35
15.5	0.45	0.67	0.65
16	1.1	0.87	0.7
16.5	1.14	0.86	0.65
17	1.43	1.05	0.5
17.5	1.41	1.1	0.55
18	1.16	1.08	0.37
18.5	1.21	1.5	0.6
19	1.27	1.54	0.6
19.5	0.91	1.16	0.53
20	0.62	1	0.44
20.5	1.12	0.27	-0.35
21	1.62	0	0

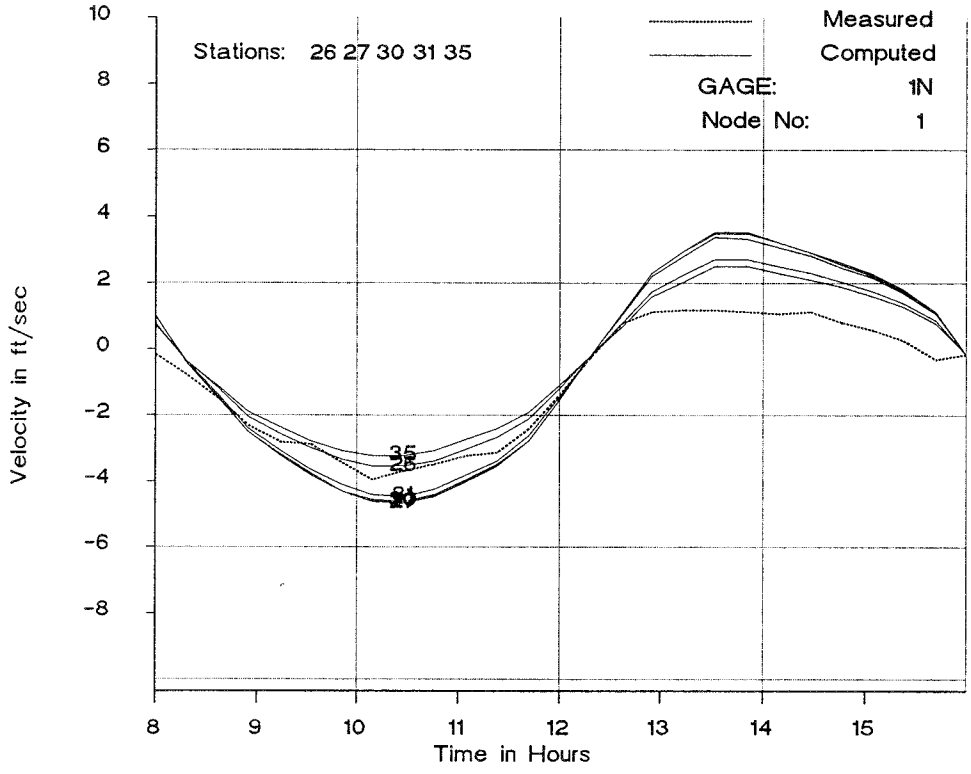
Stations: 26 27 30 31 35
Measured
Computed
GAGE: 1N
Node No: 1
Velocity in ft/sec
Time in Hours
35
26
31
30

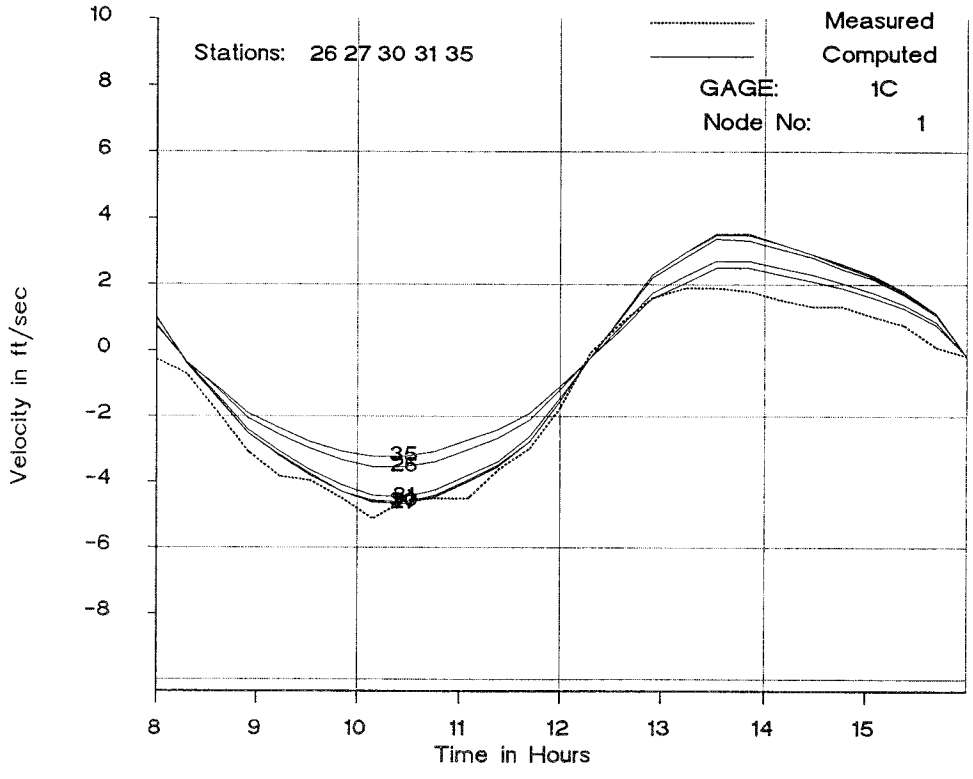
Stations: 26 27 30 31 35
Measured
Computed
GAGE: 1C
Node No: 1
Velocity in ft/sec
Time in Hours
35
26
31
30

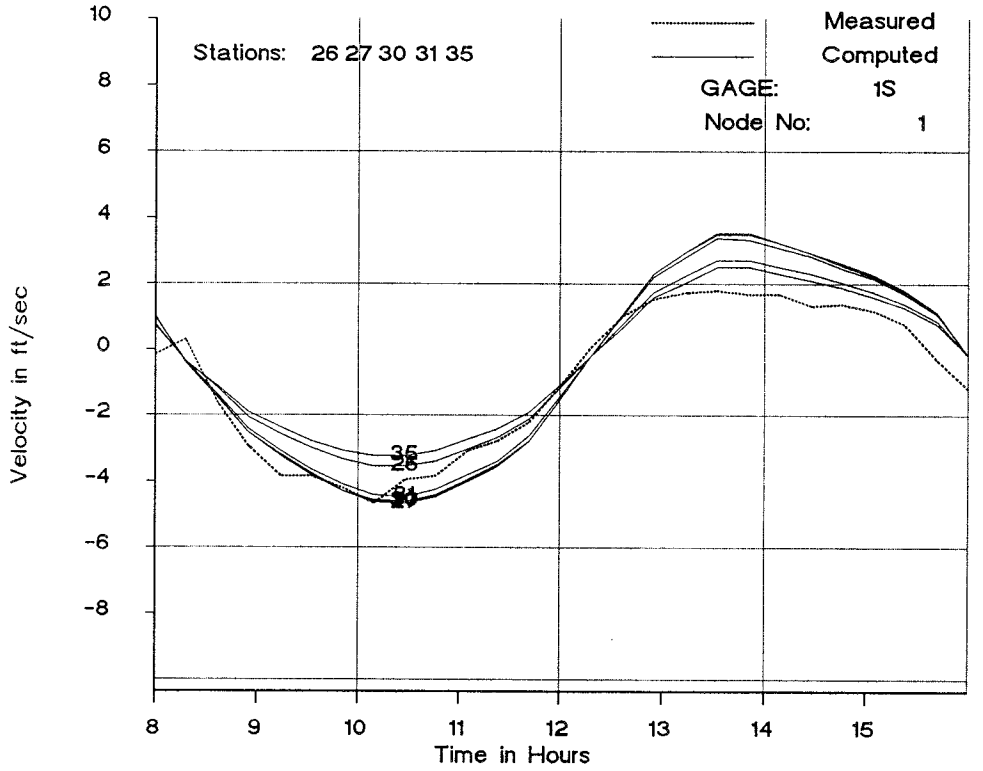
Stations: 26 27 30 31 35
Measured
Computed
GAGE: 1S
Node No: 1
Velocity in ft/sec
Time in Hours
10
8
6
4
2
0
-2
-4
-6
-8
8
9
10
11
12
13
14
15
35
26

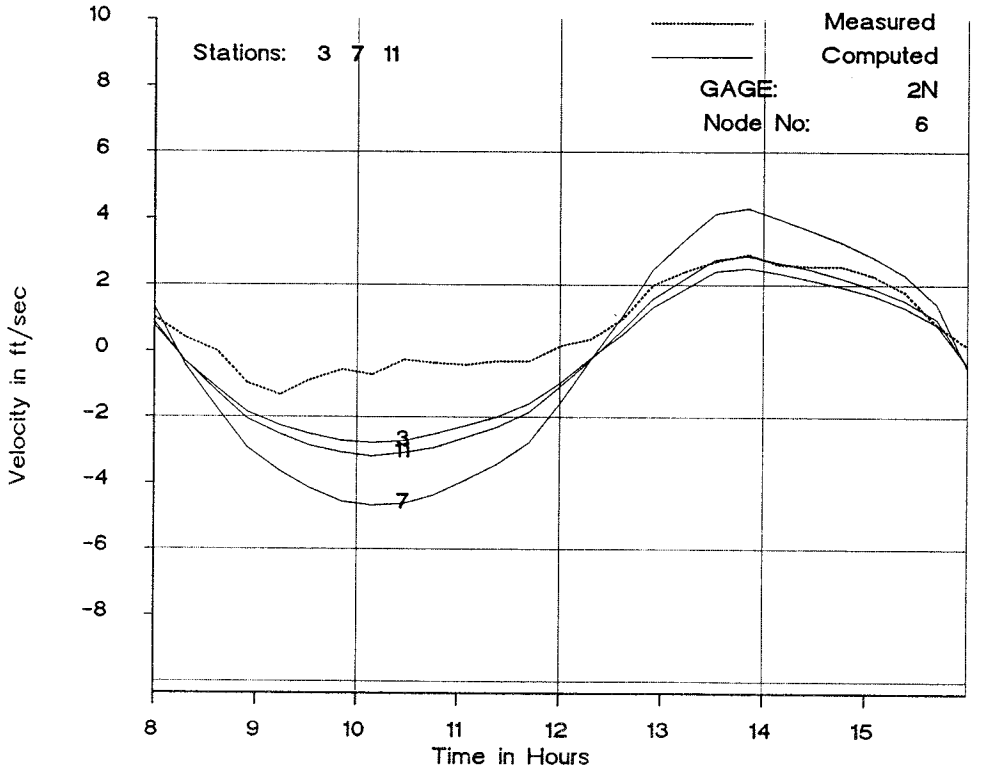
Stations: 3 7 11
Measured
Computed
GAGE: 2N
Node No: 6
Velocity in ft/sec
Time in Hours
10
8
6
4
2
0
-2
-4
-6
-8
8
9
10
11
12
13
14
15
3
11
7

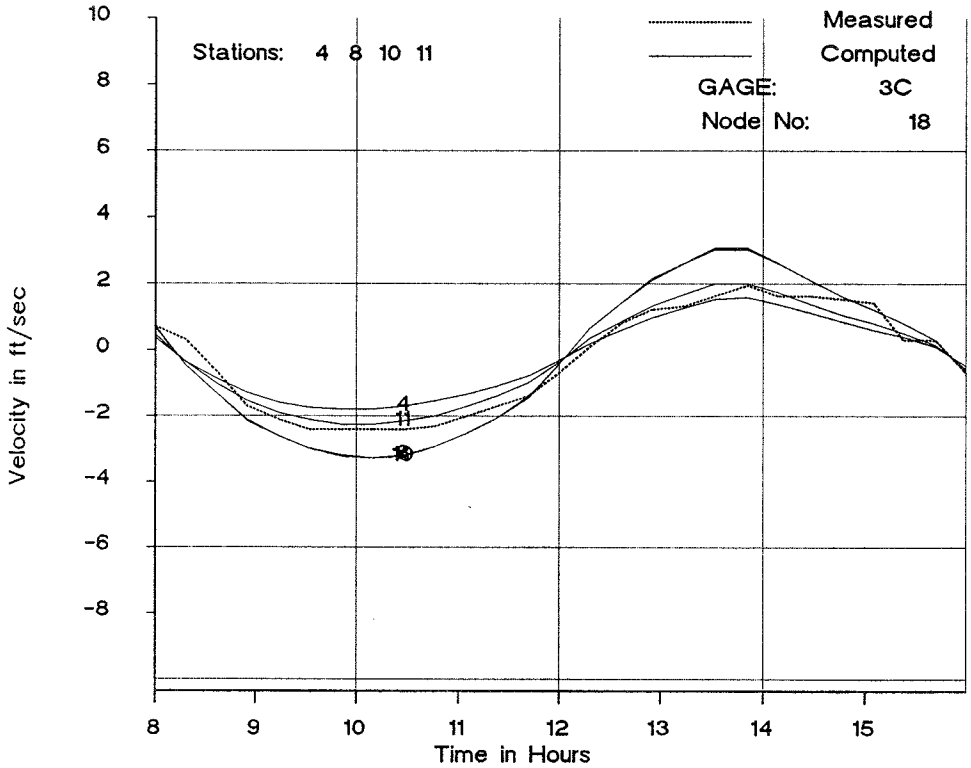
Stations: 4 8 10 11
Measured
Computed
GAGE: 3C
Node No: 18
Velocity in ft/sec
Time in Hours

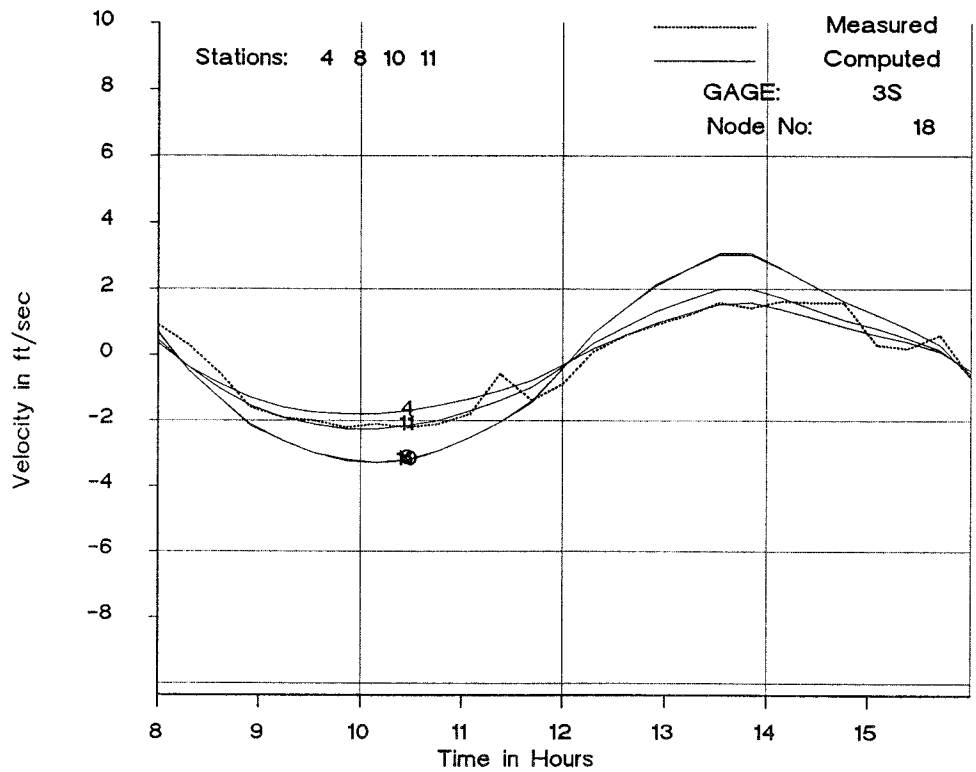
Stations: 4 8 10 11
Measured
Computed
GAGE: 3S
Node No: 18
Velocity in ft/sec
Time in Hours

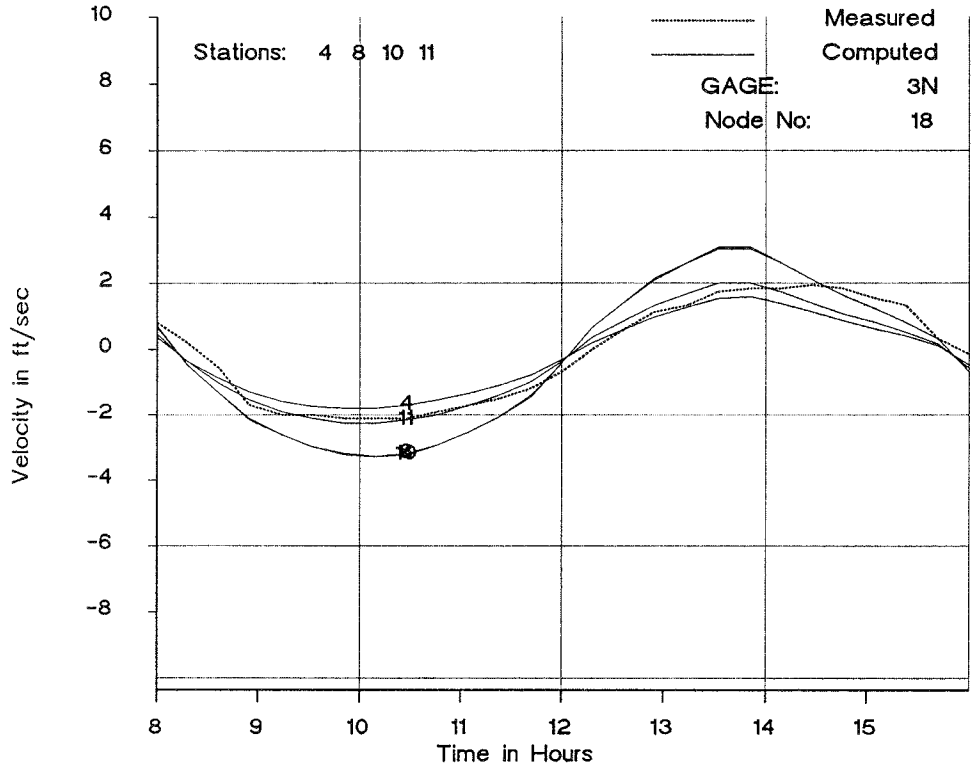
Stations: 4 8 10 11
Measured
Computed
GAGE: 3N
Node No: 18
Velocity in ft/sec
Time in Hours
10
8
6
4
2
0
-2
-4
-6
-8
8
9
10
11
12
13
14
15

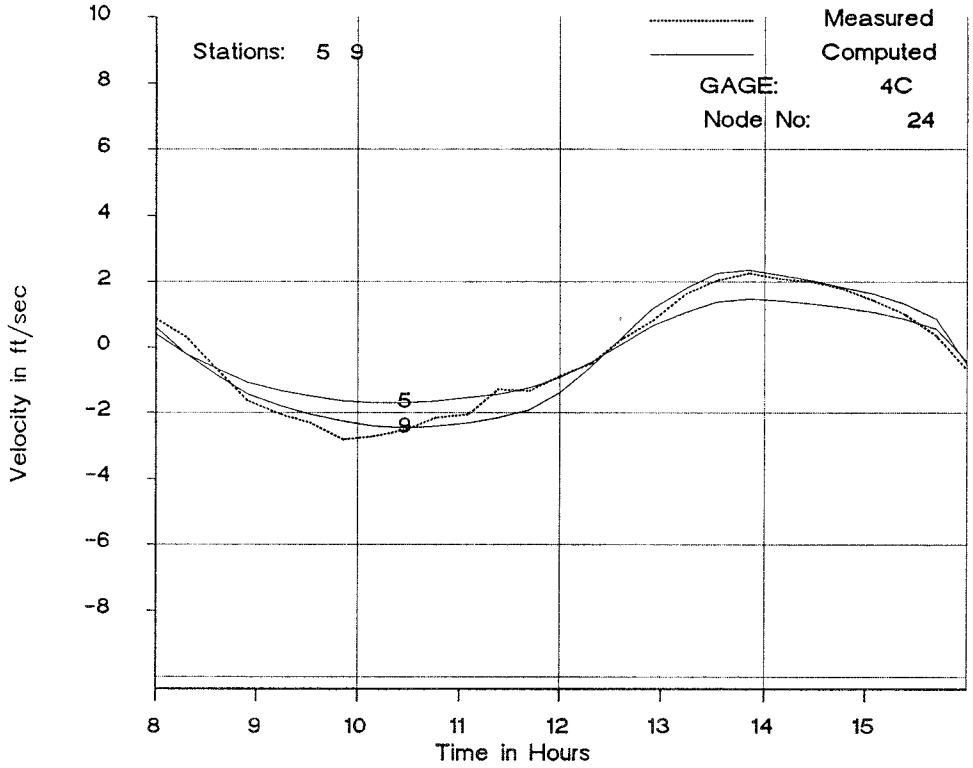
Stations: 5 9
Measured
Computed
GAGE: 4C
Node No: 24
Velocity in ft/sec
Time in Hours
10
8
6
4
2
0
-2
-4
-6
-8
8
9
10
11
12
13
14
15

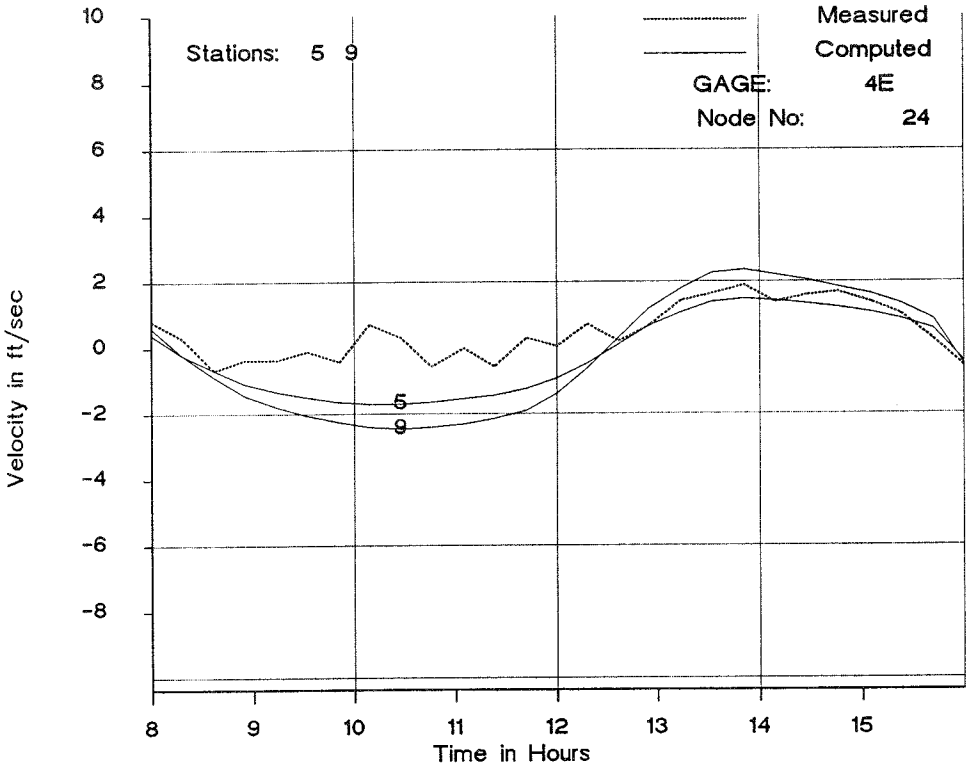
Measured
Computed
Stations: 5 9
GAGE: 4E
Node No: 24
Velocity in ft/sec
Time in Hours
5
9

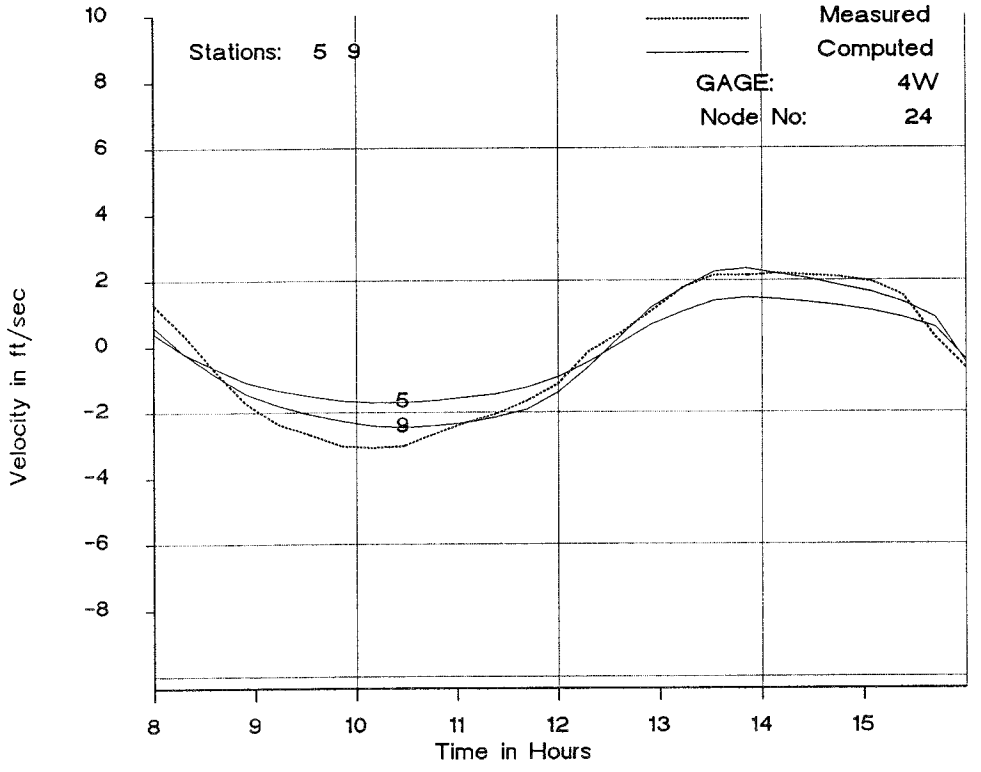
Measured
Computed
Stations: 5 9
GAGE: 4W
Node No: 24
Velocity in ft/sec
Time in Hours
5
9

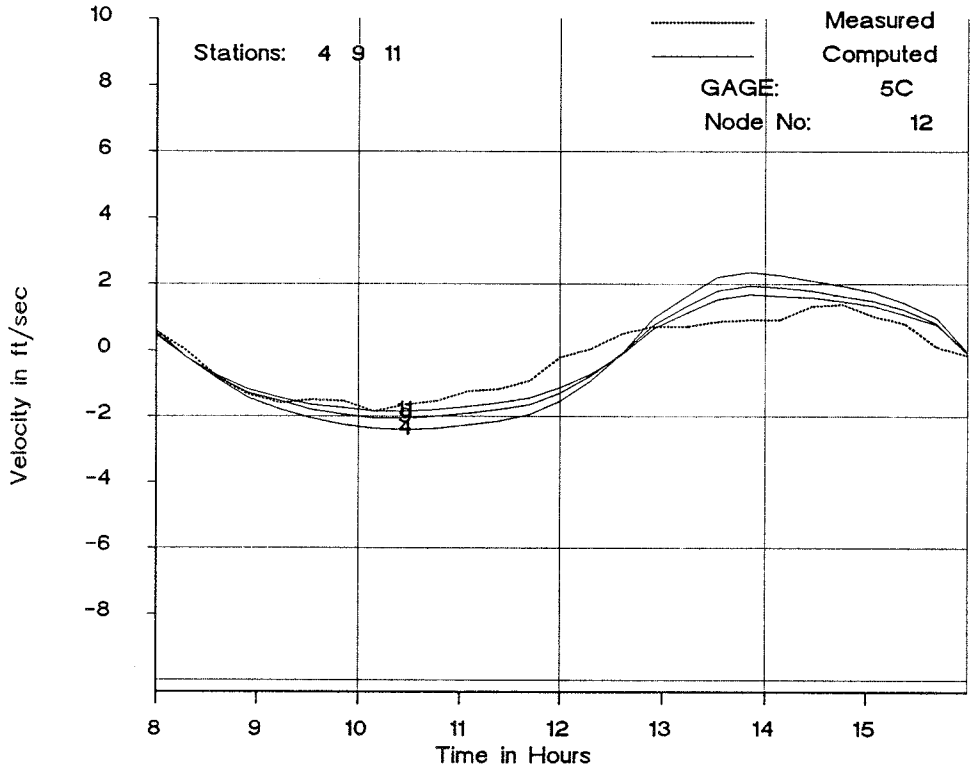
Stations: 4 9 11
Measured
Computed
GAGE: 5C
Node No: 12
Velocity in ft/sec
Time in Hours

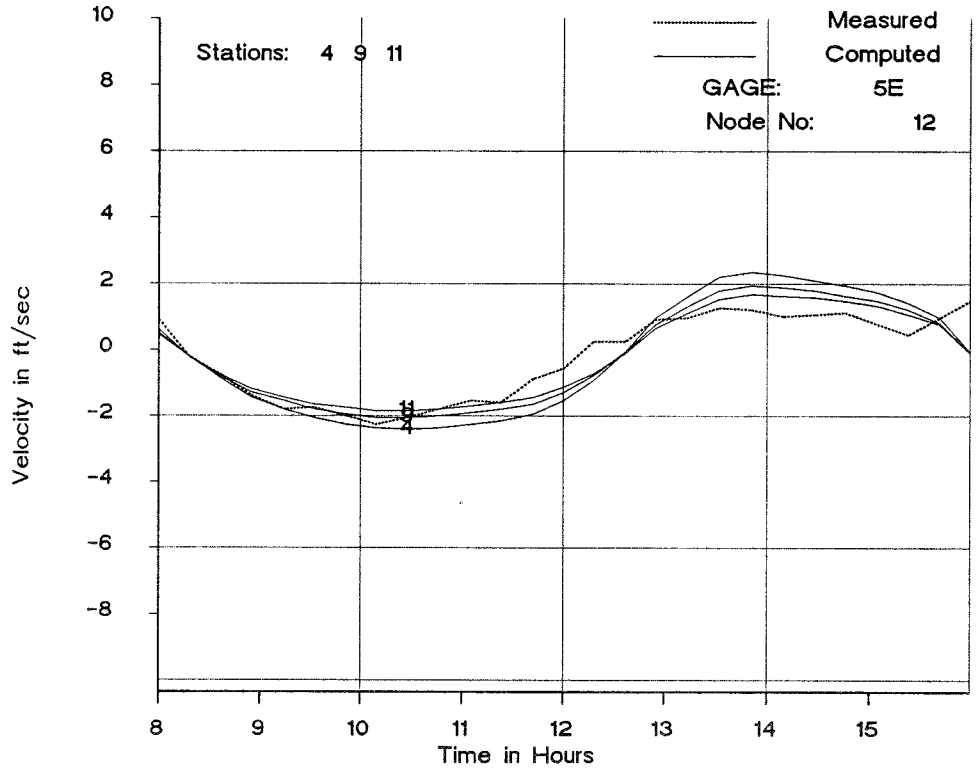
Stations: 4 9 11
Measured
Computed
GAGE: 5E
Node No: 12
Velocity in ft/sec
Time in Hours

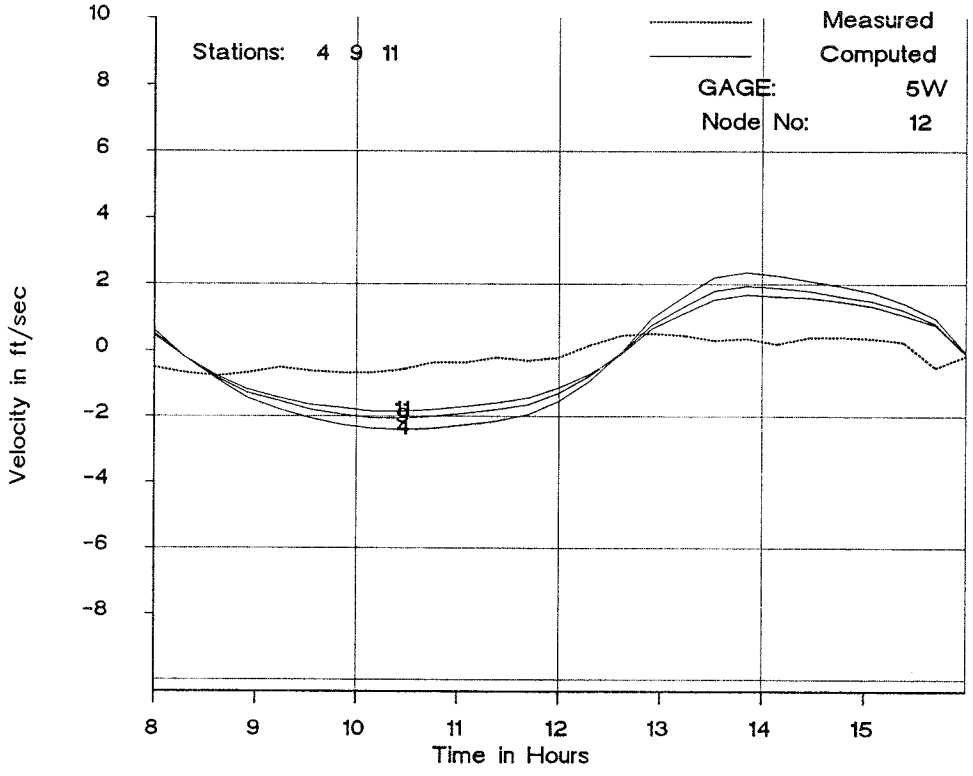
Stations: 4 9 11
Measured
Computed
GAGE: 5W
Node No: 12
Velocity in ft/sec
Time in Hours
10
8
6
4
2
0
-2
-4
-6
-8
8
9
10
11
12
13
14
15

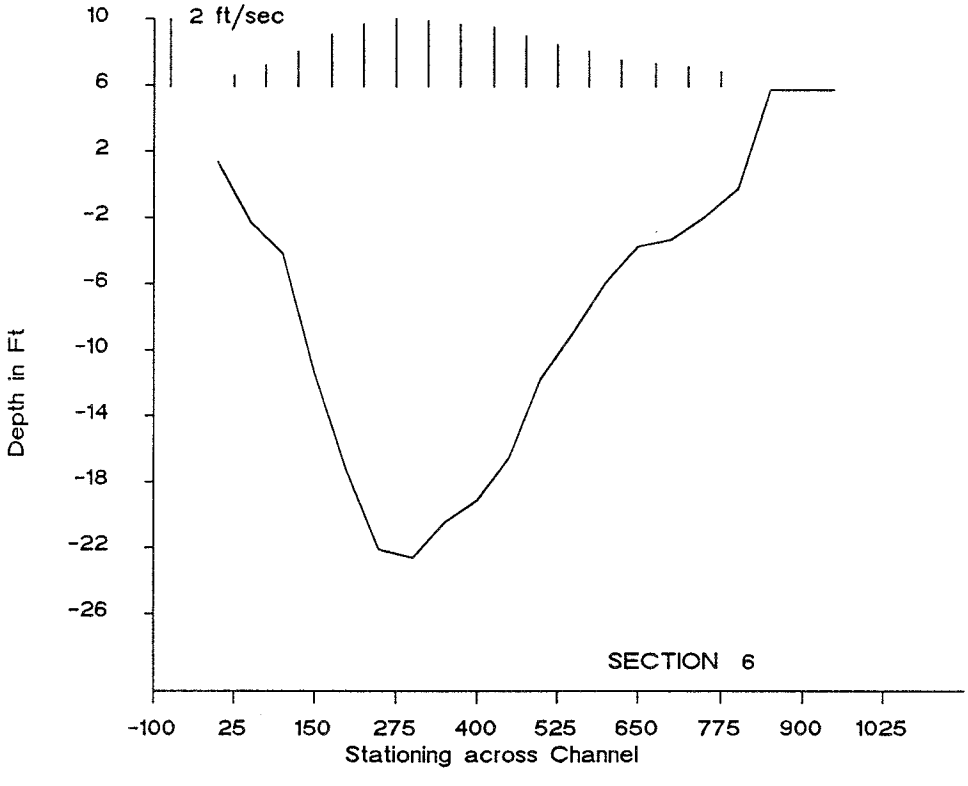
2 ft/sec
Depth in Ft
SECTION 6
Stationing across Channel
10
6
2
-2
-6
-10
-14
-18
-22
-26
-100
25
150
275
400
525
650
775
900
1025

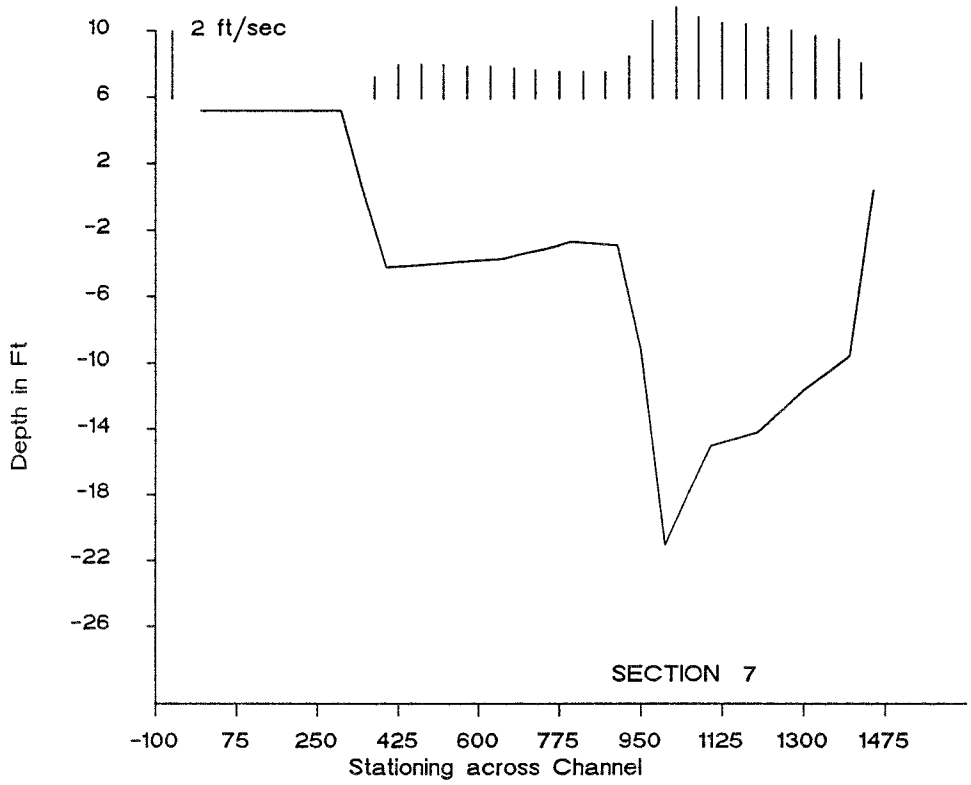
2 ft/sec
10
6
2
-2
-6
-10
-14
-18
-22
-26
Depth in Ft
SECTION 7
-100
75
250
425
600
775
950
1125
1300
1475
Stationing across Channel

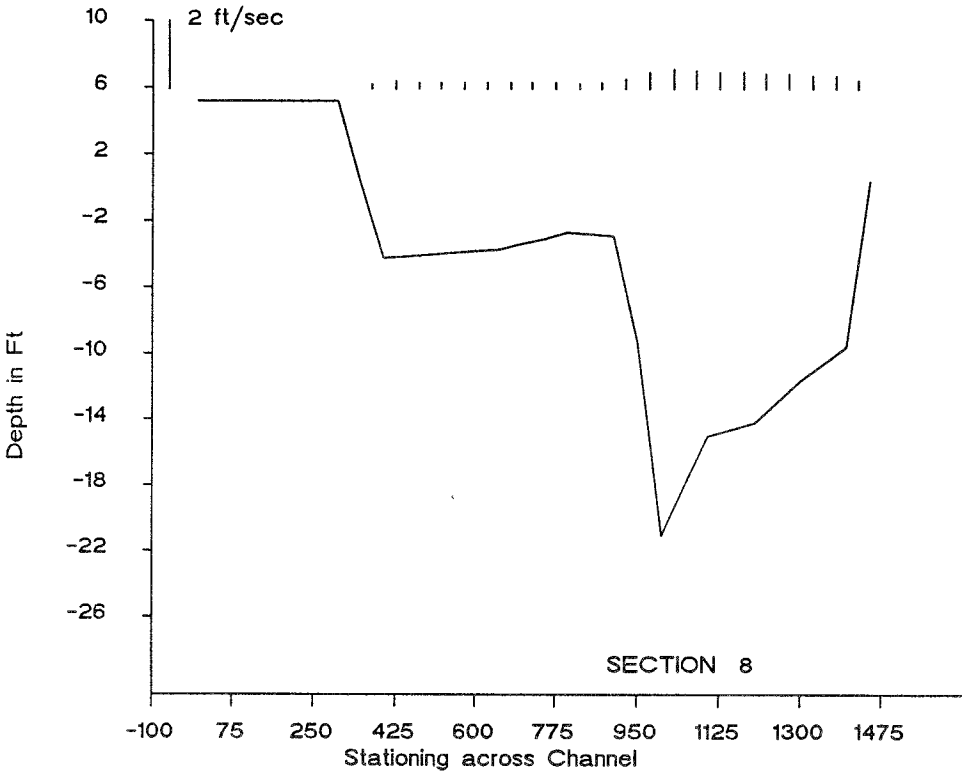
2 ft/sec
10
6
2
-2
-6
-10
-14
-18
-22
-26
Depth in Ft
SECTION 8
-100
75
250
425
600
775
950
1125
1300
1475
Stationing across Channel

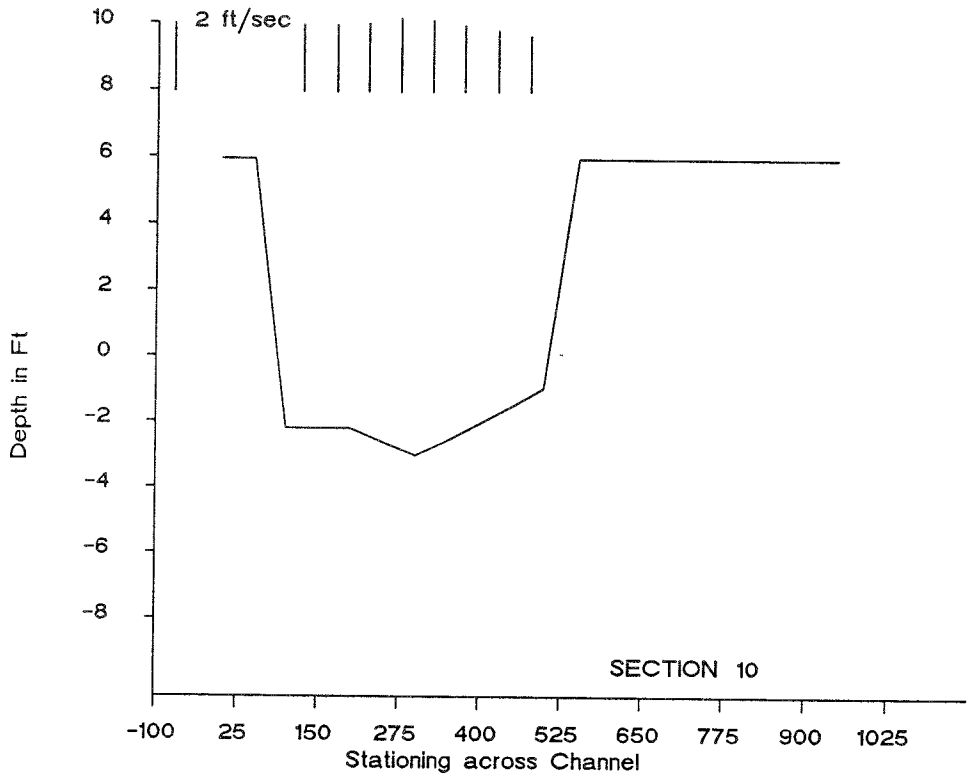
2 ft/sec
10
8
6
4
2
0
-2
-4
-6
-8
Depth in Ft
SECTION 10
-100
25
150
275
400
525
650
775
900
1025
Stationing across Channel

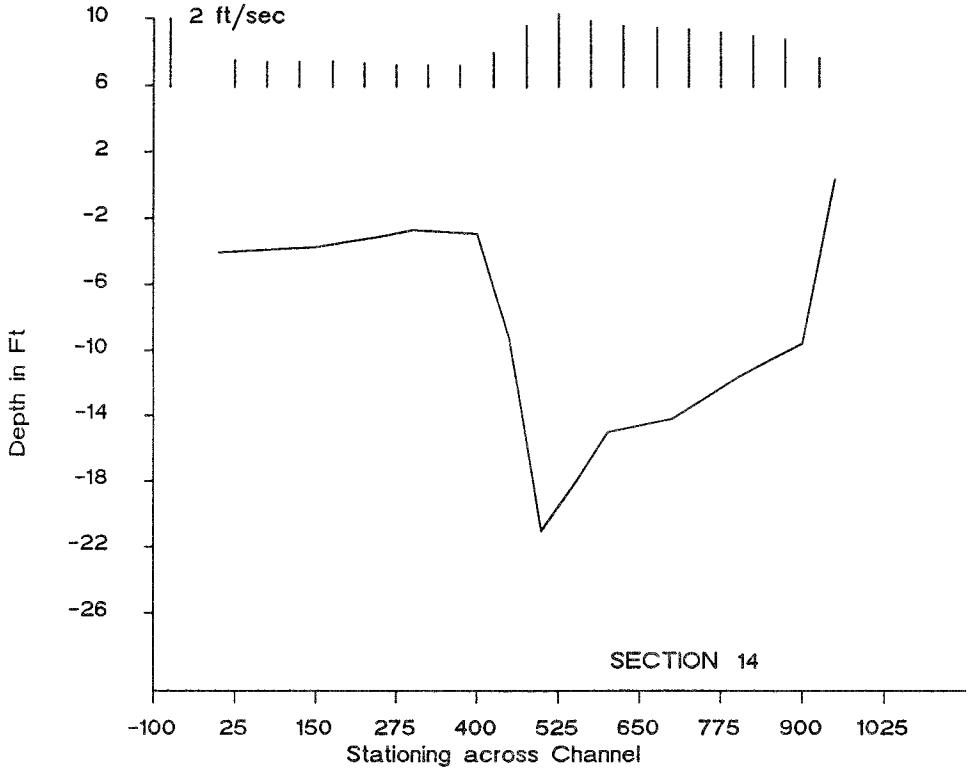
2 ft/sec
10
6
2
-2
-6
-10
-14
-18
-22
-26
Depth in Ft
SECTION 14
-100
25
150
275
400
525
650
775
900
1025
Stationing across Channel

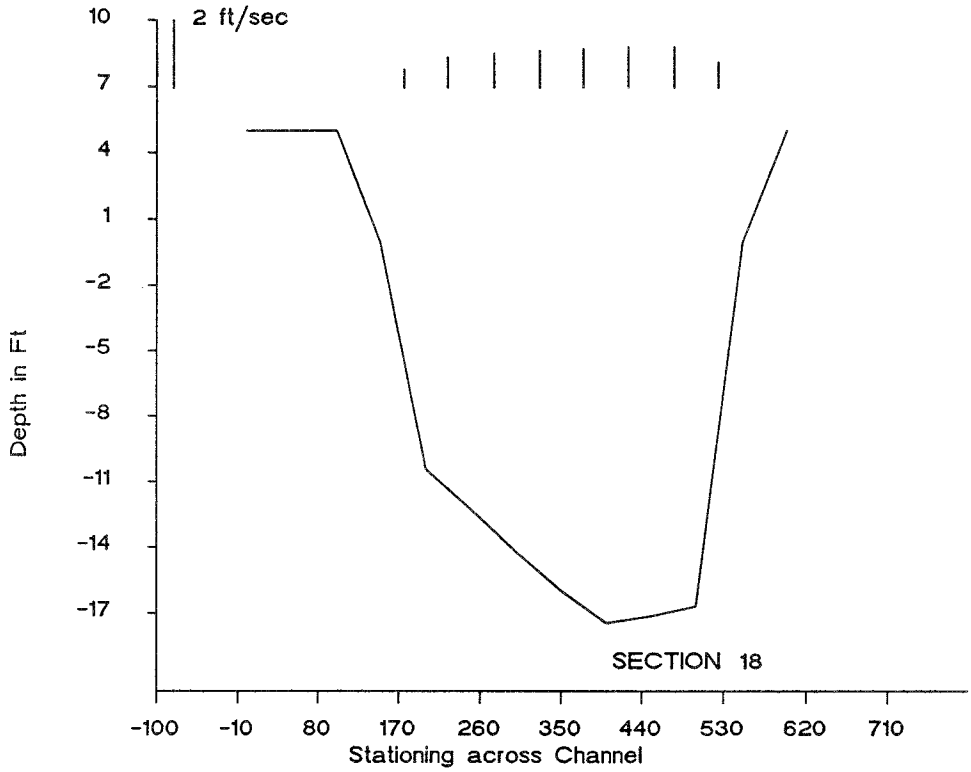
2 ft/sec
10
7
4
1
-2
-5
-8
-11
-14
-17
Depth in Ft
SECTION 18
-100
-10
80
170
260
350
440
530
620
710
Stationing across Channel

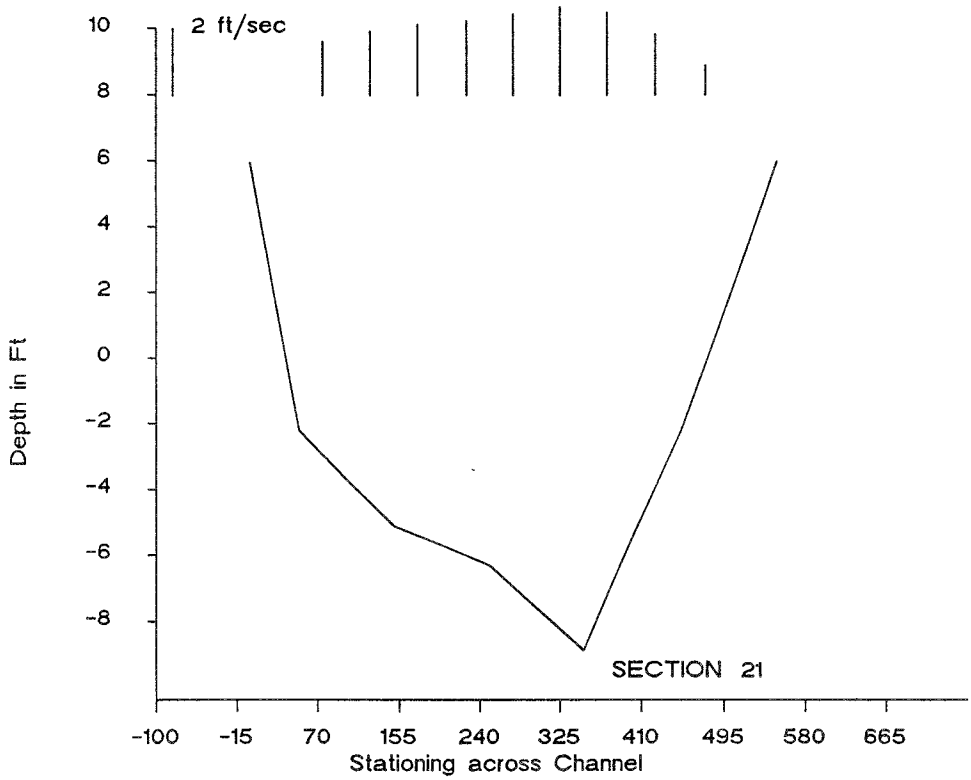
2 ft/sec
10
8
6
4
2
0
-2
-4
-6
-8
Depth in Ft
SECTION 21
-100
-15
70
155
240
325
410
495
580
665
Stationing across Channel

APPENDIX B: DATA FILES FOR INDIAN RIVER INLET

This appendix contains input and output files for the Indian River Inlet, Delaware, case study, presented in Part VI of the main text of this report. Files pertaining to both DYNLET1 and ACES-INLET are included. Plots of DYNLET1 calculations supplementing Part VI are given at the end of this appendix.

START

```
*********************************************************************
*                          DYNLET1
*********************************************************************
*         INDIAN RIVER INLET
*            INDRIVC1.DAT
*       IMPLICIT INLET DYNAMICS MODEL
*         Banded Matrix
*     3 channels and 1 junction
*        ~
*  Station 23   corresponds to Indian River Bay
*  Station 30  corresponds to Rehoboth Bay
*  Station 20, 21, 25  correspond to Junction
*  Station 1   corresponds to SEA
*         2   begins the JETTY
*  FIELD DATA BY THE US ARMY CORPS OF ENGINEERS
*  ~
*********************************************************************
A     COMPUTATIONAL PARAMETERS
*********************************************************************
A.1   TO     Tfin   yeps   Qeps  theta N   Iwind
  0.00   63.00  0.05  200.0  1.0   31     0
A.2  units
ENGLISH
A.3  UNIT OF DISTANCE
FEET
*********************************************************************
B   CHANNELS , JUNCTIONS AND EXTERNAL BOUNDARY NODES
*********************************************************************
B.1     NC  NJ  NB
      3  1     3
B.2   Channel No  Start at  End at
         1        1       20
         2       21       24
         3       25       31
B.3  Junction Number    How Many Nodes      Node numbers of Junction
      1                      3              20      21      25
B.4   Boundary Point   Node Number     Id    desc1   desc2
           1            1          1
           2           24          2
           3           31          2
*********************************************************************
C       COMPUTATIONAL PARAMETERS
*********************************************************************
C.1     Computation Time Step in sec
    1800.0
C.2   Itern
       50
C.3  Number of Printout( Display) Times NP
 49
```

```
C.4  Print Times in Hours
 39.0  39.5   40.0 40.5
 41.0  41.5  42.0  42.5   43.0            43.5   44.0  44.5   45.0 45.5
 46.0  46.5  47.0   47.5   48.0            48.5   49.0  49.5   50.0 50.5
 51.0  51.5  52.0  52.5   53.0            53.5   54.0  54.5   55.0 55.5
 56.0  56.5  57.0  57.5   58.0            58.5   59.0  59.5   60.0 60.5
 61.0  61.5  62.0  62.5   63.0
C.5  Number of Stations at which output is desired NoutN
 17
C.6  Output Stations
 4 24 21  27   1       2  3  4  5   6      10  15 20  24  26       27 28
*********************************************************************
D           NODE PARAMETERS
*********************************************************************
D.1  Values Of Distances at Channel Nodes: Node 1 to N
       0.0      6000.0    6200.0   6780.0   7200.0
    7250.0      7350.0    7500.0   7700.0   8200.0
    8470.0      8720.0    8920.0   9120.0   9750.0
   10350.0     10950.0   11550.0  13950.0  16050.0
   16050.0     23550     43050.0  45000.0      0.0
    4800.0      7300.0   10500.0   17700.0  33700.0
   40000.0
D.2    x-coordinate of left bank
-12000.0  -3000.0     -3000.0     -3000.0   -3000.0  -3000.0 -3000.0  -3000.0

-3000.0  -3000.0     -3000.0     -3000.0   -4000.0  -4000.0 -4000.0  -4000.0
-3000.0 -3000.0    -3000.0    -3000.0  -3000.0 -10000.0 -10000.0 -3000.0
    0.0      4800.0      7300.0   10500.0   17700.0  33700.0  40000.0
D.3      y coordinate of the left bank
    0.0     6000.0     6200.0     6780.0    7200.0     7250.0   7350.0  7500.0
 7700.0     8200.0    8475.0    8720.0     8920.0     9120.0   9750.0  10350.0
 10950.0   11550.0   13950.0    16050.0     20050.0   23550.0  43050.0
45000.0
 16050.0   20000.0   20300.0   20500.0     20700.0    20700.0  20000.0
D.4  Values of Lateral Inflow QL at each Node
 0.0  0.0 0.0 0.0 0.0        0.0 0.0 0.0 0.0 0.0
 0.0  0.0 0.0 0.0 0.0        0.0 0.0 0.0 0.0 0.0
 0.0  0.0 0.0 0.0 0.0        0.0 0.0 0.0 0.0 0.0
0.0
D.5   Values of Reference Elevation Z
 0.0  0.0 0.0 0.0 0.0        0.0 0.0 0.0 0.0 0.0
 0.0  0.0 0.0 0.0 0.0        0.0 0.0 0.0 0.0 0.0
 0.0  0.0 0.0 0.0 0.0        0.0 0.0 0.0 0.0  0.0
0.0
D.6  Values of Channel Alignment Angles
   90.0   90.0   90.0   90.0   90.0   90.0  90.0  90.0  90.0  275.0
  275.0  275.0  275.0  275.0  275.0   90.0  90.0  90.0  90.0  135.0
  135.0  135.0  135.0  135.0  135.0  135.0 135.0 135.0  135.0 135.0
 135.0
```

```
D.7  Transition Loss Coefficients
  0.00   0.40  0.40  0.40  0.40         0.40  0.40  0.40  0.60  0.60
  0.60   0.6  0.6  0.4  0.4         0.4  0.4  0.4  0.4  0.4
  0.4   0.4  0.4  0.4  0.4         0.4  0.4  0.4  0.4  0.4
  0.4
D.8  Values of Initial water surface  elev  ZIN (ft)
     2.30   2.30    2.30    2.30     2.30    2.30    2.30    2.30    2.30
2.30
     2.30   2.30    2.30    2.30     2.30    2.30    2.30    2.30    2.30
2.30
     2.30   2.30    2.30    2.30     2.30    2.30    2.30    2.30    2.30
2.30
     2.30
D.9  Values of Initial Discharge   QIN
 0.0  0.0  0.0  0.0  0.0
 0.0  0.0  0.0  0.0  0.0
 0.0  0.0  0.0  0.0  0.0
 0.0  0.0  0.0  0.0  0.0
 0.0  0.0  0.0  0.0  0.0
 0.0  0.0  0.0  0.0  0.0
0.0
```

SECTION

```
*********************************************************************
E        Cross-Section Geometry and Friction Coefficients, Indian River
*********************************************************************
E.1   Section ID   Number of Elevation Points
    1        7
E.2 Stations and Elevations
      0.0    -35.0  3333.0  -37.00 6666.00  -40.00 10000.00 -39.00
  13333.0    -39.00  16666.0 -38.0  20000.0 -34.0
E.3   Manning's Coefficient of Friction
  0.0300  0.0300  0.0300  0.0300  0.0300  0.0300  0.0300
E.1 Section ID   Number of Elevation Points
    2        12
E.2 Stations and Elevations
     0.0    0.00   80.00  -30.00  120.00  -40.00  220.00  -60.00
  300.00  -70.0  310.0  -80.00  340.00  -82.50  400.00  -70.00
  430.00  -50.00  480.00  -20.00   560.0  -7.50  660.00  -19.50
E.3  Manning's Coefficient of Friction
  0.0300 0.0300 0.0300 0.0300 0.0300 0.0300 0.0300  0.030  0.030 0.030
  0.0300 0.0300
E.1   Section ID   Number of Elevation Points
    3        13
E.2 Stations and Elevations
   0.00    5.00    1.0  -1.00   40.00  -10.00   90.00  -30.00
 150.00  -40.00  290.00  -70.00  340.00  -61.30  380.00  -40.00
 390.00  -35.00  400.00  -25.00  440.00  -10.00  469.0  -1.00
 470.00  5.00
```

```
E.3  Manning's Coefficient of Friction
  0.0300 0.0300 0.0300 0.0300 0.0300 0.0300 0.0300 0.0300 0.0300 0.0300
  0.0300 0.0300 0.0300
E.1   Section ID   Number of Elevation Points
    4        13
E.2 Stations and Elevations
  00.00    5.00    1.00   -1.00   50.00  -10.00  100.00  -30.00
 150.00  -50.00  200.00  -45.00  250.00  -40.00  300.00  -41.00
  350.00  -42.00  400.00  -38.00 450.00  -30.00  500.00   -1.00
  510.00    5.00
E.3  Manning's Coefficient of Friction
  0.0300 0.0300 0.0300 0.0300 0.0300 0.0300 0.0300 0.0300 0.0300 0.0300
  0.0300 0.0300 0.0300
E.1   Section ID   Number of Elevation Points   <<50 FT EAST OF BRIDGE>>
    5        19
E.2 Stations and Elevations
   0.00    5.00    1.00   -1.00   30.00   -5.00   50.00  -10.00
  90.00  -20.00  110.00  -25.00  150.00  -50.00  200.00  -61.00
 240.00  -74.00  260.00  -70.00 340.00  -60.00  360.00  -50.00
 390.00  -40.00  430.00  -36.00  450.00  -25.00 470.00  -20.00
 480.00  -10.00  509.00  -1.00   510.00    5.00
E.3  Manning's Coefficient of Friction
 0.0300 0.0300 0.0300 0.0300 0.0300 0.0300 0.0300 0.0300 0.0300 0.0300
  0.0300 0.0300 0.0300 0.0300 0.0300 0.0300 0.0300 0.0300 0.0300
E.1   Section ID   Number of Elevation Points   <<AT BRIDGE>>
    6        31
E.2 Stations and Elevations
  00.00    5.00    1.00   -1.00    50.00   -8.00   70.00  -25.00
 100.00  -34.00  110.00  -25.00  123.00  -25.00   130.00  -25.00
  130.10   5.00   140.00    5.00 140.10  -25.00  150.00  -20.00
  170.00  -20.00  180.00  -30.00  190.00  -40.00 200.00  -46.00
 230.00  -65.00   240.00  -70.00  280.00  -65.00  320.00  -60.00
 380.00  -60.00  380.10    5.00   390.0     5.00  390.10  -50.00
 400.00  -40.00 410.00  -35.00  440.00  -29.00   450.00  -20.00
 480.00  -11.00  509.00   -1.00  510.00    5.00
E.3  Manning's Coefficient of Friction
  0.0450 0.0450 0.0450 0.0450 0.0450 0.0450 0.0450 0.0450 0.0450 0.0450
  0.0450 0.0450 0.0450 0.0450 0.0450 0.0450 0.0450 0.0450 0.0450 0.0450
  0.0450 0.0450 0.0450 0.0450 0.0450 0.0450 0.0450 0.0450 0.0450 0.0450
  0.0450
E.1   Section ID   Number of Elevation Points    <<100 FT WEST OF BRIDGE>>
    7        18
E.2 Stations and Elevations
   0.00    5.00    1.00   -1.00   50.00   -8.00   70.00  -25.00
  100.00  -40.00  120.00  -50.00  170.00  -53.00  200.00  -52.00
 250.00  -49.00  270.00  -50.00  300.00  -57.00  350.00  -60.00
 410.00  -50.00  420.00  -27.00  450.00  -25.00  470.00   -8.00
 509.00   -1.00  510.00    5.00
E.3  Manning's Coefficient of Friction
  0.0450 0.0450 0.0450 0.0450 0.0450 0.0450 0.0450 0.0450 0.0450 0.0450
  0.0450 0.0450 0.0450 0.0450 0.0450 0.0450 0.0450 0.0450
```

```
E.1   Section ID   Number of Elevation Points
    8         26
E.2 Stations and Elevations
   0.00     5.00     1.00  -1.00     50.00  -15.00    70.00  -25.00
  80.00  -30.00    90.00  -40.00  110.00  -46.00  120.00  -45.00
 140.00  -40.00  150.00  -30.00  180.00  -32.00  210.00  -38.00
 250.00  -25.00  280.00  -36.00  300.0   -38.0   320.00  -35.0
 350.00  -30.00  360.00  -25.00  400.00  -40.00  430.00  -30.00
 440.00  -25.00  450.00  -20.00  480.00  -20.00  490.00  -10.00
 509.00   -1.00  510.00    5.00
E.3  Manning's Coefficient of Friction
  0.0450 0.0450 0.0450 0.0450 0.0450 0.0450 0.0450 0.0450 0.0450 0.0450
  0.0450 0.0450 0.0450 0.0450 0.0450 0.0450 0.0450 0.0450 0.0450 0.0450
  0.0450 0.0450 0.0450 0.0450 0.0450 0.0450
E.1  Section ID  NO. Elev Pts
    9         29
E.2 Stations and Elevations
  00.00     5.00     1.00   -1.00    70.00  -15.00  120.00  -25.00
150.00  -25.00  180.00  -50.00  190.00  -60.00  200.00  -70.00
 220.00  -79.00  250.00  -89.00  270.00  -93.00  300.00  -90.00
 350.00  -80.00  400.00  -70.00  460.00  -75.00  500.00  -78.00
 550.00  -76.00  600.00  -60.00  610.00  -50.00  620.00  -45.00
 640.00  -30.00  650.00  -20.00  680.00  -15.00  700.00  -10.00
 720.00  -12.00 730.00  -10.00  750.00   -5.00  799.00   -1.00
 800.00    5.00
E.3  Manning's Coefficient of Friction
 0.0450 0.0450 0.0450 0.0450 0.0450 0.0450 0.0450 0.0450 0.0450 0.0450
 0.0450 0.0450 0.0450 0.0450 0.0450 0.0450 0.0450 0.0450 0.0450 0.0450
 0.0450 0.0450 0.0450 0.0450 0.0450 0.0450 0.0450 0.0450 0.0450
E.1   Section ID   Number of Elevation Points
    10       22
E.2 Stations and Elevations
   0.00     5.00     1.00   -1.00    45.00  -15.00    50.00  -20.00
70.00  -30.00  100.00  -40.00  200.00  -40.00  250.00  -37.00
300.00  -36.00  350.00  -36.00  400.00  -32.00  450.00  -28.00
500.00  -26.00  550.00  -27.00  600.00  -31.00  650.00  -33.00
 700.00  -33.00  740.00  -25.00  760.00  -20.00  780.00  -10.00
 799.00   -1.00  800.00    5.00
E.3  Manning's Coefficient of Friction
  0.0450  0.0450  0.0450  0.0450  0.0450  0.0450  0.0450  0.0450
  0.0450  0.0450  0.0450  0.0450  0.0450  0.0450  0.0450  0.0450
  0.0450  0.0450  0.0450  0.0450  0.0450  0.0450
E.1   Section ID   Number of Elevation Points
   11         21
E.2 Stations and Elevations
   0.00     5.00     1.00   -1.00    40.00  -10.00  100.00  -20.00
  150.00  -25.00  300.00  -28.00  400.00  -27.00  500.00  -25.00
  600.00  -23.00  650.00  -20.00  700.00  -14.00  800.00  -12.00
  900.00  -12.50  950.00  -14.00 1000.00  -20.00 1050.00  -24.00
 1100.00  -25.00 1150.00  -19.00 1180.00  -15.00 1189.00  -10.00
1190.0     5.00
```

```
E.3  Manning's Coefficient of Friction
  0.0450  0.0450  0.0450  0.0450  0.0450  0.0450  0.0450  0.0450
  0.0450  0.0450  0.0450  0.0450  0.0450  0.0450  0.0450  0.0450
  0.0450  0.0450  0.0450  0.0450  0.0450
E.1   Section ID   Number of Elevation Points
   12        21
E.2 Stations and Elevations
  00.00   -5.00   40.00  -10.00  100.00  -13.00  150.00  -14.00
  220.00  -20.00  330.00  -23.00  420.00  -22.00  500.00  -21.00
  600.00  -21.00  800.00  -20.00  900.00  -21.00 1020.00  -22.00
 1050.00  -25.00 1100.00  -26.00 1140.00  -30.00 1160.00  -40.00
 1200.00  -50.00 1240.00  -40.00 1280.00  -30.00 1399.00  -24.00
1400.00    5.00
E.3  Manning's Coefficient of Friction
  0.0450  0.0450  0.0450  0.0450  0.0450  0.0450  0.0450  0.0450
  0.0450  0.0450  0.0450  0.0450  0.0450  0.0450  0.0450  0.0450
  0.0450  0.0450  0.0450  0.0450  0.0450
E.1   Section ID   Number of Elevation Points
   13        22
E.2 Stations and Elevations
   0.00   -5.00   40.00  -10.00  100.00  -13.00  180.00  -15.00
  200.00  -17.00  300.00  -21.00  400.00  -20.00  500.00  -20.00
 600.00  -18.00  700.00  -16.00  800.00  -16.80  900.00  -18.00
1000.00  -17.00 1100.00  -21.00 1200.00  -25.00 1250.00  -40.00
 1300.00  -45.00 1370.00  -40.00 1400.00  -35.00 1450.00  -20.00
1500.00   -8.00 1550.00   -5.00
E.3  Manning's Coefficient of Friction
  0.0350  0.030  0.030  0.030  0.030  0.030  0.030  0.030  0.030  0.030
  0.030  0.030  0.030  0.030  0.030  0.030  0.030  0.030  0.030  0.030
  0.030  0.030
E.1   Section ID   Number of Elevation Points  y-coordinate 599+00
   14        20
E.2 Stations and Elevations
   0.00   -5.00  100.00  -16.00  200.00  -15.00  300.00  -20.00
 400.00  -18.00  500.00  -18.00  550.00  -18.20  600.00  -16.30
 700.00  -14.60  800.00  -12.80 1000.00  -15.00 1120.00  -17.00
 1170.00  -19.00 1200.00  -17.3  1350.00 -24.00 1450.00  -27.20
1470.00  -25.00 1490.00  -20.00 1550.00  -12.00 1600.00   -7.80
E.3  Manning's Coefficient of Friction
  0.030 0.030 0.030 0.030 0.030 0.030 0.030 0.030 0.030 0.030
  0.030 0.030 0.030 0.030 0.030 0.030 0.030 0.030 0.030 0.030
E.1   Section ID   Number of Elevation Points  y-coordinate  598+380
   15        22
E.2 Stations and Elevations
   0.00   -8.80  100.00  -12.60  200.00  -19.60  300.00  -19.60
 400.00  -15.20  500.00  -15.30  600.00  -12.50  700.00  -12.00
 800.00   -9.70  900.00  -10.40 1000.00  -12.50 1100.00  -16.00
 1200.00  -17.50 1250.00  -20.00 1300.00  -22.00 1400.00  -23.20
 1450.00  -26.30 1500.00  -26.50 1600.00  -21.90 1650.00  -12.00
1700.00   -6.60 1800.00   -2.30
```

```
E.3  Manning's Coefficient of Friction
  0.030 0.030 0.030 0.030 0.030 0.030 0.030 0.030 0.030 0.030
  0.030 0.030 0.030 0.030 0.030 0.030 0.030 0.030 0.030 0.030
  0.030 0.030
E.1   Section ID   Number of Elevation Points
   16        20
E.2 Stations and Elevations
   0.00   -3.00  150.00  -15.40  250.00  -20.0   350.00  -20.00
 450.00  -16.00  550.00  -12.40  650.00  -12.50  750.00  -12.00
 850.00  -12.30  950.00  -12.00 1050.00  -10.00 1150.00   -4.00
 1250.00   -7.00 1350.00  -14.00 1450.00  -22.00 1550.00  -31.20
 1650.00  -34.00 1750.00  -22.50 1850.00  -12.80 1950.00   -5.00
E.3  Manning's Coefficient of Friction
  0.030 0.030 0.030 0.030 0.030 0.030 0.030 0.030 0.030 0.030
  0.030 0.030 0.030 0.030 0.030 0.030 0.030 0.030 0.030 0.030
E.1   Section ID   Number of Elevation Points
   17        21
E.2  Stations and Elevations
   0.00   -4.00  200.00  -12.20  300.00  -14.00  400.00  -15.00
 500.00  -14.00  600.00  -11.00  700.00  -11.50  800.00   -6.00
  900.00   -9.00 1000.00   -9.00 1100.00  -13.00 1200.00  -16.70
1300.00  -21.60 1400.00  -25.10 1500.00  -27.00 1600.00  -27.70
 1700.00  -31.00 1800.00  -30.00 1850.00  -26.40 1900.00  -16.50
1980.00   -9.00
E.3 Manning's Coefficient of Friction
  0.030 0.030 0.030 0.030 0.030 0.030 0.030 0.030 0.030 0.030
  0.030 0.030 0.030 0.030 0.030 0.030 0.030 0.030 0.030 0.030
  0.030
E.1   Section ID   Number of Elevation Points
   18        24
E.2 Stations and Elevations
   0.00   -4.00  50.00  -10.00  200.00   -6.00   300.00   -8.00
 400.00  -10.50  500.00  -11.80  600.00  -13.00  700.00  -14.00
 800.00  -15.50  900.00  -18.00 1000.00  -18.40 1100.00  -19.00
1200.00  -20.00 1300.00  -18.20 1350.00  -16.70 1400.00  -20.50
 1450.00  -24.00 1500.00  -26.30 1550.00  -27.50 1700.00  -28.30
1830.00  -25.00 1870.00  -20.00 1910.00  -15.00 1930.00  -10.00
E.3  Manning's Coefficient of Friction
  0.030 0.030 0.030 0.030 0.030 0.030 0.030 0.030 0.030 0.030
  0.030 0.030 0.030 0.030 0.030 0.030 0.030 0.030 0.030 0.030
  0.030 0.030 0.030 0.030
E.1   Section ID   Number of Elevation Points
   19        21
E.2 Stations and Elevations
   0.00    0.00  800.00   -4.00 1600.00   -4.60 2400.00   -3.20
 3200.00   -3.70 4000.00   -3.90 4800.00   -3.60 5600.00   -2.7
  6400.00   -2.20 7200.00   -1.60 8000.00   -1.70 8400.00  -18.70
 8800.00  -10.00 9200.0    -9.00 9600.00   -5.00  10000.0   -5.00
10400.0  -11.0 10800.0   -16.0 11200.0    -5.0 11600.0    -3.0
11601.0    5.0
```

```
E.3  Manning's Coefficient of Friction
  0.030  0.030  0.030  0.030  0.030  0.030  0.030  0.030  0.030  0.030
  0.030  0.030  0.030  0.030  0.030  0.030  0.030  0.030  0.030  0.030
  0.030
E.1   Section ID   Number of Elevation Points
   20        26
E.2 Stations and Elevations
   0.00     0.00  800.00   -1.80 1600.00   -2.60 2400.00   -6.00
 3200.00   -4.00 4000.00   -4.10 4800.00   -3.50 5600.00   -3.9
 6400.00   -4.00 7200.00   -2.00 8000.00   -1.90 8400.00   -3.00
 8800.00   -5.00 8960.0   -10.00 9600.00   -3.00  10000.0   -1.00
  10400.0   -0.5 10800.0    -9.0 11200.0    -5.5 12000.0    -3.6
  12800.0   -6.5  13600.0   -1.0 14400.0    -1.5 15200.0    -1.5
  15599.0    -1.0 15600.0    5.0
E.3  Manning's Coefficient of Friction
  0.030  0.030  0.030  0.030  0.030  0.030  0.030  0.030  0.030  0.030
  0.030  0.030  0.030  0.030  0.030  0.030  0.030  0.030  0.030  0.030
  0.030  0.030  0.030  0.030  0.030  0.030
E.1   Section ID   Number of Elevation Points
   21        26
E.2 Stations and Elevations
   0.00     0.00  800.00   -1.80 1600.00   -2.60 2400.00   -6.00
3200.00   -4.00 4000.00   -4.10 4800.00   -3.50 5600.00   -3.9
6400.00   -4.00 7200.00   -2.00 8000.00   -1.90 8400.00   -3.00
8800.00   -5.00 8960.0   -10.00 9600.00   -3.00 10000.0   -1.00
 10400.0   -0.5 10800.0    -9.0 11200.0    -5.5 12000.0    -3.6
12800.0   -6.5  13600.0   -1.0 14400.0    -1.5 15200.0    -1.5
15599.0    -1.0  15600.0    5.0
E.3  Manning's Coefficient of Friction
  0.030  0.030  0.030  0.030  0.030  0.030  0.030  0.030  0.030  0.030
  0.030  0.030  0.030  0.030  0.030  0.030  0.030  0.030  0.030  0.030
  0.030  0.030  0.030  0.030  0.030  0.030
E.1   Section ID   Number of Elevation Points
   22        26
E.2 Stations and Elevations
   0.00     0.00  800.00   -1.80 1600.00   -2.60 2400.00   -6.00
 3200.00   -4.00 4000.00   -4.10 4800.00   -3.50 5600.00   -3.9
 6400.00   -4.00 7200.00   -2.00 8000.00   -1.90 8400.00   -3.00
 8800.00   -5.00 8960.0   -10.00 9600.00   -3.00 10000.0   -1.00
 10400.0   -0.5 10800.0    -9.0 11200.0    -5.5 12000.0    -3.6
12800.0   -6.5  13600.0   -1.0 14400.0    -1.5 15200.0    -1.5
15599.0    -1.0  15600.0    5.0
E.3  Manning's Coefficient of Friction
  0.030  0.030  0.030  0.030  0.030  0.030  0.030  0.030  0.030  0.030
  0.030  0.030  0.030  0.030  0.030  0.030  0.030  0.030  0.030  0.030
  0.030  0.030  0.030  0.030  0.030  0.030
E.1  Section ID   Number of Elevation Points
   23  9
E.2 Stations and Elevations
   0.00   -1.00  900.00   -5.00 1300.00   -5.60 2400.00   -6.00
 3800.00   -6.50  8400.0   -3.3   8600.0   -1.70  8800.0   -4.1
  8900.0    -3.7
```

```
E.3  Manning's Coefficient of Friction
  0.030  0.030  0.030  0.030  0.030  0.035   0.035   0.035   0.035
E.1  Section ID   Number of Elevation Points
   24  5
E.2 Stations and Elevations
   0.00   -1.00  500.00   -2.00 1000.00   -5.00 1500.00   -2.00
2000.00   -2.00
E.3 Manning's Coefficient of Friction
  0.030  0.030  0.030  0.030  0.030
E.1  Section ID   Number of Elevation Points
   25       26
E.2 Stations and Elevations
   0.00    0.00  800.00   -1.80 1600.00   -2.60 2400.00   -6.00
 3200.00   -4.00 4000.00   -4.10 4800.00   -3.50 5600.00   -3.9
 6400.00   -4.00 7200.00   -2.00 8000.00   -1.90 8400.00   -3.00
 8800.00   -5.00 8960.0   -10.00 9600.00   -3.00 10000.0   -1.00
 10400.0   -0.5 10800.0    -9.0 11200.0    -5.5 12000.0    -3.6
12800.0   -6.5  13600.0   -1.0 14400.0    -1.5 15200.0    -1.5
15599.0    -1.0  15600.0    5.0
E.3  Manning's Coefficient of Friction
  0.030  0.030  0.030  0.030  0.030  0.030  0.030  0.030  0.030  0.030
  0.030  0.030  0.030  0.030  0.030  0.030  0.030  0.030  0.030  0.030
  0.030  0.030  0.030  0.030  0.030  0.030
E.1   Section ID   Number of Elevation Points
   26        16
E.2 Stations and Elevations
   0.00   -4.60  160.00  -15.00  240.00   -7.60  400.00   -9.00
  480.00  -10.00  481.00    5.0  1280.00    5.00  1281.0   -2.00
 1400.00   -3.60  1500.0   -1.50  1700.0  -10.50 1900.00   -8.40
 2000.0   -9.4  2100.00   -6.1   2400     -1.5   2800.0    -1.0
E.3  Manning's Coefficient of Friction
  0.030  0.030  0.030  0.030  0.030  0.030  0.030  0.030  0.030  0.030
  0.030  0.030  0.030  0.035   0.03    0.03
E.1   Section ID   Number of Elevation Points
   27         10
E.2 Stations and Elevations
   0.00    0.00  400.00   -3.00  800.00   -4.00  1300.0   -4.00
   1600.00   -9.00 2000.00   -3.00 2400.00   -2.5  2800.00   -3.50
   3200.0   -1.70  3300.00    0.0
E.3  Manning's Coefficient of Friction
  0.030  0.030  0.030  0.030  0.030  0.030  0.030  0.030  0.030  0.030
E.1   Section ID   Number of Elevation Points
   28        16
E.2 Stations and Elevations
   0.00    0.00  400.00   -1.00  800.00   -1.90 1200.00   -2.00
1600.00   -1.00  2000.00   -4.00 2400.00   -2.90 2800.0    -0.60
 3200.0    -2.00  3600.0   -2.30  4000.0   -2.60  4400.00   -6.5
  4800.0    -6.0  5200.0    -1.5   5600.0   -1.7  6000.0    0.0
E.3  Manning's Coefficient of Friction
  0.030  0.030  0.030  0.030  0.030  0.030  0.030  0.030  0.030  0.030
  0.030  0.030  0.030  0.030  0.030  0.030
```

```
E.1   Section ID   Number of Elevation Points
   29         19
E.2 Stations and Elevations
   0.00     0.00  160.00   -1.80  800.00   -5.00 1600.00   -6.00
 2400.00   -7.00  3200.00   -6.00 4000.00   -5.80 4800.00   -5.80
5600.00   -5.4  6400.00   -4.40  7200.00   -4.70 8000.00   -4.90
8800.00   -5.00 9600.0    -4.0 10400.0    -2.50 13200.0   -2.0
14000.0    -1.0 14800.0    -1.0 14801.0     0.0
E.3  Manning's Coefficient of Friction
  0.030  0.030  0.030  0.030  0.030  0.030  0.030  0.030  0.030  0.030
  0.030  0.030  0.030  0.030  0.030  0.030  0.030  0.030  0.030
E.1   Section ID   Number of Elevation Points
   30          9
E.2 Stations and Elevations
   0.00     0.00  160.00   -3.00  3000.0   -3.0 6000.00   -1.00
 9000.0 -5.00 12000.0   -4.0 16000.0    -3.0   18000.0  -1.0
  18001.0    0.0
E.3  Manning's Coefficient of Friction
  0.030  0.030  0.030  0.030  0.030  0.030 0.030 0.030 0.030
E.1   Section ID   Number of Elevation Points
   31          9
E.2 Stations and Elevations
   0.00     0.00  160.00   -3.00  3000.0   -3.0 6000.00   -1.00
  9000.0 -5.00  12000.0   -4.0 16000.0    -3.0   18000.0  -1.0
  18001.0    0.0
E.3  Manning's Coefficient of Friction
  0.030  0.030  0.030  0.0
30  0.030  0.030 0.030 0.030 0.030
```

EXTER

```
*************************************************************************
F       Time-Dependent Data   Indian River Inlet
*************************************************************************
F.1  index time  Ust(1,L)  Ust(2,L) Ust(3,L)
 1   0.5      2.30      0.0       0.0
 2   1.0      2.40      0.0       0.0
 3   1.5      2.50      0.0       0.0
 4   2.00     2.61      0.0       0.0
 5   2.50     2.92      0.0       0.0
 6   3.00     2.92      0.0       0.0
 7   3.5      2.89      0.0       0.0
 8   4.00     2.73      0.0       0.0
 9   4.50     2.40      0.0       0.0
10   5.00     2.04      0.0       0.0
11   5.50     1.62      0.0       0.0
12   6.00     1.22      0.0       0.0
13   6.5      0.63      0.00      0.0
14   7.00    -0.06      0.00      0.0
15   7.50    -0.65      0.00      0.0
```

16	8.00	-1.11	0.00	0.0
17	8.50	-1.57	0.00	0.0
18	9.00	-1.80	0.00	0.0
19	9.50	-1.92	0.00	0.0
20	10.00	-1.89	0.00	0.0
21	10.50	-1.79	0.00	0.0
22	11.00	-1.47	0.00	0.0
23	11.50	-1.24	0.00	0.0
24	12.00	-0.91	0.00	0.0
25	12.50	-0.48	0.00	0.0
26	13.00	0.01	0.00	0.0
27	13.50	0.40	0.00	0.0
28	14.00	0.80	0.00	0.0
29	14.50	1.09	0.00	0.0
30	15.00	1.19	0.0	0.0
31	15.50	1.26	0.0	0.0
32	16.00	1.16	0.0	0.0
33	16.50	0.56	0.00	0.0
34	17.00	0.86	0.00	0.0
35	17.50	0.63	0.00	0.0
36	18.00	0.24	0.00	0.0
37	18.50	-0.12	0.00	0.0
38	19.00	-0.68	0.00	0.0
39	19.50	-1.11	0.00	0.0
40	20.00	-1.57	0.0	0.0
41	20.50	-1.86	0.0	0.0
42	21.00	-1.99	0.0	0.0
43	21.50	-2.02	0.00	0.0
44	22.00	-1.76	0.00	0.0
45	22.50	-1.50	0.00	0.0
46	23.00	-1.11	0.00	0.0
47	23.50	-0.68	0.00	0.0
48	24.00	-0.19	0.00	0.0
49	24.50	0.40	0.00	0.0
50	25.00	1.06	0.0	0.0
51	25.50	1.62	0.0	0.0
52	26.00	2.27	0.0	0.0
53	26.50	2.70	0.00	0.0
54	27.00	3.12	0.00	0.0
55	27.50	3.28	0.00	0.0
56	28.00	3.38	0.00	0.0
57	28.50	3.29	0.00	0.0
58	29.00	2.99	0.00	0.0
59	29.50	2.70	0.00	0.0
60	30.00	2.27	0.0	0.0
61	30.50	1.78	0.0	0.0
62	31.00	1.16	0.0	0.0
63	31.50	0.66	0.00	0.0
64	32.00	0.04	0.00	0.0
65	32.50	-0.62	0.00	0.0
66	33.00	-1.17	0.00	0.0
67	33.50	-1.57	0.00	0.0

68	34.00	-1.76	0.00	0.0
69	34.50	-1.79	0.00	0.0
70	35.00	-1.69	0.0	0.0
71	35.50	-1.40	0.0	0.0
72	36.00	-1.14	0.0	0.0
73	36.50	-0.82	0.00	0.0
74	37.00	-0.39	0.00	0.0
75	37.50	0.24	0.00	0.0
76	38.00	0.66	0.00	0.0
77	38.50	1.09	0.00	0.0
78	39.00	1.48	0.00	0.0
79	39.50	1.62	0.00	0.0
80	40.00	1.75	0.0	0.0
81	40.50	1.75	0.0	0.0
82	41.00	1.68	0.0	0.0
83	41.50	1.45	0.00	0.0
84	42.00	1.16	0.00	0.0
85	42.50	0.96	0.00	0.0
86	43.00	0.50	0.00	0.0
87	43.50	0.07	0.00	0.0
88	44.00	-0.55	0.00	0.0
89	44.50	-1.04	0.00	0.0
90	45.00	-1.44	0.0	0.0
91	45.50	-1.69	0.0	0.0
92	46.00	-1.76	0.0	0.0
93	46.50	-1.82	0.00	0.0
94	47.00	-1.60	0.00	0.0
95	47.50	-1.24	0.00	0.0
96	48.00	-0.85	0.00	0.0
97	48.50	-0.35	0.00	0.0
98	49.00	0.11	0.00	0.0
99	49.50	0.73	0.00	0.0
100	50.00	1.35	0.0	0.0
101	50.50	2.01	0.0	0.0
102	51.00	2.53	0.0	0.0
103	51.50	3.05	0.00	0.0
104	52.00	3.38	0.00	0.0
105	52.50	3.55	0.00	0.0
106	53.00	3.42	0.00	0.0
107	53.50	3.32	0.00	0.0
108	54.00	3.12	0.00	0.0
109	54.50	2.80	0.00	0.0
110	55.00	2.34	0.0	0.0
111	55.50	1.85	0.0	0.0
112	56.00	1.12	0.0	0.0
113	56.50	0.34	0.00	0.0
114	57.00	-0.49	0.00	0.0
115	57.50	-0.94	0.00	0.0
116	58.00	-1.44	0.00	0.0
117	58.50	-1.66	0.00	0.0
118	59.00	-1.69	0.00	0.0
119	59.50	-1.73	0.00	0.0

120	60.00	-1.50	0.0	0.0
121	60.50	-1.27	0.0	0.0
122	61.00	-0.88	0.0	0.0
123	62.00	-0.48	0.00	0.0
124	62.00	-0.19	0.00	0.0
125	62.50	0.40	0.00	0.0
126	63.00	0.76	0.00	0.0
127	63.50	1.26	0.00	0.0

PARAM (Indian River Inlet)

Number of Gages in the Field
2
Number of Stations at the Gage
3
Identification of Stations
IST1 IST2 IST3
Computed Velocity Cross Section Number
4
Number of Velocity Output Locations Station Numbers
5 4 5 6 7 10
Number of Stations in the Gage
4
Identification of Stations
MIST1 MIST2 MIST3 MIST4
Computed Velocity Cross Section Number
26
Number of Velocity Output Locations Station Numbers
3 2 4 11
Number of Tide Gages
5
Identification of Tide Gages
Inlet Potnets Vines Massey Dewey
12 22 23 26 28

VOBSD.DAT

FILE FOR INDIAN RIVER INLET
(VALUES OF MEASURED VELOCITIES AT GAGING STATIONS)

Time hour	istatla velocity ft/s	Istat2a	Istat3a
39.0	4.72	4.75	5.50
39.5	4.34	4.66	5.33
40.0	3.97	4.57	4.67
40.5	3.12	3.59	3.67
41.0	2.27	2.62	2.67
41.5	1.28	1.60	1.88
42.0	-2.07	-0.58	-0.80
42.5	-3.50	-2.40	-2.57
43.0	-4.93	-4.22	-4.03
43.5	-5.42	-4.74	-4.85
44.0	-5.90	-5.27	-5.67
44.5	-6.04	-5.43	-5.95
45.0	-5.98	-5.58	-5.57
45.5	-5.72	-5.16	-5.08
46.0	-5.20	-4.73	-4.60
46.5	-4.25	-3.87	-3.73
47.0	-3.30	-3.00	-2.85
47.5	-2.03	-1.71	-2.37
48.0	2.00	0.42	-1.88
48.5	2.98	1.88	2.31
49.0	3.97	3.33	4.13
49.5	4.77	4.65	5.23
50.0	5.57	5.97	6.33
50.5	5.64	6.00	6.88
51.0	5.58	6.03	7.43
51.5	5.56	6.05	7.85
52.0	5.53	6.02	7.60
52.5	5.34	5.53	6.83
53.0	5.15	5.03	6.07
53.5	4.44	4.25	4.93
54.0	3.73	3.47	3.80
54.5	1.78	3.05	2.30
55.0	-0.97	0.58	-3.10
55.5	-3.47	-2.79	-4.22
56.0	-5.97	-4.13	-5.33
56.5	-6.39	-5.11	-6.37
57.0	-6.82	-6.08	-7.40
57.5	-6.53	-6.52	-7.77
58.0	-6.25	-6.38	-7.80
58.5	-5.90	-6.24	-6.97
59.0	-5.55	-6.10	-6.13
59.5	-5.01	-5.03	-5.22

60.0	-4.47	-3.97	-4.30
60.5	-3.33	-2.97	-3.10
61.0	-2.20	-1.97	-1.90
61.5	0.97	1.94	0.63
62.0	1.23	2.25	1.73
62.5	3.13	0.00	3.07
63.0	3.93	0.00	0.00

Time hour	Mstatla velocity (ft/s)	Mstat2a	Mstat3a	Mstat4a
39.0	1.59	1.68	0.84	0.82
39.5	1.68	1.86	1.04	1.26
40.0	1.77	1.93	1.24	1.72
40.5	1.77	1.87	1.36	1.79
41.0	1.79	1.82	1.47	1.66
41.5	1.50	1.41	1.20	1.46
42.0	1.23	1.00	0.93	1.26
42.5	1.04	0.58	0.75	0.88
43.0	-0.84	-0.63	-0.56	-0.53
43.5	-1.30	-1.08	-0.96	-0.78
44.0	-1.75	-1.58	-1.37	-1.04
44.5	-1.96	-1.83	-1.69	-1.12
45.0	-2.18	-2.08	-2.00	-1.20
45.5	-2.28	-2.42	-2.30	-1.24
46.0	-2.39	-2.52	-2.64	-1.23
46.5	-2.28	-2.32	-2.68	-1.13
47.0	-2.06	-2.11	-2.72	-1.04
47.5	-1.81	-1.84	-2.43	-0.98
48.0	-1.55	-1.58	-2.15	-0.93
48.5	-1.07	-0.96	-1.79	-0.86
49.0	-0.59	0.70	-1.43	-0.80
49.5	0.62	1.25	-1.16	0.42
50.0	1.55	1.80	-0.88	0.87
50.5	1.82	2.07	1.24	1.24
51.0	2.08	2.35	1.60	1.62
51.5	2.29	2.64	1.96	1.83
52.0	2.51	2.94	2.31	2.04
52.5	2.63	3.02	2.43	2.22
53.0	2.75	3.10	2.55	2.40
53.5	2.87	3.13	2.43	2.62
54.0	2.64	3.15	2.33	2.58
54.5	2.37	2.66	2.11	2.56
55.0	2.09	2.18	1.89	2.28
55.5	2.01	1.63	1.18	1.72
56.0	-2.09	0.62	0.51	1.47
56.5	-2.15	0.33	-0.14	-0.12
57.0	-2.21	-1.63	-1.10	-0.21
57.5	-2.27	-1.86	-1.50	-0.39
58.0	-2.34	-1.94	-2.41	-1.63
58.5	-2.39	-2.01	-2.55	-1.68
59.0	-2.43	-2.08	-2.64	-1.68
59.5	-2.49	-2.13	-2.65	-1.66

60.0	-2.55	-2.18	-2.66	-1.63
60.5	-2.45	-2.14	-2.66	-1.54
61.0	-2.34	-2.09	-2.65	-1.44
61.5	-1.83	-1.68	0.00	-1.30
62.0	-1.33	-1.28	0.00	-1.16
62.5	-0.56	-0.66	0.00	-0.92
63.0	0.00	0.87	0.00	-0.68

FTIDE (Indian River Inlet)

Measured Stages

time	inlet	potnets	vines	massey	dewey
		12	22	23	26	29
hr	ft	ft	ft	ft	ft	
39.00	1.08	0.38	0.73	0.43	0.28
39.50	1.24	0.64	0.99	0.55	0.34
40.00	1.35	0.86	1.17	0.69	0.4
40.50	1.43	1.05	1.33	0.8	0.54
41.00	1.33	1.21	1.45	0.88	0.66
41.50	1.28	1.3	1.54	0.95	0.79
42.00	1.16	1.32	1.49	0.98	0.88
42.50	0.88	1.29	1.33	0.96	0.98
43.00	0.61	1.18	1.1	0.9	1.01
43.50	0.16	1	0.8	0.81	0.98
44.00	-0.14	0.78	0.56	0.66	0.94
44.50	-0.49	0.55	0.4	0.49	0.86
45.00	-0.79	0.33	0.19	0.33	0.75
45.50	-0.94	0.1	-0.05	0.16	0.68
46.00	-1.1	-0.12	-0.27	0.01	0.55
46.50	-1.08	-0.32	-0.46	-0.14	0.45
47.00	-0.92	-0.49	-0.63	-0.26	0.36
47.50	-0.68	-0.64	-0.77	-0.34	0.25
48.00	-0.38	-0.72	-0.88	-0.4	0.16
48.50	-0.09	-0.73	-0.88	-0.36	0.08
49.00	0.24	-0.62	-0.68	-0.21	0
49.50	0.63	-0.4	-0.27	-0.03	-0.01
50.00	1	-0.13	0.12	0.12	-0.02
50.50	1.36	0.19	0.47	0.27	0.08
51.00	1.67	0.52	0.83	0.45	0.14
51.50	1.95	0.86	1.15	0.66	0.25
52.00	2.15	1.19	1.44	0.83	0.4
52.50	2.28	1.49	1.73	1.01	0.57
53.00	2.38	1.74	1.99	1.17	0.74
53.50	2.41	1.96	2.19	1.32	0.92
54.00	2.37	2.12	2.34	1.46	1.08
54.50	2.25	2.22	2.42	1.59	1.2
55.00	2.02	2.26	2.46	1.68	1.32
55.50	1.62	2.23	2.5	1.68	1.45
56.00	1.16	2.1	2.25	1.6	1.53

56.50	0.72	1.88	1.84	1.51	1.55
57.00	0.27	1.61	1.5	1.36	1.48
57.50	−0.12	1.36	1.23	1.15	1.41
58.00	−0.42	1.1	0.98	0.96	1.33
58.50	−0.56	0.84	0.69	0.77	1.23
59.00	−0.73	0.58	0.41	0.62	1.15
59.50	−0.71	0.34	0.19	0.46	1.02
60.00	−0.71	0.13	0.01	0.33	0.91
60.50	−0.51	−0.06	−0.16	0.21	0.8
61.00	−0.29	−0.2	−0.32	0.11	0.7
61.50	−0.1	−0.28	−0.39	0.05	0.61
62.00	0.24	−0.3	−0.36	0.04	0.51
62.50	0.46	−0.21	−0.17	0.15	0.42
63.00	0.78	−0.01	0.18	0.31	0.37

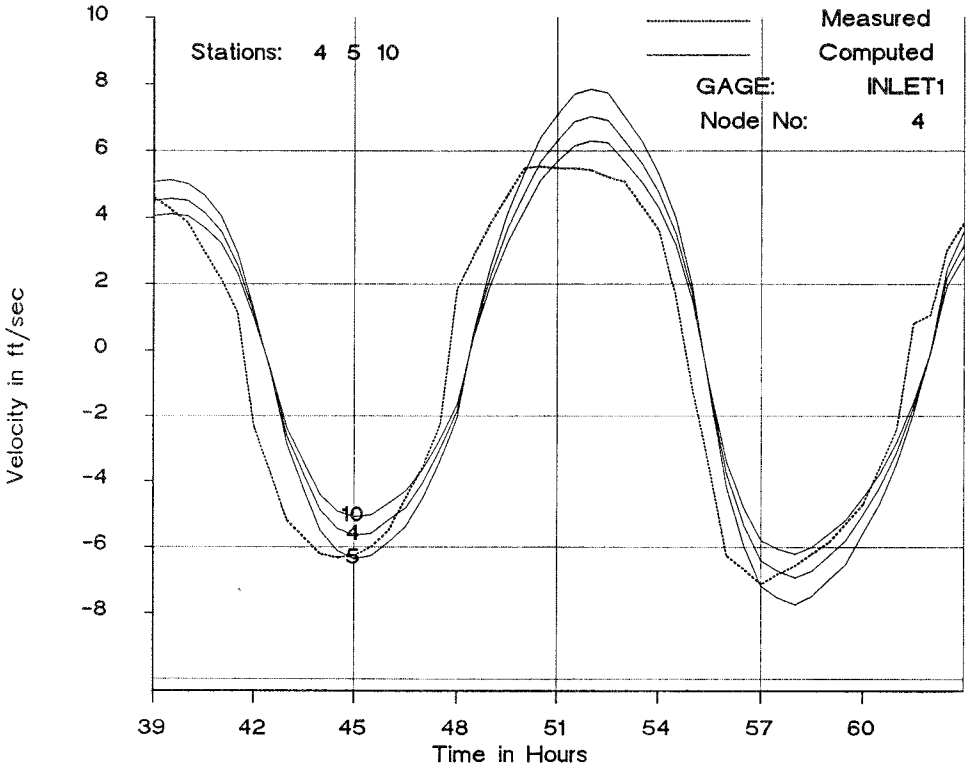
Stations: 4 5 10
Measured
Computed
GAGE: INLET1
Node No: 4
Velocity in ft/sec
Time in Hours
10
8
6
4
2
0
-2
-4
-6
-8
39
42
45
48
51
54
57
60
10
4
5

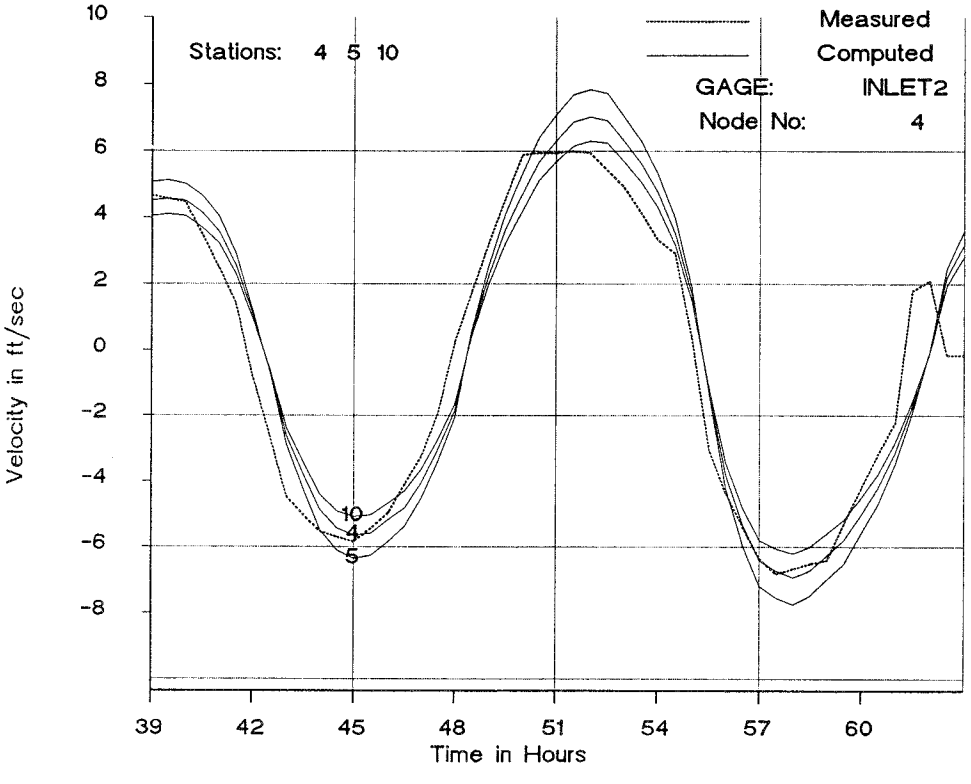
Stations: 4 5 10
Measured
Computed
GAGE: INLET2
Node No: 4
Velocity in ft/sec
Time in Hours
10
8
6
4
2
0
-2
-4
-6
-8
39
42
45
48
51
54
57
60
10
4
5

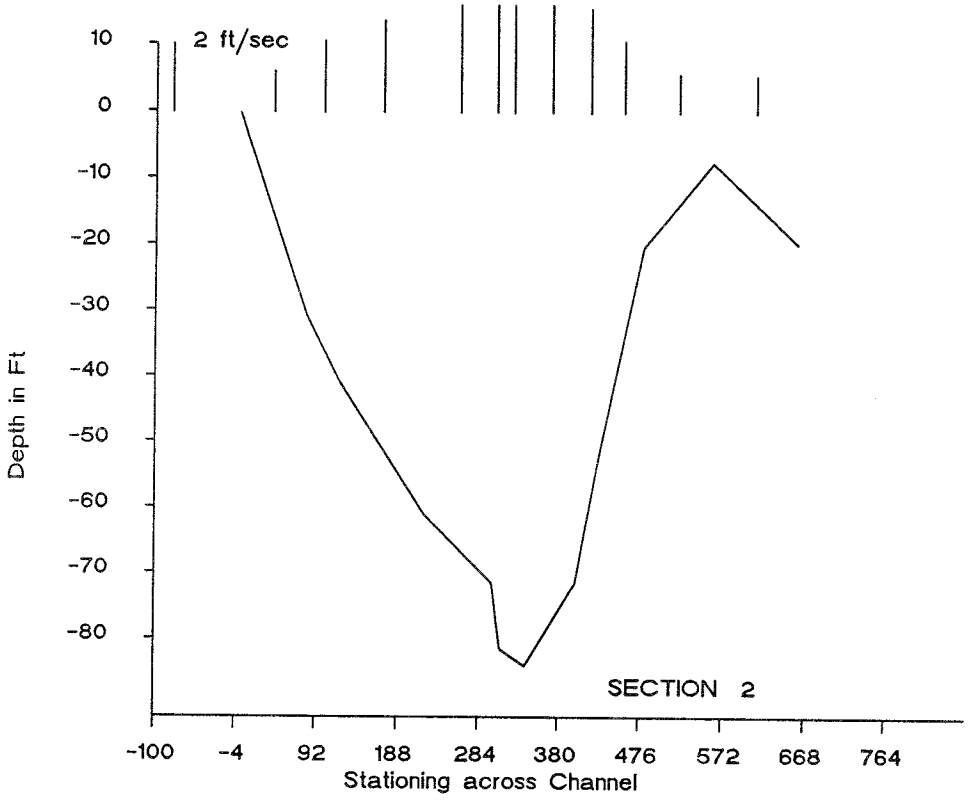
2 ft/sec
10
0
-10
-20
-30
-40
-50
-60
-70
-80
Depth in Ft
SECTION 2
-100
-4
92
188
284
380
476
572
668
764
Stationing across Channel

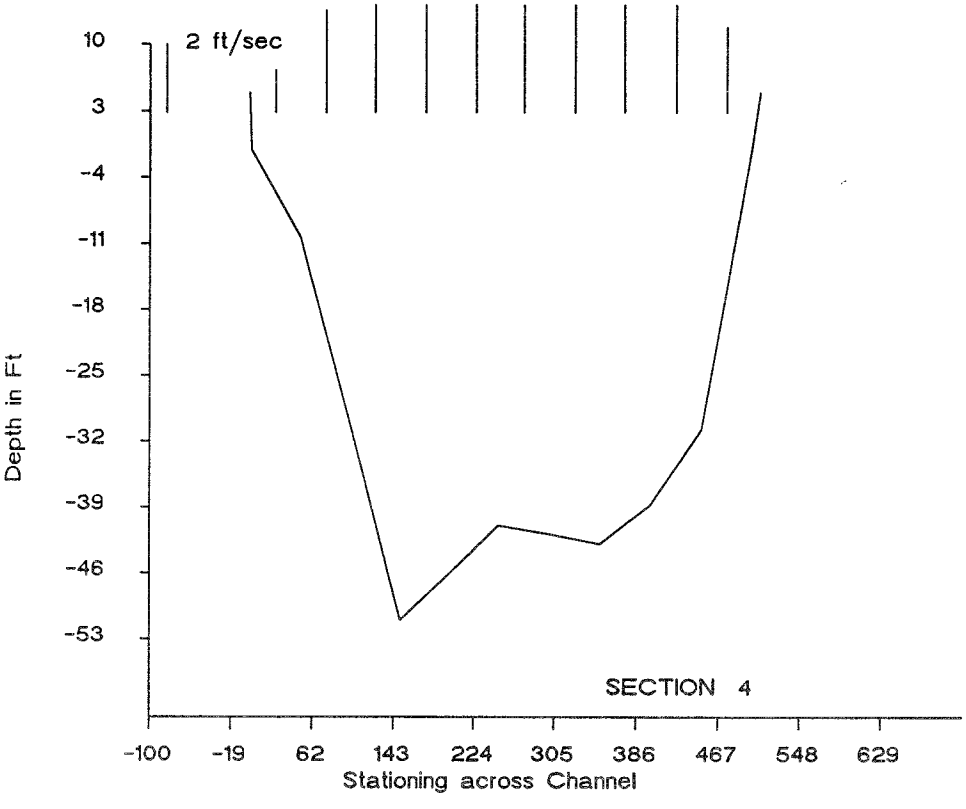
2 ft/sec
10
3
-4
-11
-18
-25
-32
-39
-46
-53
Depth in Ft
SECTION 4
-100
-19
62
143
224
305
386
467
548
629
Stationing across Channel

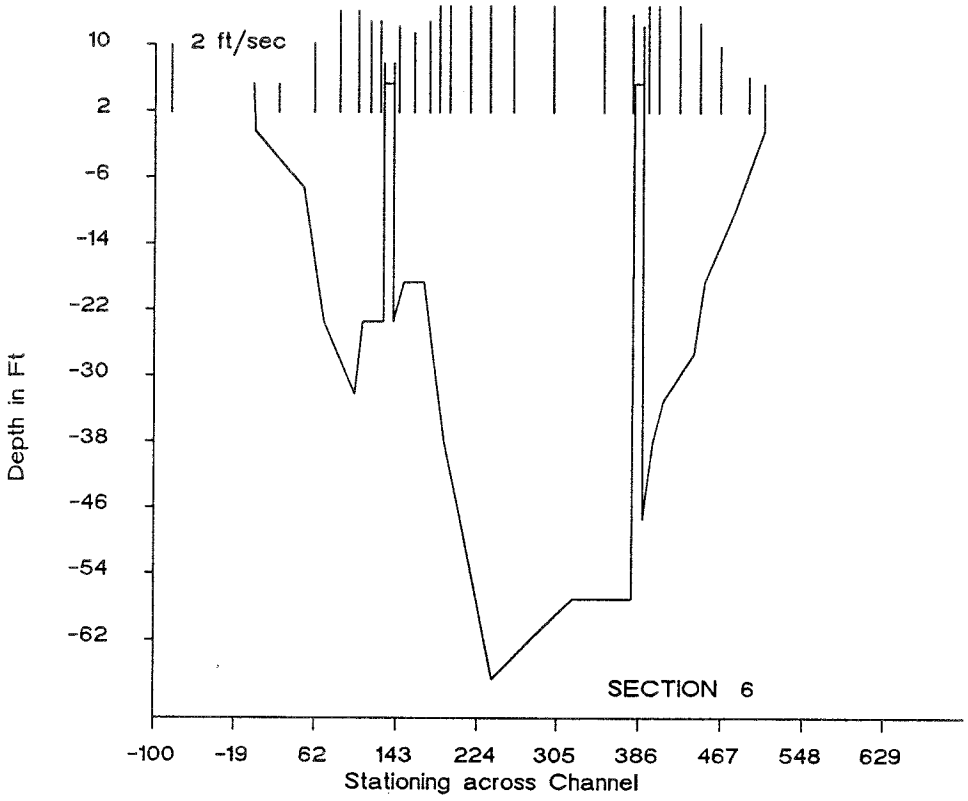
2 ft/sec
10
2
-6
-14
-22
-30
-38
-46
-54
-62
Depth in Ft
SECTION 6
-100
-19
62
143
224
305
386
467
548
629
Stationing across Channel

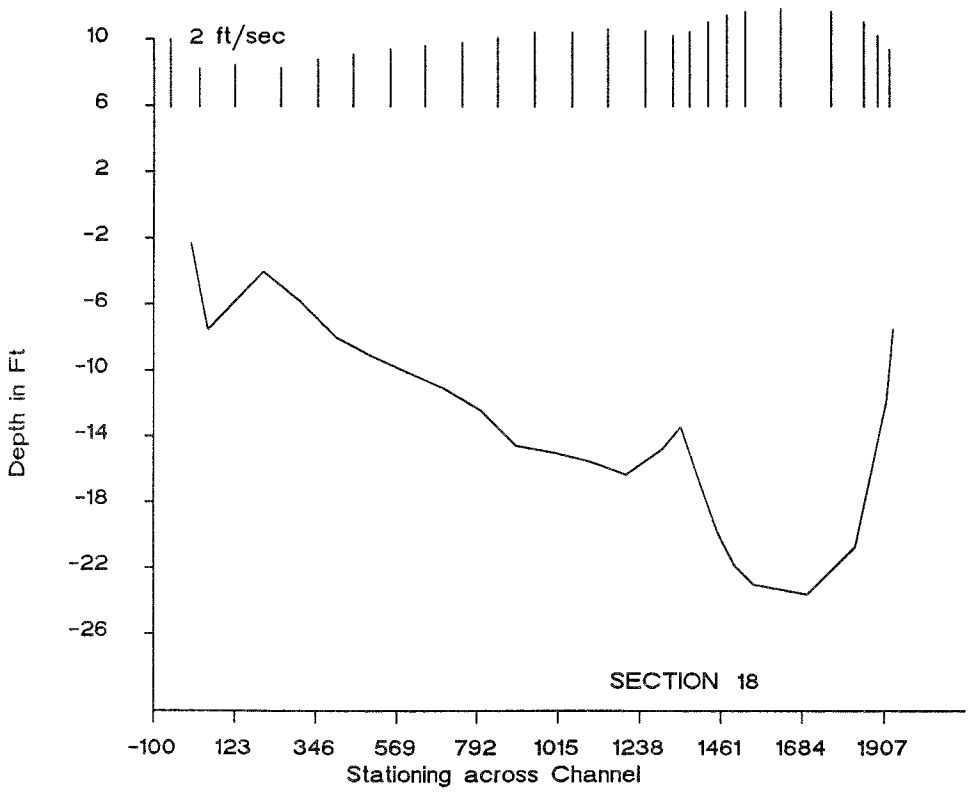
2 ft/sec
10
6
2
-2
-6
-10
-14
-18
-22
-26
Depth in Ft
SECTION 18
-100
123
346
569
792
1015
1238
1461
1684
1907
Stationing across Channel

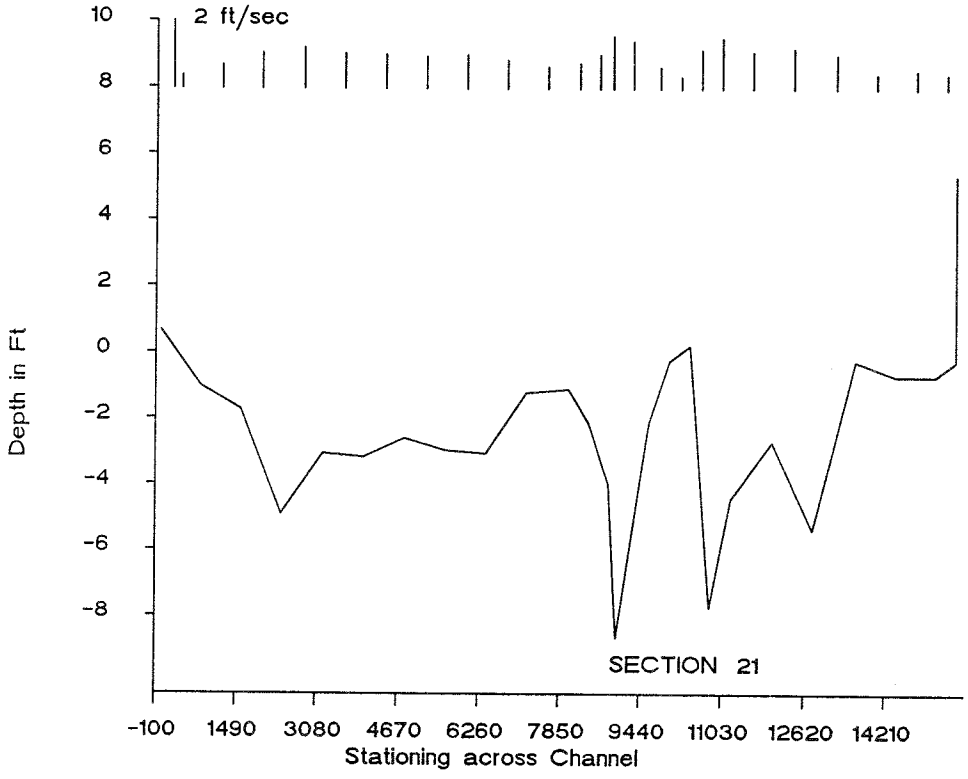
2 ft/sec
10
8
6
4
2
0
-2
-4
-6
-8
Depth in Ft
SECTION 21
-100
1490
3080
4670
6260
7850
9440
11030
12620
14210
Stationing across Channel

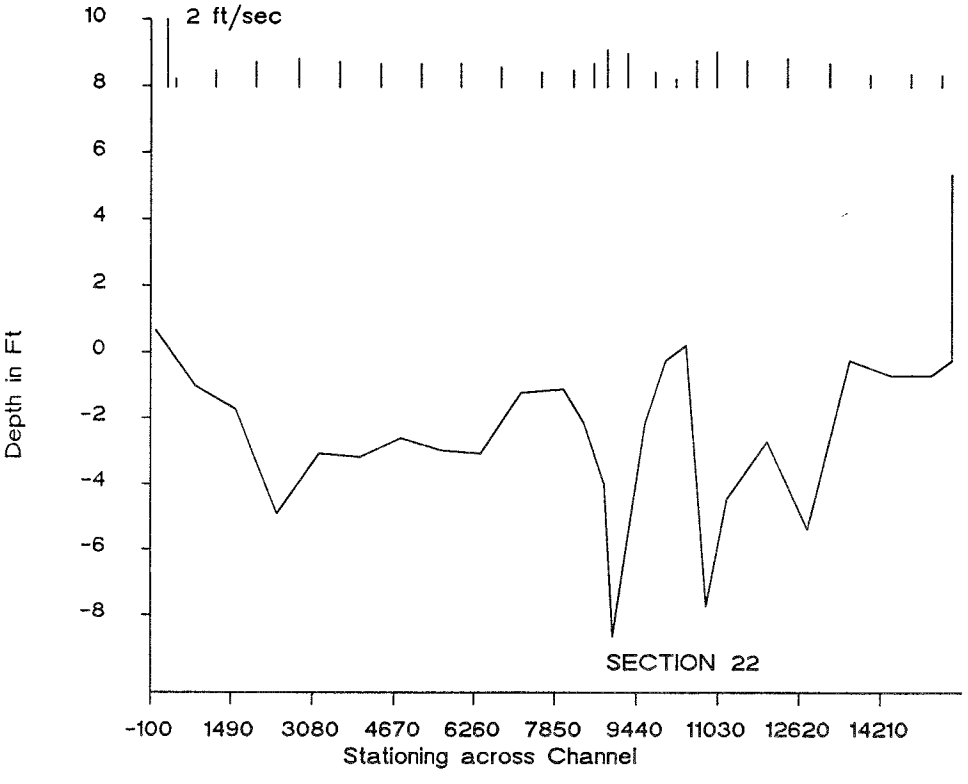
2 ft/sec
10
8
6
4
2
0
-2
-4
-6
-8
Depth in Ft
SECTION 22
-100
1490
3080
4670
6260
7850
9440
11030
12620
14210
Stationing across Channel

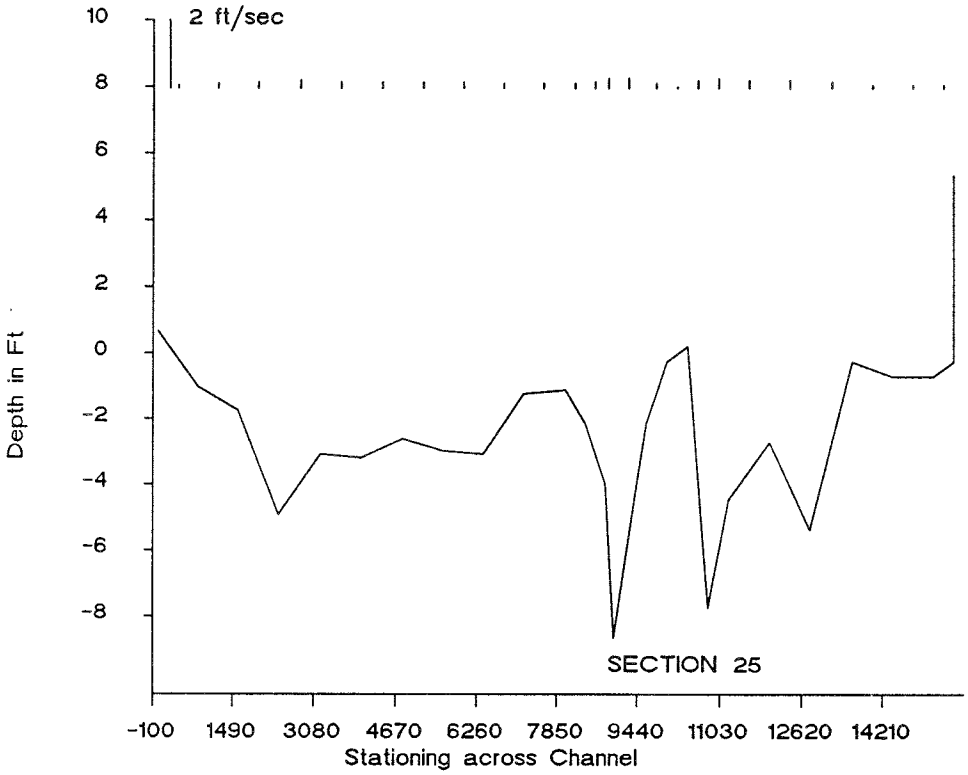
2 ft/sec
10
8
6
4
2
0
-2
-4
-6
-8
Depth in Ft
SECTION 25
-100
1490
3080
4670
6260
7850
9440
11030
12620
14210
Stationing across Channel

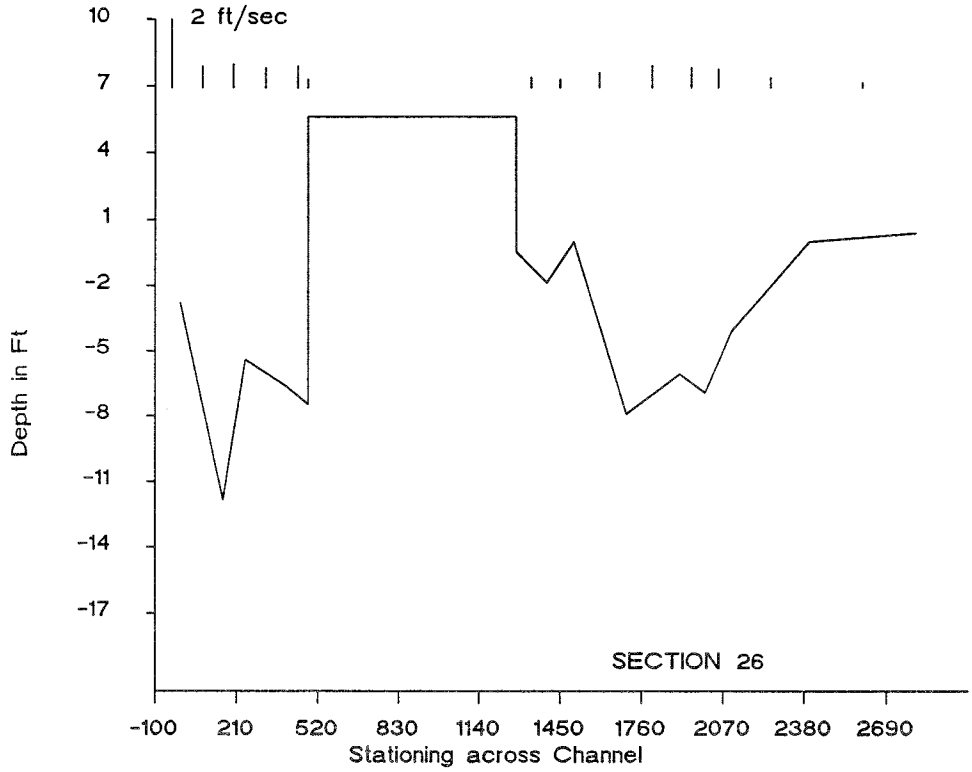
2 ft/sec
10
7
4
1
-2
-5
-8
-11
-14
-17
Depth in Ft
SECTION 26
-100
210
520
830
1140
1450
1760
2070
2380
2690
Stationing across Channel

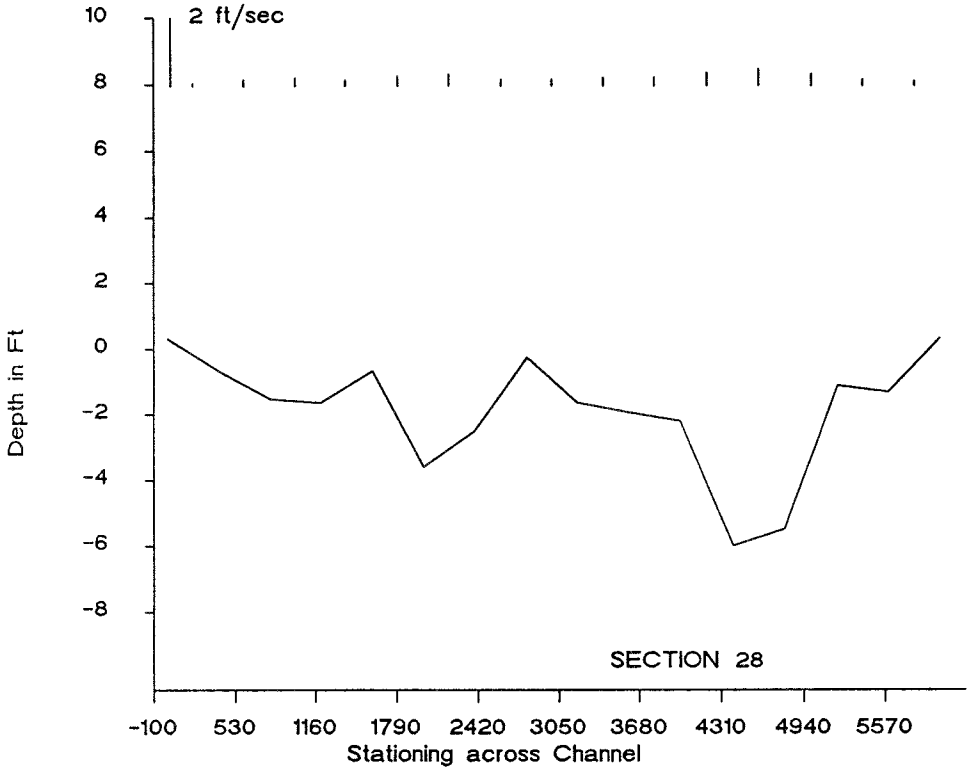
2 ft/sec
10
8
6
4
2
0
-2
-4
-6
-8
Depth in Ft
SECTION 28
-100
530
1160
1790
2420
3050
3680
4310
4940
5570
Stationing across Channel

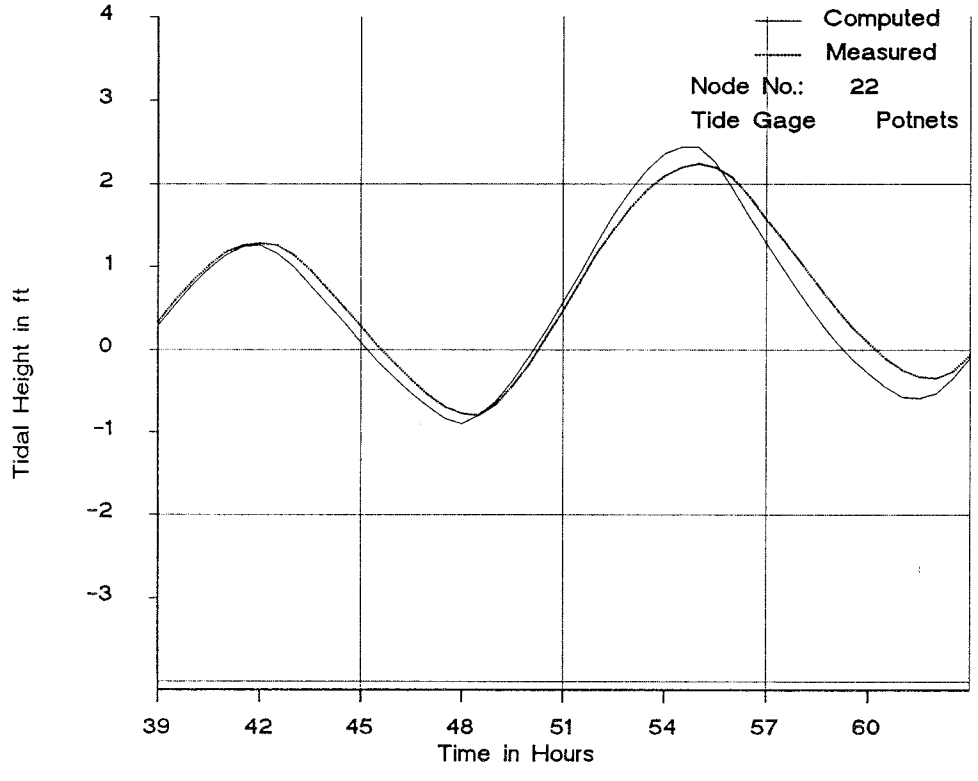
Computed
Measured
Node No.: 22
Tide Gage Potnets
4
3
2
1
0
-1
-2
-3
Tidal Height in ft
39
42
45
48
51
54
57
60
Time in Hours

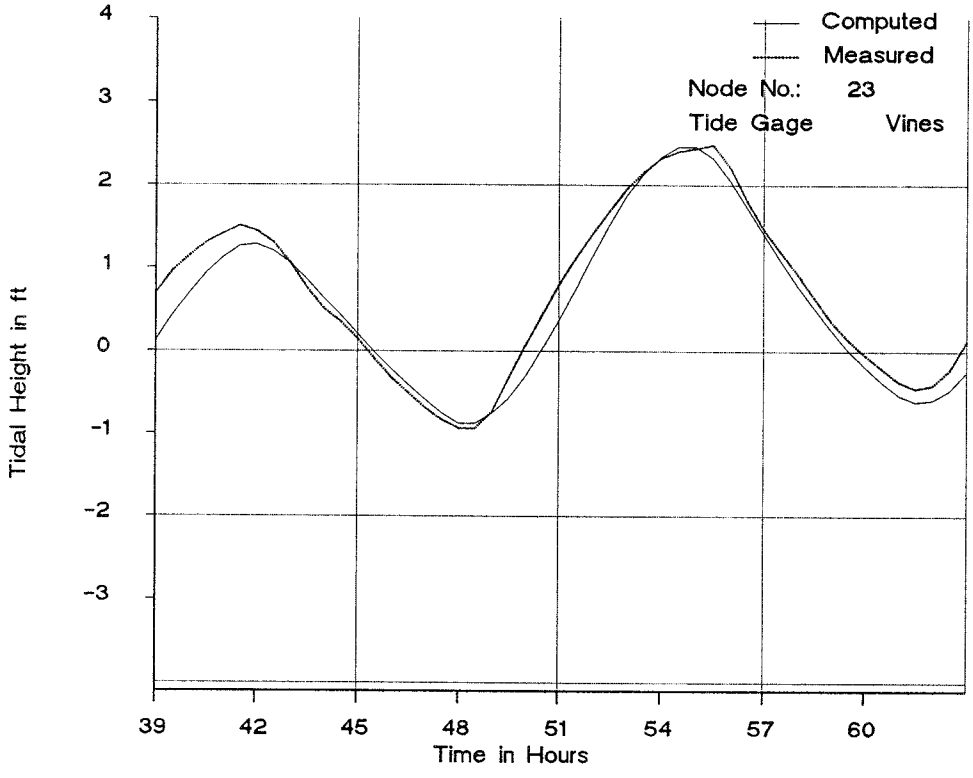
Computed
Measured
Node No.: 23
Tide Gage Vines
Tidal Height in ft
4
3
2
1
0
-1
-2
-3
39
42
45
48
51
54
57
60
Time in Hours

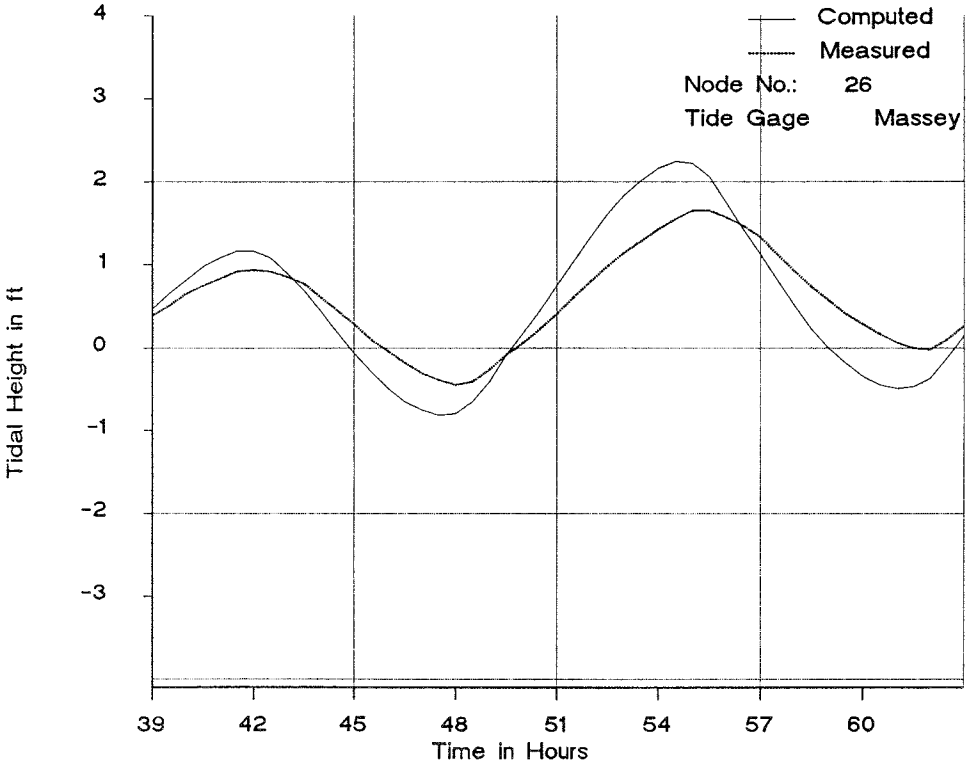
Computed
Measured
Node No.: 26
Tide Gage Massey
Tidal Height in ft
4
3
2
1
0
-1
-2
-3
39
42
45
48
51
54
57
60
Time in Hours

APPENDIX C: NOTATION

A	Cross-sectional area
B	Width of top of channel cross section
C	Constants obtained in evaluation of finite-difference solution
C_f	Coefficient of wind drag
F	Governing functional relation in finite-difference form
g	Acceleration due to gravity
h	Water depth from the channel bottom to the free surface
i	Grid space coordinate; also, arbitrary node number
j	Grid time coordinate; also, space coordinate a cross section subchannel
k	Arbitrary node number
K	Conveyance
K_e	Empirical form-drag coefficient for transition loss
l	Arbitrary node number
m	Arbitrary node number
M	Arbitrary grid point on space and time solution grid
n	Manning's coefficient of friction
n_j	Manning's coefficient of friction for subchannel j
N	Total number of nodes
P	Wetted perimeter of channel cross section
q	Lateral inflow or outflow per unit channel length per unit time
Q	Volume flow rate (discharge)
R_{hj}	Hydraulic radius of subchannel j
S_e	Rate of longitudinal head loss (transition loss)
S_f	Friction slope
t	Time
v	Average water flow velocity
V_w	Wind speed
x	Coordinate identifying position (stations) or distance across a channel cross section

y	Coordinate identifying position or lateral distance along a channel axis
z	Water surface elevation
z_b	Channel bottom elevation (reference datum)
α	Arbitrary variable in basic equations
ρ	Density of water
ρ_a	Density of air
τ_b	Bottom shear stress (due to bottom friction)
τ_b	Surface shear stress (due to wind)